[redacted]

POSTFLIGHT EVALUATION OF ATLAS-CENTAUR AC-5

(Launched March 2, 1965)

Centaur Project Office

and

Advanced Development and Evaluation Division

Lewis Research Center
Cleveland, Ohio

(NASA-TM-X-57043) POSTFLIGHT EVALUATION OF ATLAS-CENTAUR AC-5, LAUNCHED 2 MARCH 1965 (NASA) 102 p LIMIT NASA

X75-74675

Unclas
00/98 27404

[redacted]

C65-9277

CONFIDENTIAL

POSTFLIGHT EVALUATION OF ATLAS-CENTAUR AC-5 [redacted]

(Launched March 2, 1965)

Centaur Project Office

and

Advanced Development and Evaluation Division

Lewis Research Center
Cleveland, Ohio

Restriction/Classification Cancelled

GROUP 4
Downgraded at 3 year intervals;
declassified after 12 years

~~This material contains information affecting the national defense of the United States within the meaning of the espionage laws, Title 18, U.S.C., Secs. 793 and 794, the transmission or revelation of which in any manner to an unauthorized person is prohibited by law.~~

NOTICE Restriction/Classification Cancelled
This docum
satisfied y
of in accor
tions or the
Security M
Information.

CONFIDENTIAL

CONTENTS

I. SUMMARY

The Atlas-Centaur AC-5 vehicle was launched from ETR Complex 36A on March 2, 1965 at 8:25.04 a.m. EST. Within about 1 second after launch the thrust of the Atlas booster engine decayed rapidly; the vehicle settled back on the launch pad and was quickly destroyed by fire and explosion. Considerable damage was sustained by the launch complex and its associated equipment.

Loss of booster engine thrust was due to fuel depletion at the turbopump inlets, which is attributed to closure of the fuel prevalve or the staging valve. To preclude the recurrence of either of these fuel valving malfunctions, the following corrective action has been taken: The remote control actuator has been replaced by manual operation of the Atlas fuel prevalve; the internal passage dimensions in the staging valve have been increased to lessen the hydraulic load on the valve poppet.

In addition to the Atlas fuel system malfunction, a failure in the power control circuitry of the Centaur guidance computer resulted in partial removal of power at umbilical ejection. To prevent such a guidance system failure on future flights some redundant circuitry has been eliminated and more rigorous checkout procedures have been adopted. No further anomalies were discovered in the telemetered data prior to the Atlas booster thrust decay.

A prime objective of the AC-5 flight was to place a dynamic model of the Surveyor spacecraft in a simulated lunar transfer trajectory. An important facet of this problem is the demonstration of a launch-on-time capability in accordance with the proper Earth-moon relation. The window opening time was established at 8:25 a.m. EST; thus the actual launch occurred within 4 seconds of the planned time.

II. INTRODUCTION

The Atlas-Centaur AC-5 vehicle, which was launched from ETR Complex 36A on March 2, 1965, at 8:25.04 a.m. EST, was the fifth in a series of developmental flights. Shortly after lift-off, Atlas booster engine thrust was lost, and the vehicle settled back to the launcher and was destroyed by explosion and fire. Loss of thrust was caused by fuel starvation of the Atlas booster engines.

This flight was to have been the first to attempt to place a dynamic model of the Surveyor spacecraft (SD-1) in a simulated lunar transfer trajectory. (All abbreviations and symbols are defined in the appendix.) In order to place the spacecraft in this type of trajectory with a second-stage single-propulsion phase (direct ascent), the launch vehicle must demonstrate a launch-on-time capability in accordance with the proper Earth-moon relation. The vehicle was targeted for the actual lunar opportunity of October 10, 1964. The launch window opening for this particular day was biased by 7 hours to provide for a daylight launch that was required for photographic coverage. The resulting window opening time was established as 8:25 a.m. EST with the actual launch occurring at 8:25.04 a.m. EST thereby successfully demonstrating a lunar launch-on-time capability.

Several major changes to vehicle systems were incorporated on AC-5:

(1) An advanced Centaur propellant utilization system

(2) A payload separation system

(3) A Surveyor dynamic model that includes research and development instrumentation and an S-band transponder

(4) Uprated Rocketdyne MA-5 propulsion system with 165k booster engines

(5) Agena timer and auxiliary electronic module

The test control parameters for this flight were as follows:

Separation System

(1) To demonstrate the spacecraft separation system

(2) To verify the satisfactory operation of the Atlas-Centaur separation system

(3) To verify the satisfactory operation of the insulation-panel and nose-fairing-jettison system

Propulsion System

(1) To verify the ability of the Centaur propulsion system to start in the

flight environment and burn to guidance cutoff

(2) To obtain data on the performance of the Centaur main engine system

(3) To obtain data on the performance of the H_2O_2 attitude control system

Basic Structure

(1) To verify the structural integrity of the Atlas and Centaur vehicles during all powered phases of flight

(2) To verify the structural and thermal integrity of the Centaur nose-fairing and insulation panels

Guidance System

(1) To verify the integrity of the guidance system

(2) To demonstrate the overall measuring accuracy of the guidance system

(3) To verify that the guidance system provides proper discrete and steering signals to the Atlas and Centaur flight control systems

(4) To demonstrate that the guidance equations and associated trajectory parameters are satisfactory

(5) To obtain data on Atlas-Centaur lunar orbit injection accuracy by post-injection DSIF tracking of the Surveyor dynamic model S-band transponder

Centaur Vehicle Systems

(1) To verify that the flight control system supplies proper signals for attitude control and dynamic stability of the Centaur vehicle

(2) To obtain data on the capability of the Centaur to perform a retro-maneuver

(3) To obtain data on the Centaur propellant-utilization-system performance

(4) To obtain data on the performance of the Centaur hydraulic, pneumatic, and electrical systems

(5) To obtain data on the performance of the Centaur RF systems, telemetry, Azusa, and C-band beacon

(6) To demonstrate the capability of the Agena timer for a one-burn mission

Atlas Vehicle

(1) To obtain data on the performance of all Atlas systems

(2) To demonstrate the operation of the uprated MA-5 booster engines (LV-3C), 165k pounds of thrust

Launch Capability

(1) To obtain data on the simulated lunar launch-on-time capability (variable launch azimuth) of the Atlas-Centaur

Environment

(1) To obtain data on the spacecraft environment during the launch-to-spacecraft separation phase of flight

(2) To obtain data on the flight environments, including pressures, temperatures, and vibration levels

(3) To obtain data on the orbital environments, terminal behavior, and general postmission performance of Centaur systems until loss of all data links

The AC-5 planned sequence of flight events is presented in table II-I. A schematic diagram of the planned flight is shown in figure II-1, and an illustration of the general arrangement of the Centaur stage is presented in figure II-2.

This report consists mainly of an evaluation of the Atlas propulsion system failure, the Centaur guidance system failure, and their respective failure analyses. Other Atlas and Centaur airborne systems are evaluated up to vehicle destruction, including an evaluation of ground-support systems and launch-area damage.

TABLE II-I. - PLANNED SEQUENCE OF AC-5 FLIGHT EVENTS (REF. 1)

Event	Programer time, sec	Preflight nominal time, sec
Guidance to flight mode		T - 8.37
Unnull Atlas displacement gyros		T - 3.95
Programer start, 2-in. rise		T + 0
Unnull Atlas servointegrators (8-in. rise)		
Activate autopilot control (42-in. rise)		
Initiate roll program		T + 4
Initiate pitch program		T + 15
LOX tank pressure change		T + 20
Vent insulation panel purge		T + 40
Open LH_2 vent valve command		T + 74
Displacement and rate gyro gain to low		T + 110
Enable booster staging		T + 135
Booster engine cutoff, close LH_2 vent valve command, activate sustainer control, rate gyro gain to high	BECO + 0	T + 141.6
Deactivate booster control, null integrators	BECO + 1	T + 142.6
Deactivate sustainer control	BECO + 3	T + 144.6
Jettison booster package	BECO + 3.1	T + 144.7
Open LH_2 vent valve command	BECO + 7	T + 148.6
Admit guidance steering, disable displacement gyros	BECO + 8	T + 149.6
Jettison insulation panels	BECO + 30	T + 171.6
Unlatch nose fairings	BECO + 54.5	T + 196.1
Fire thrustor bottles	BECO + 55	T + 196.6
Start Centaur boost pumps, unlatch insulation-panel hinges	BECO + 66	T + 207.6
Enable sustainer engine cutoff	BECO + 88	T + 229.6
Sustainer engine cutoff, vernier engine cutoff, start Centaur programer, close LOX and LH_2 vent valves, pressurize LOX and LH_2 tanks	SECO + 0	T + 238.0
Energize electrical disconnect	SECO + 0.1	T + 238.1

TABLE II-I. - Concluded. PLANNED SEQUENCE OF AC-5 FLIGHT EVENTS (REF. 1)

Event	Programer time, sec	Preflight nominal time, sec
Start hydraulic recirculating pump, PU segmented signal	SECO + 0.5	T + 238.5
Boost pump accelerating valve	SECO + 1	T + 239.0
Separate first and second stages	SECO + 1.9	T + 239.9
Fire retrorockets	SECO + 2	T + 240.0
Prestart, steering reference to Centaur	SECO + 3.5	T + 241.5
Start main engines, unnull main engine integrators, energize igniters, low rate gain	SECO + 8.5	T + 246.5
Admit guidance for steering	SECO + 12.5	T + 250.5
Reset programer	SECO + 30	T + 268.0
Unnull PU signal	SECO + 98.5	T + 336.5
PU segmented signal	SECO + 333.5	T + 571.5
Enable main engine cutoff	SECO + 403.5	T + 641.5
Main engine cutoff, H_2O_2 separate on, H_2O_2 roll integrator unnulled, low displacement gain, high rate gain	MECO + 0	T + 664.0
MECO backup, PU null	SECO + 450.5(t)	T + 688.5
Safe Surveyor destruct	SECO + 451	T + 689.0
Preseparation arming, extend landing gear, null main engine integrators	t + 18	T + 706.5
Unlock omni antenna	t + 28.5	T + 717.0
Preseparation arming off, high power on	t + 49	T + 737.5
Spacecraft electrical disconnect, switch guidance/spacecraft TLM channels	t + 54.5	T + 743.0
Separate spacecraft	t + 60	T + 748.5
Start 180° turn, admit guidance for attitude control	t + 65	T + 753.5
End 180° turn, start hydraulic recirculating pump, prestart, start retrothrust	t + 265	T + 953.5
Calibrate telemetry	t + 641	T + 1329.5
Open LOX and LH_2 vent valves	t + 1165	T + 1853.5
End retrothrust, power off	t + 1166	T + 1854.5

CONFIDENTIAL

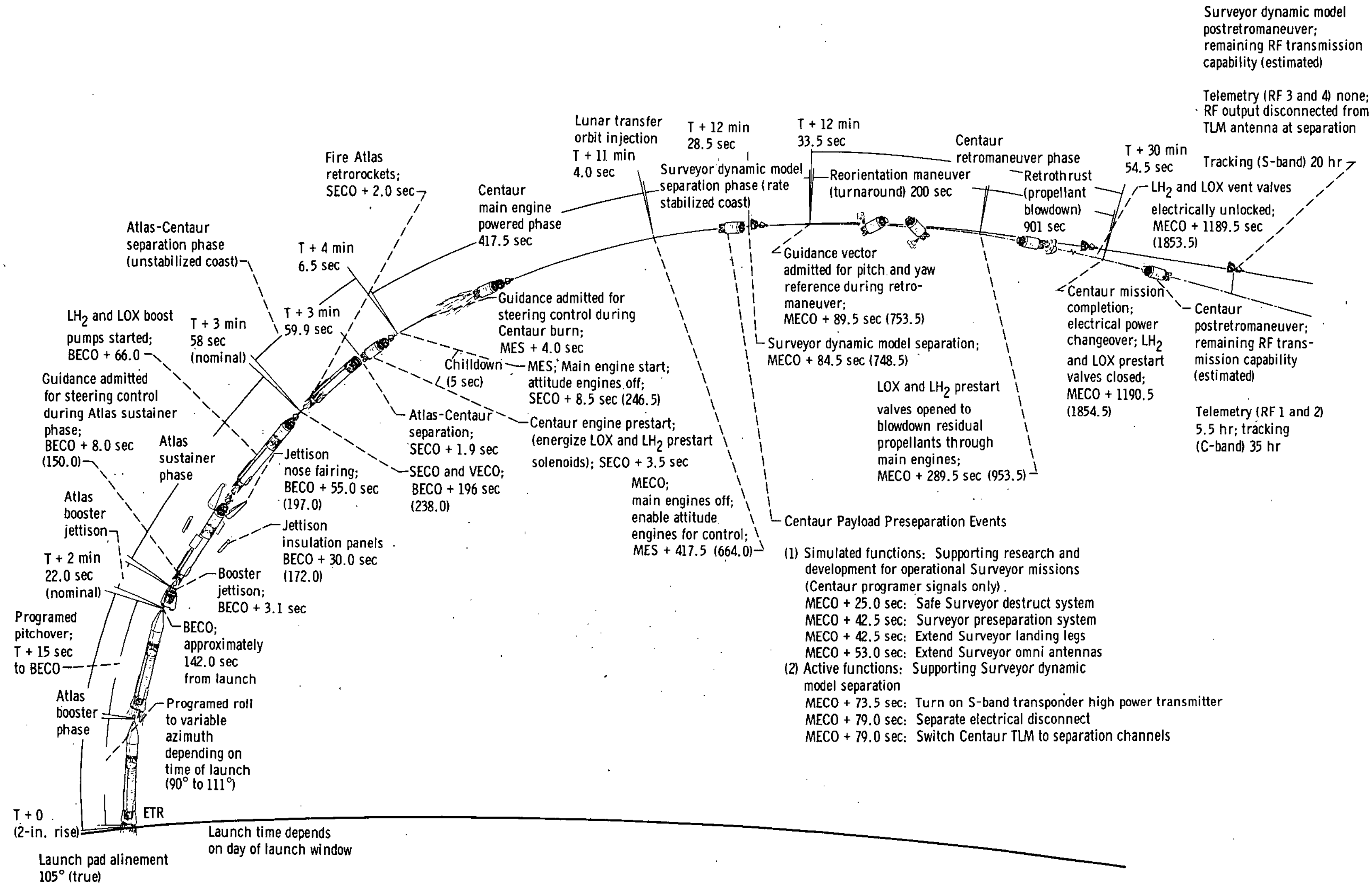

Figure II-1. - Planned AC-5 flight compendium (ref. 1).

CONFIDENTIAL

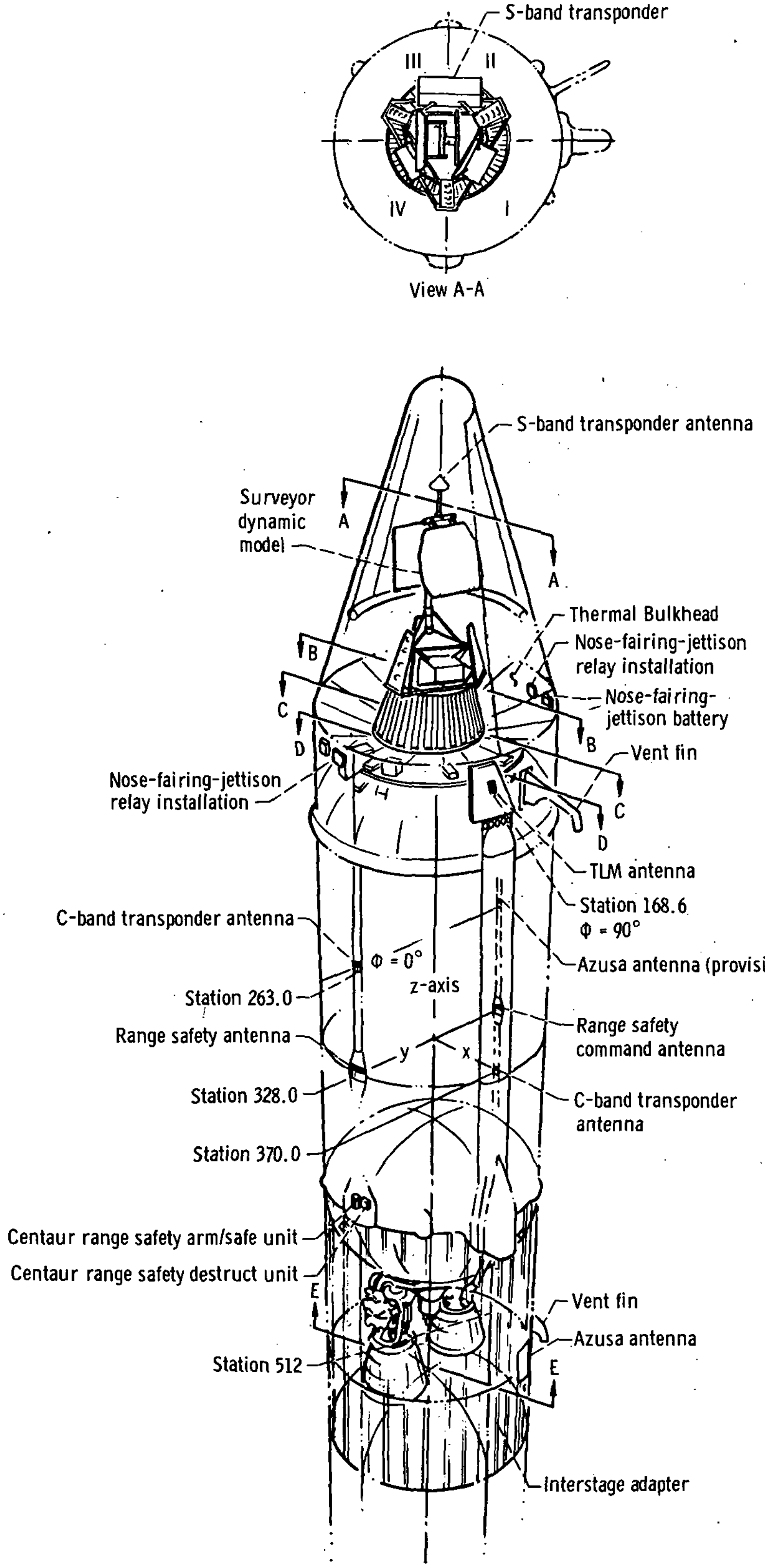

(a) Overall view.

Figure II-2. - General arrangement of

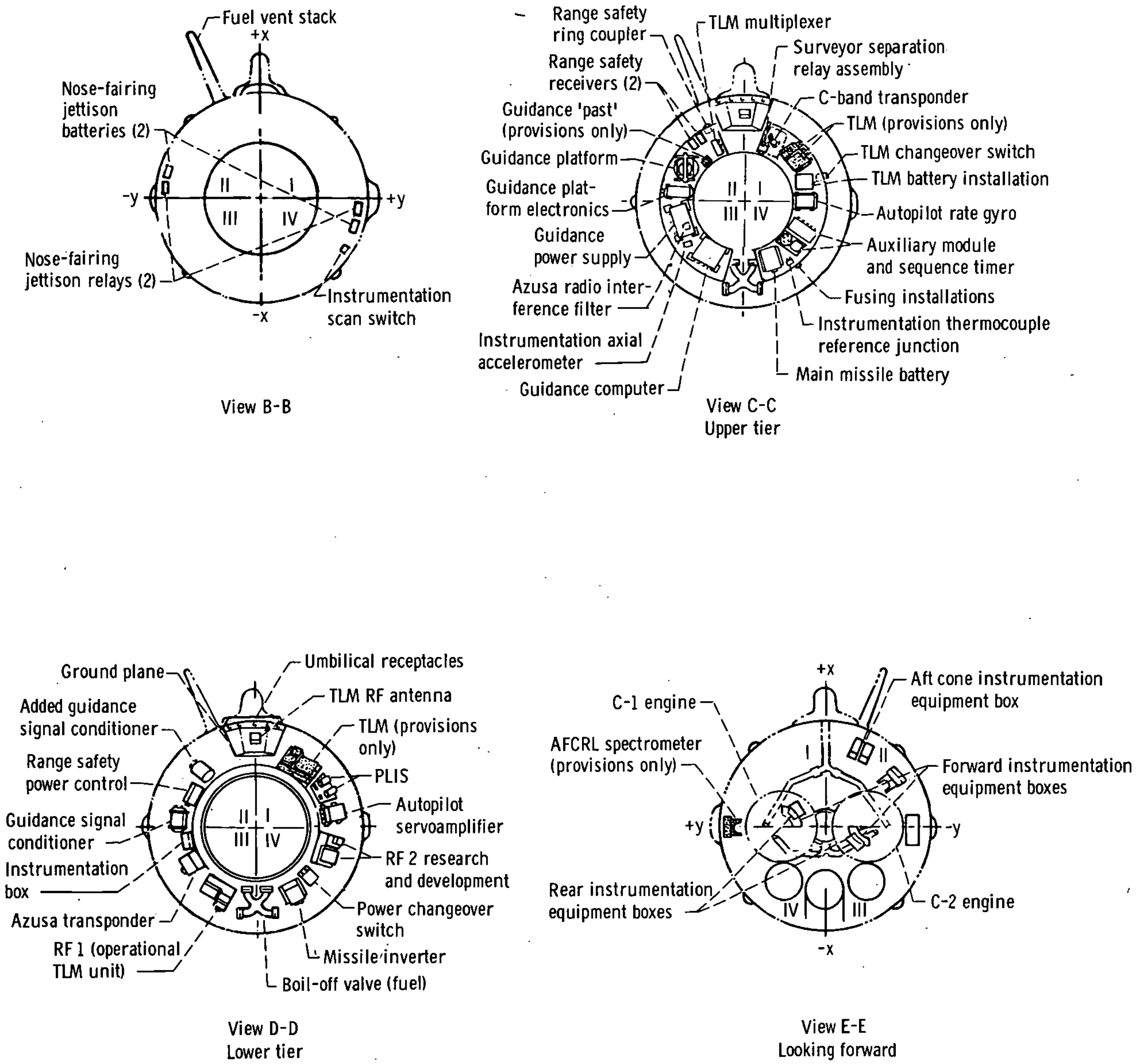

(b) Sectional views.

Centaur stage (6C)(ref. 1).

III. PRELAUNCH HISTORY

Summary

Prior to launching, the flight vehicle undergoes a series of preflight tests, which consist of (1) propellant tanking integrated test, (2) flight acceptance and composite test, and (3) composite readiness test, to ensure that all airborne and ground-support systems are within specifications to support a successful launch.

Arrival and Erection

The Atlas 156D booster arrived at ETR on January 7, 1965, followed by the Centaur 6C, and the interstage adapter (I/A) on January 9. The Atlas-Centaur launch vehicle erection started on January 14 with the Atlas 156D booster, I/A on January 15, and Centaur 6C on January 16.

Propellant Tanking Integrated Test

The propellant tanking integrated test (quad tanking, ref. 1) is conducted to verify that the launch vehicle can be tanked with propellants and that all vehicle and spacecraft systems will function properly under cryogenic conditions and in a radiofrequency environment. This test was conducted on February 11 for AC-5. Prior to the tanking test, two problems were encountered during the Atlas RP-1 tanking. The first was a leaking flex line in the ground transfer system that required replacement, and the second was a leak in the sustainer turbopump seals. This leak occurred after a pressure of 60 psig was reached (sequence II). The decision was to close the fuel prevalves and proceed with the tanking test. The test began at 1730 EST and proceeded normally through T - 0 with no holds except the 40-minute built-in hold at T - 10 minutes. Other than the leak in the sustainer turbopump seal, the test was completed with satisfactory results.

Special RP-1 Tanking Test

On February 15, this special tanking test was conducted to verify the sustainer turbopump seal leak and to record the leakage rate. Prior to the tanking of RP-1, the turbopump was pressurized to 30 psig with gas, and flowmeters were attached to the seal drain lines. This gas leakage test was conducted under both static and dynamic conditions. A leakage of 0.7 standard cubic inch per minute was recorded under dynamic conditions. RP-1 was tanked, and only a slight amount of leakage was evident. This leakage ceased after the tank pressures were cycled several times between 13 and 60 psig (sequences I and II); as a result, the existing sustainer engine was used.

Flight Acceptance Composite Test

The flight acceptance composite test (FACT, ref. 2) was conducted to verify that the combined Atlas-Centaur-Surveyor dynamic model system is capable of operation with no detrimental interference when subjected to conditions simulating flight. This test for AC-5 was conducted on February 18. The test began at 1443 EST and proceeded normally until T - 5 minutes at which time a preplanned guidance "no-go" signal was issued. The preplaned signal was a launch-on-time requirement to determine a time interval to reset the computer for a new launch window. The time interval to accomplish this task was 15 minutes. Prior to resuming the count, a power fluctuation was detected from power supply 3. The hold was extended, and the difficulty was traced to a faulty safety switch. The switch was bypassed, and the test proceeded normally with T - 0 occurring at 1618 EST. Other than the hold at T - 5 minutes for guidance system launch on time and the power supply, the test was completed with satisfactory results.

Composite Readiness Test

The composite readiness test (CRT, ref. 3) was conducted to revalidate and verify the proper operation of the vehicle and GSE electrical systems. This test for AC-5 was conducted on February 25. Prior to conducting the test, guidance system 19A was removed from the vehicle for a clock pulse generator board change. Accelerometer pulse count shifts due to the board change resulted in the system becoming unacceptable for flight and the backup system 26 became the flight item. The test began at 1235 EST and was completed satisfactorily.

Payload

The 1400-pound Surveyor dynamic model arrived at ETR on January 22. Encapsulation of the dynamic model within the flight nose fairing was accomplished on February 3 and then mated to the launch vehicle on February 5. The encapsulated payload was demated on February 19 following quad tanking and FACT for final flight preparations. The encapsulated payload was remated to the launch vehicle on February 26 in preparation for launch on March 2.

Launch

The Atlas-Centaur launch vehicle AC-5, consisting of Centaur 6C and Atlas 156D, was launched from ETR Complex 36A at 0825:04 EST on March 2. The launch ended in destruction of the vehicle approximately 3 seconds after 2-inch motion. The failure was caused by the loss of booster engine thrust, which was attributed to fuel starvation of the booster engines.

Weather

The atmospheric conditions on launch day were favorable. All wind velocities (fig. III-1) were within vehicle specification, and the conditions for photographic coverage were excellent.

Time	0825 EST
Surface temperature	68° F
Relative humidity	92 percent
Surface winds	14 knots at 175° true North
Visibility	10 miles
Cloud coverage	50 percent strato-cumulus base at 4000 ft 10 percent alto-cumulus base at 16 000 ft

AC-5 Prelaunch History - 1965

Atlas 156D arrival	January 7
Centaur 6C arrival	January 9
Interstage adapter arrival	January 9
Atlas 156D erection	January 14
I/A erection	January 15
Centaur 6C erection	January 16
Insulation panel arrival	January 21
Nose-fairing payload arrival	January 22
Insulation panel erection	January 29
Encapsulate payload	February 3
Barrel section erection	February 5
Mate encapsulated payload	February 5
Quad tanking	February 11
Special RP-1 tanking	February 15
FACT	February 18
Demate payload	February 19
CRT	February 25
Remate payload	February 26
Launch	March 2

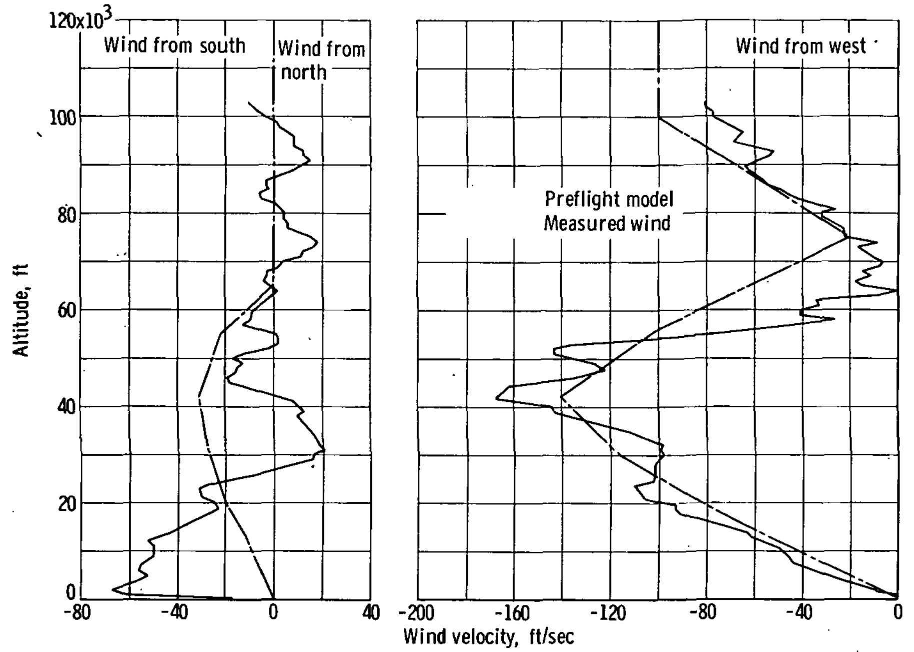

(a) North wind component.

(b) East wind component.

Figure III-1. - Wind conditions measured prior to AC-5 launch as determined by Rawinsonde run at 0824 EST on March 2, 1965 (preflight data).

IV. LAUNCH ON TIME

The AC-5 launch demonstrated two important launch-on-time objectives essential to the development of a capability to adjust to unknown factors that could cause the miss of a launch window. These factors were (1) to demonstrate the capability to preplan a countdown operation and execute the countdown to achieve a precise vehicle lift-off time and (2) to demonstrate the ability of the launch vehicle to hold for a preplanned length of time in a fully tanked condition without systems degradation.

The Atlas-Centaur AC-5 launch vehicle was launched on March 2, 1965, at 0825:04 EST, which was 4 seconds after the window opening time. Although shortly after lift-off the vehicle failed, the launch countdown was successful thus demonstrating the ability to launch on time.

The launch window for AC-5 was derived from the actual launch window of October 10, 1964. The window opening was established at 0825 EST and was biased by 7 hours to provide maximum launch opportunity and to permit range photographic coverage.

The Range countdown was scheduled for 280 minutes with preplanned holds of 60 and 40 minutes at T - 90 and T - 5 minutes, respectively. These hold times were planned into the countdown to increase the launch-on-time capability.

The countdown began at 0205 EST and continued without a hold until T - 90 minutes. At T - 140 minutes, the complex encountered a facility power failure that caused the guidance-autopilot test start time to be delayed 40 minutes. The preplanned hold of 60 minutes absorbed this 40 minutes thus allowing the countdown to proceed on schedule upon resuming the count at T - 90 minutes. The countdown continued without a hold until T - 5 minutes, at which time the 40-minute hold was started. The only anomaly at this time was that the Centaur LOX topping extended into the hold period by 2 minutes to complete topping to 100 percent. The 40-minute hold demonstrated the ability of the Atlas-Centaur vehicle to hold for a preplanned length of time in a fully tanked condition without apparent systems degradation.

V. ATLAS PROPULSION SYSTEM

Summary

The Atlas propulsion system operated normally through lift-off for the AC-5 launch. At approximately 1.0 second (all times are referenced to vehicle lift-off) the booster engines began losing thrust as a result of fuel depletion to the turbopump inlets. The loss of thrust resulted in the vehicle settling back on the launch pad at 2.8 seconds. Several possibilities exist as to the cause of fuel depletion, although closure of the fuel prevalve and the staging valve are considered the primary suspects. Although the exact cause of the failure has not been ascertained, comprehensive corrective actions taken for future vehicles are such that all known AC-5 failure modes have been eliminated.

System Description and Performance

The Atlas propulsion system consists of two booster, one sustainer, and two vernier engines. (See system schematic in fig. V-1.) At engine start, the propellants are supplied from a LOX and a fuel start tank, each pressurized to approximately 600 psia. One gas generator drives the sustainer turbopump and another drives the two booster turbopumps. When the turbopumps approach their normal operating speeds, the systems revert to the main propellant supply consisting of a LOX tank pressurized to approximately 40 psia and a fuel tank pressurized to approximately 73 psia (ref. 5).

The fuel system from the main supply tank to the engine injector contains a prevalve, a staging valve and disconnect, a turbopump, and a main fuel valve for the booster system. The sustainer system has a prevalve, a turbopump, and a propellant utilization (PU) valve. The LOX system has the same elements except that the main LOX valve replaces the main fuel valve for the boosters, and a head supression valve replaces the PU valve for the sustainer.

All Atlas propulsion system parameters were normal through lift-off for the AC-5 launch. Table V-I compares some propulsion system nominal values with those obtained at lift-off on AC-5. The first indication of trouble occurred with the loss of fuel pump inlet pressure (FPIP). From 0.7 to 0.9 second the B-1 FPIP decayed from 56.0 to 5.5 psia, and the B-2 FPIP from 56.0 to 8.0 psia (fig. V-2). Following 1.1 seconds the inlet pressures for both the B-1 and B-2 sides remained below 3.0 psia. The fuel tank ullage pressure remained essentially constant until vehicle disintegration at 2.8 seconds, indicating the source of the problem was somewhere between the main fuel supply and the turbopump inlets. The B-1 and B-2 thrust chamber pressures (fig. V-3) were 560 psia at 0.8 second. At 1.1 seconds, the B-1 pressure was 487 psia and the B-2 was 530 psia. By 1.5 seconds both chamber pressures had decayed to approximately 40 psia. The sustainer chamber pressure remained normal, approximately 700 psia, until flight termination.

The booster gas generator chamber pressure (fig. V-4) was 515 psia at 1.0 second and decayed to 30 psia by 1.5 seconds. The gas generator should have reverted to start tank operation but did not. For gas generator operation the gas generator blade valve is in the open position. Hardware recovery indicated the blade valve was in the closed position. Two theories have been advanced as to why the blade valve closed. One states that following the loss of fuel at the turbopump inlets, the ducts collapsed severing the electrical connection to the blade valve solenoid control. The other states that the overspeeding of the turbopumps loosened the electrical connections. In either case, the closure of the gas generator blade valve is considered a result of the vehicle failure.

The B-1 turbopump started to overspeed from its normal speed of 6350 rpm at 0.8 second (see fig. V-5). The B-2 turbopump started to overspeed at 0.95 second with a value of 6150 rpm, reached a peak value of 6850 rpm at 1.1 seconds, and decayed to 1500 rpm by 2.7 seconds. The turbopumps initially oversped because the loss of fuel unloaded the system. The only discrepancies in the sustainer system and the booster LOX system performance (fig. V-6) are considered a result of the vehicle failure.

The length of time the thrust chambers could operate under steady-state conditions following the loss of fuel at the turbopump inlets was calculated to be about 0.25 second. With the sequence of events occurring in the order described and from the study of flight films, starvation of fuel to the turbopump inlets has been concluded as the AC-5 failure mode.

Failure Analysis

Fuel starvation to the booster engines could have been caused by the following possible failure modes (ref. 6):

(1) Closure of the prevalve

(2) Closure of the staging valve

(3) Low pressure ducting rupture

(4) Blockage of the low pressure ducts

(5) Fill and drain valve remaining open

(6) Generation of, and reaction to, a BECO signal

A schematic describing the critical area between the main fuel supply and the turbopump inlets is shown in figure V-7. Figures V-8 to 11 show the prevalve assembly, the prevalve actuator and crank arms, the butterfly valve, and the "spider" in the staging disconnect, respectively.

<u>Prevalve</u>. - Examination of hardware after the fire indicated that the prevalve actuator was unlocked and the butterfly valve was near the closed position. Evaluation of data revealed there was no command given to close the prevalve. Flow tests indicated the maximum torque that fuel flow can exert on the butterfly valve was approximately 260 inch-pounds. With the prevalve in the locked open position the minimum torque required to cause system failure was de-

termined to be approximately 2000 inch-pounds. Additional tests indicated that it was possible to actuate the prevalve toward the open position, have the microswitches indicate the prevalve open, and not have the actuator in the locked open position. The flow tests also indicated that if the prevalve was greater than 4° from the full open position, the valve would slam shut in approximately 0.8 second. If this were the case for AC-5, the prevalve would have shut prior to lift-off.

If the prevalve failed on AC-5, it did not fail in the locked open position. The valve was either locked and became unlocked prior to failure, or was partially open but unlocked.

The AC-5 prevalve actuator was recovered, disassembled, and examined for failure analysis. Testing and examination of the components were compared with failure history reports on other actuators. The only significant anomaly was the presence of a foreign fluid behind the actuator piston. The fluid was analyzed and found to be a mixture of RP-1 fuel and "firex" water. Firex water was used to quench the flames after vehicle impact. The fluid is assumed to have entered the actuator following vehicle destruction.

Although the variation of closure time from actuator to actuator often can be considerable, the times for one particular actuator are usually consistent. The AC-5 actuator required 2.1 seconds to close during quad tanking and only required 0.9 second to close on X - 2 days. Both values are within specifications; however, the significant time reduction on X - 2 could have indicated that the actuator was not locked open. This also opens the possibility that the actuator was not locked open on launch day (unpublished GD/C data).

Possibilities of the prevalve closing are that some shock, pneumatic surge, or false electrical signal to the pneumatic ground control was sufficient to drive the valve closed. Tests and analysis have been conducted on the following to determine if a sufficient shock or surge existed on AC-5:

(1) Evaluate pressure pulses resulting from the unique configuration of the launcher flame buckets on Complex 36A combined with the effect of 165k booster engines. This was the first Atlas-Centaur launch using 165k boosters.

(2) Analyze launcher deflections for vehicle AC-5 and launch pad 36A. Determine spring and unloading effect of launcher on vehicle.

(3) Determine the possible effect of overpressurization of the launcher pneumatic system.

(4) Investigate electrical power transients to determine the effect on the prevalve electrical system.

(5) Install pneumatic purge box accelerometer instrumentation on a future Atlas vehicle flight. Evaluate data to determine the vibration levels in this area.

(6) Determine force necessary to separate a frozen rise off disconnect panel and the force necessary under normal separation.

(7) Evaluate the possibility of high pressure not venting from the pneumatic system at lift-off.

Analysis of the preceding areas have revealed no source considered adequate to drive the fuel prevalve from the locked open to the closed position.

Staging valve. - A schematic drawing of the staging valve and disconnect is shown in figure V-12. The main components of the valve are the housing, the spring loaded poppet, and the valve seat. The disconnect contains a "spider" member that supports the staging valve poppet through booster engine operation. The nominal dimension between the flange of the staging valve and the flange of the staging disconnect is 17.5±0.2 inches (see fig. V-12). This results in a nominal longitudinal separation of 1.5±0.2 inches between the poppet and its seat. At booster engine cutoff (BECO) the booster section of the Atlas separates from the remainder of the vehicle. At this time the staging disconnect pulls away from the poppet and the spring drives the poppet to its seat, terminating flow to the booster engines.

Closure of the staging valve can be accomplished by buckling of the spider member, buckling of the staging disconnect, failure of the main support, displacement of the booster structure, or combinations of these (see fig. V-12). Results of unpublished GD/C analysis have eliminated displacement of the booster structure alone as a possible failure mode. Investigations have been conducted to evaluate the remaining failure modes.

Flow tests have been performed to determine the load produced by the poppet on the spider at different settings of clearance between the poppet and its seat for a range of flow rates. Figure V-13 summarizes the results of this test. The figure demonstrates that the maximum allowable setting is in an area where a rapid change in poppet load results from a small increase in valve setting. The load increases sharply as a result of the effect of the poppet blocking the flow stream. At a flange-to-flange separation of 17.87 inches, the member began to yield; at a separation of 18.10 inches, the spider member and the staging disconnect housing buckled before rated flow was obtained. The buckled hardware was similar in appearance to that recovered following AC-5.

From the foregoing investigation it was concluded that an allowable flange-to-flange valve setting of up to 17.7 inches could be dangerous - particularly on the AC-5 launch where an abnormally high longitudinal vibration (see Section XI. VEHICLE DYNAMICS) may have resulted in catastrophic loading on the staging valve poppet.

Static load tests were conducted to determine the strength and deflection of the spider and of the staging disconnect. Figure V-13 also contains a plot of spider deflection as a function of load. The deflection of these members during operation would allow the poppet to near the seat and thus increase the poppet load exerted by flow. The spider member buckled at 2700 pounds of load, and the staging disconnect buckled at 6500 pounds. Although the static tests revealed the staging disconnect to be considerably stronger than the spider member, both members buckled during the flow tests. The staging disconnect could have buckled with the lower loads as the result of an eccentric loading following the buckling of the spider member.

During the AC-5 tanking test, fuel was drained from the main propellant tank by opening the prevalve and allowing the propellant to surge into the low pressure ducting. It was feared that the load created by the fuel may have been sufficient to overstress the main support strut shown in figure V-12. The yielding of this strut could then have been sufficient to allow the staging disconnect to move and the poppet to seat, thus terminating fuel flow to the engine. A test has been run duplicating the conditions on AC-5, however, and indicated that the force was well below the 18 000 pounds necessary to cause the support to yield.

Duct failure and fill and drain. - The low pressure ducting to the booster engines was recovered in the collapsed condition. Both the B-1 and B-2 fuel pump inlet pressures were maintained at less than 3.0 psia from 1.1 seconds until termination of flight. The pressure differential between the atmosphere and the ducting was more than adequate to cause the ducts to collapse. Analysis shows a critical buckling differential of 5.5 psi. However, the fact that the ducts were able to maintain vacuum condition until flight termination indicates that the system remained intact. This eliminates duct rupture and an open fuel fill and drain valve as AC-5 failure modes.

Duct blockage. - Hardware inspection of the pertinent areas uncovered no obstruction considered adequate to block fuel flow. It is highly doubtful that a foreign object could have so completely terminated flow as to result in the rapid pressure decay indicated in figure V-2.

False BECO. - A review of the flight films and analysis of data have revealed no thrust section explosion and no generation of a false BECO signal. No incorrect electrical or pneumatic connections have been discovered.

Corrective Action

Loss of the AC-5 vehicle soon after lift-off, the ensuing failure analysis, and associated test programs resulted in isolating the cause of the catastrophe to fuel starvation of the booster engines. A study of the fuel system indicated that malfunction of the prevalve pneumatic remote control actuators or the staging valve and disconnect could have caused fuel starvation of the engines. Hardware and procedural changes to future vehicles are detailed below.

Booster prevalve actuation. - Of all the possible failure modes considered, none has been clearly identified as the prime cause of this malfunction. Since the Atlas vehicle is the booster stage of the Atlas-Agena system, flight schedules dictated an interim modification. For the Atlas-Centaur vehicle it was decided to eliminate remote control actuation and revert to manual operation and locking of the prevalve. The various modifications are detailed in the following paragraphs.

In order to avoid impacting Atlas-Agena missions, an interim fix was decided on. This modification consists of attaching a wedge to the actuator housing that physically holds the prevalve in the open position. The installation details of the wedge are shown in figure V-14. The wedge is installed during countdown after requirements for remote pneumatic power operation have been fulfilled. All pneumatic lines are disconnected at this time. From figure V-14 it can be seen that, with the torque induced by fuel flow, loads on the prevalve butterfly try to turn the bell-crank in the direction indicated. To accomplish this motion the actuator must pivot about the trunion. The rotation about the trunion is prevented by the presence of the wedge.

Permanent fix: Design of a permanent modification of the prevalve actuator for the Atlas-Centaur consisted of substituting a manual handle on the butterfly shaft to replace the pneumatic actuator. The manual handle has the capability of being locked in the prevalve open and closed positions by two bolts either of which is capable of reacting fuel flow loads induced by the prevalve butterfly. Figure V-15 shows the details of this modification. In order to obviate similar failure of the sustainer fuel prevalve, remote pneumatic actuation on this valve was also deleted. This was replaced by an Atlas series "E" manually operated prevalve. An improved locking device is to be incorporated to assure positive locking in the open position by means of a clamping bracket. This device is illustrated in figure V-16. To establish the load-carrying capability of the various elements of the prevalve system, a static load test was accomplished. The results of this test are shown in figure V-17. The load was applied to the butterfly shaft with a moment arm of 24 inches, subjecting the shaft to a static torque. This torsion was transmitted to

(1) The AC-5 actuator, which was in the prevalve open mode, and

(2) The manual actuator design to be used on AC-6 and on vehicles, also in the prevalve open mode

In the first case, failure of the bell-crank occurred at a torque of 2064 inch-pounds, establishing the weakest element of the system. Since the bell-crank is deleted in the modification, it was established that the system is capable of at least reaching a torque of over 2064 inch-pounds. The manual actuation design (aluminum handle) showed no failure at a torque value of 4320 inch-pounds. This compares with a maximum value of 260 inch-pounds of torque induced by fuel flow based on a flow rate for 165k booster engines.

Thrust section access door: This modification provides for convenient access for manual operation of the prevalves. It consists of an 8- by 6-inch door cut in the thrust section, opposite the location of the prevalves. The effectivity of this modification is Atlas 194D (AC-9) vehicle. It was decided not to incorporate this modification on the next flight vehicle (AC-6) because of the associated schedule impact.

Procedure: As a result of the deletion of fuel prevalve actuator, the countdown procedure has been modified by dropping those items in the sequence associated with the remote actuation of the prevalve.

<u>Booster staging valve</u>. - To preclude excessive loading on the poppet valve and spider on the AC-6 vehicle, it has been decided to decrease the nominal valve setting dimension from 17.5 to 17.25 inches; thus moving to the left of the poppet loading curve shown in figure V-13. This decrease in the valve setting is to be accomplished by introducing a 0.25-inch shim between the aft

flange of the staging disconnect and the forward flange of the downstream fuel ducting.

In order to confirm the position of the poppet in relation to its seat on the flight vehicle, it has been decided to X-ray the installation. On the AC-6 vehicle, this will be done on the launch pad.

Booster fuel system low pressure ducting. - Unusual loads induced in the booster low pressure ducting during the tanking test are suspected of having weakened the support structure sufficiently to have caused AC-5 failure. The sequence of events that led to the suspected over-stressing were:

(1) Closure of the fuel prevalve

(2) Draining of fuel from the low pressure ducting through the fill and drain valve (This resulted in a partial vacuum in the ducting noted during the tanking test.)

(3) Opening of the prevalve permitting fuel to rush into the ducting under existing partial vacuum conditions

The on-rush of fuel may have created a transient dynamic load condition that overstressed the ducting and support structure. Flow tests duplicating the preceding conditions show that induced loads are quite low and well within the capability of the support structure and ducting. However, it has been decided to eliminate this source of load on future vehicles. This will be accomplished by avoiding the sequence of events previously detailed. Test site personnel have been instructed accordingly.

TABLE V-I. - COMPARISON OF PREDICTED AND CALCULATED ATLAS SYSTEM PROPULSION VALUES AT LIFT-OFF

Parameter	Units	Calculated or data value at lift-off	Predicted or nominal value
Booster thrust	lb force	324 220	326 190
Sustainer thrust	lb force	56 260	56 240
Vernier thrust	lb force	1 720	1 710
Total thrust	lb force	382 460	384 140
Booster specific impulse	$\frac{\text{lb force-sec}}{\text{lb mass}}$	252.1	252.0
Sustainer (plus vernier) specific impulse	$\frac{\text{lb force-sec}}{\text{lb mass}}$	213.4	211.6
B-1 chamber pressure	psia	565	580
B-2 chamber pressure	psia	568	575
Sustainer chamber pressure	psia	715	706
B-1 FPIP	psia	61.5	69.9
B-2 FPIP	psia	64.0	69.9
Sustainer FPIP	psia	69.0	72.0
B-1 pump speed	rpm	638	6 306
B-2 pump speed	rpm	612	6 256
Sustainer pump speed	rpm	1 012	10 098
Booster gas generator chamber pressure	psia	525	526
Sustainer gas generator discharge pressure	psia	575	No data
B-1 LOX pump inlet pressure	psia	52.0	54.0
B-2 LOX pump inlet pressure	psia	52.0	54.0
Sustainer LOX pump inlet pressure	psia	59.0	58.6

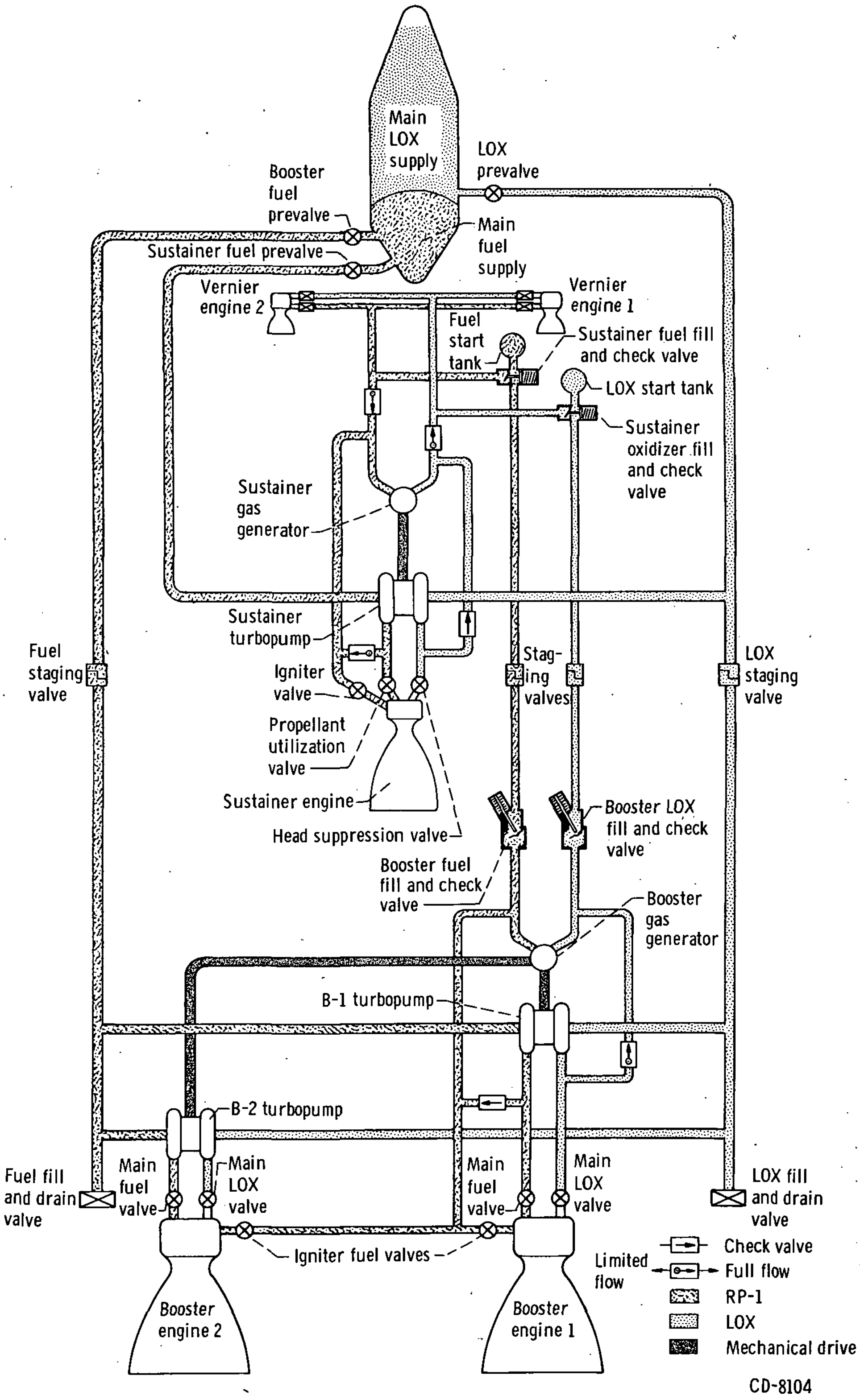

Figure V-1. - Propulsion system schematic.

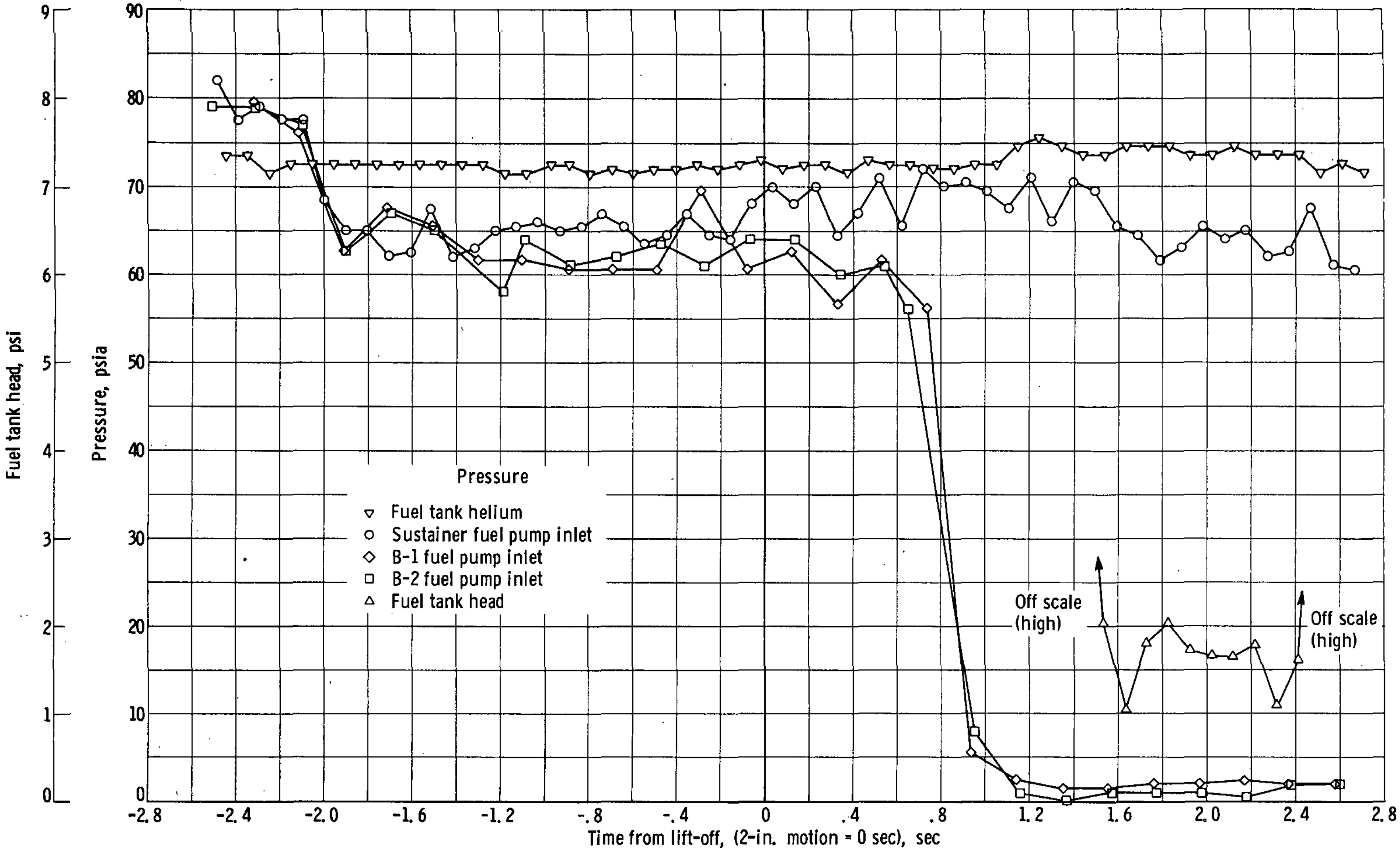

Figure V-2. - Atlas fuel pump inlet and tank pressures as function of time from AC-5 flight data.

CONFIDENTIAL

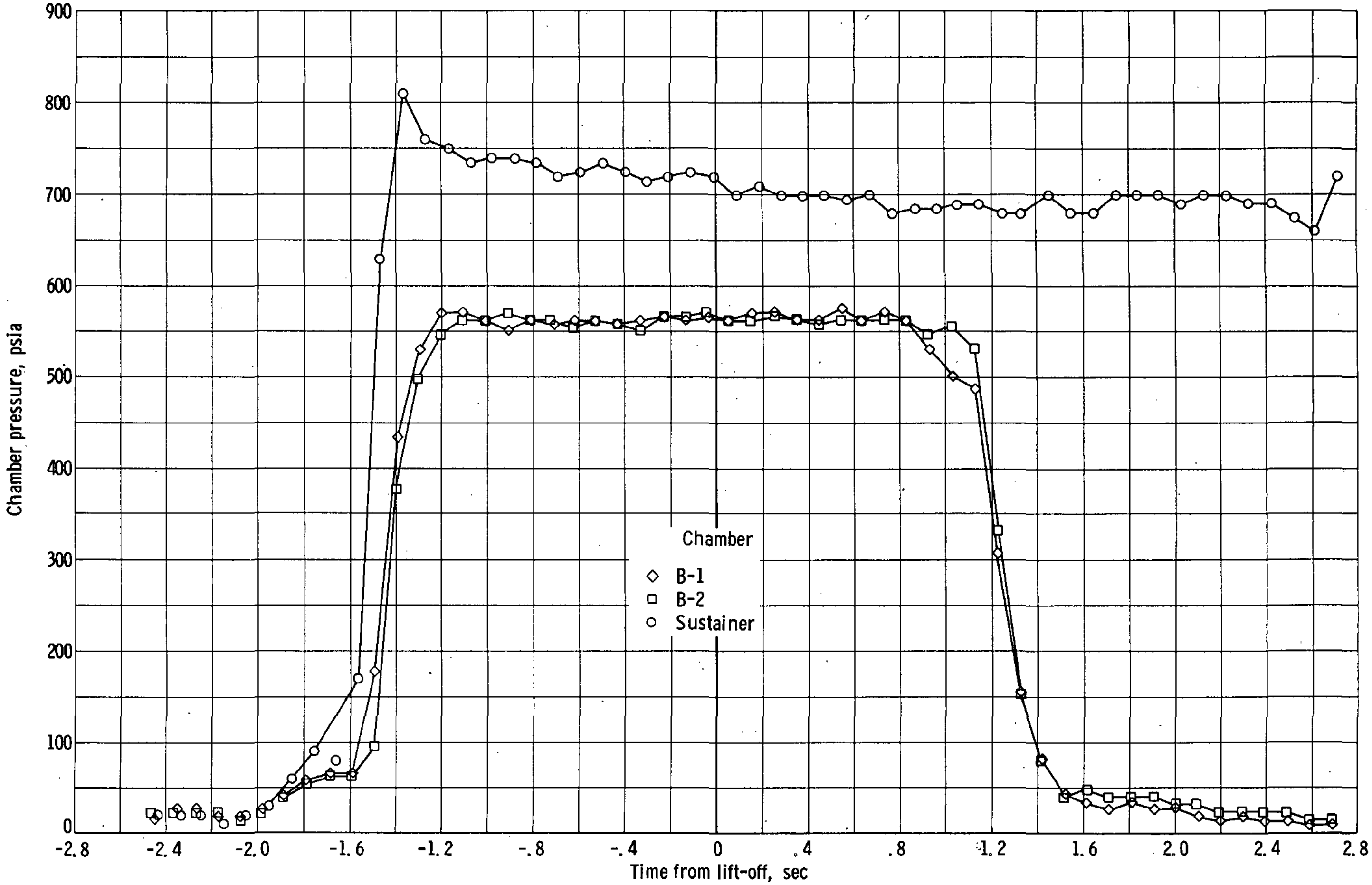

Figure V-3. - Atlas engine chamber pressures for AC-5 flight.

CONFIDENTIAL

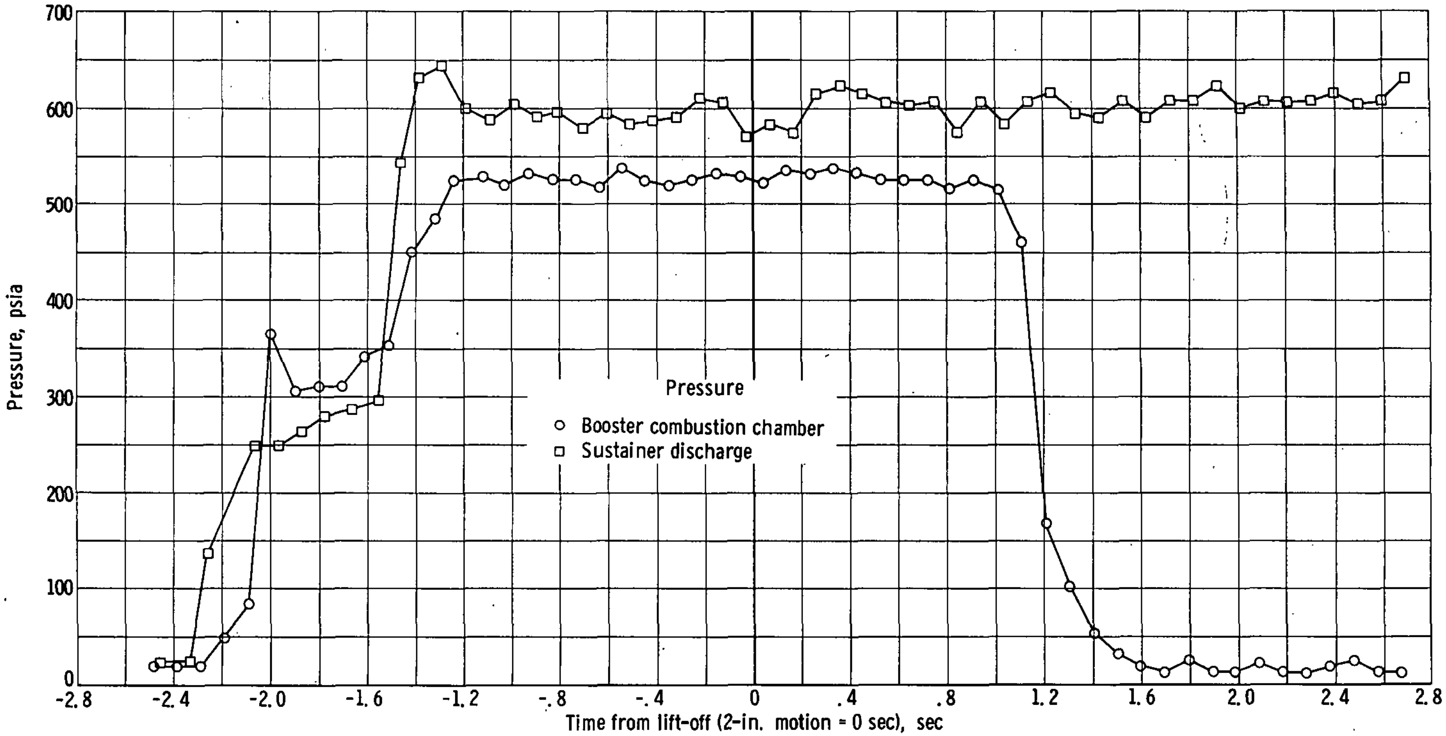

Figure V-4. - Atlas gas generator pressure for AC-5 flight.

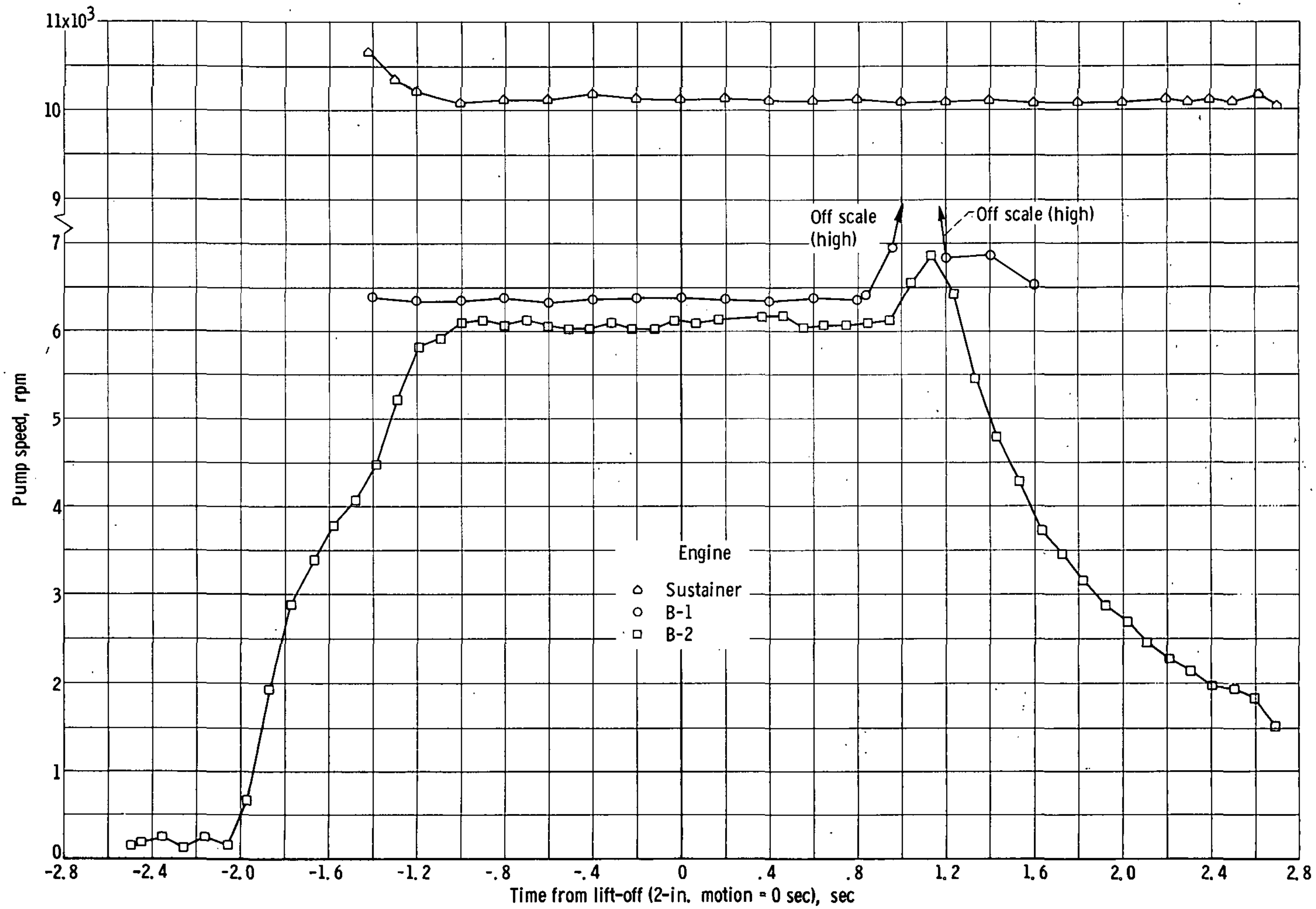

Figure V-5. - Atlas engine rpm as function of time for AC-5 flight.

[redacted]

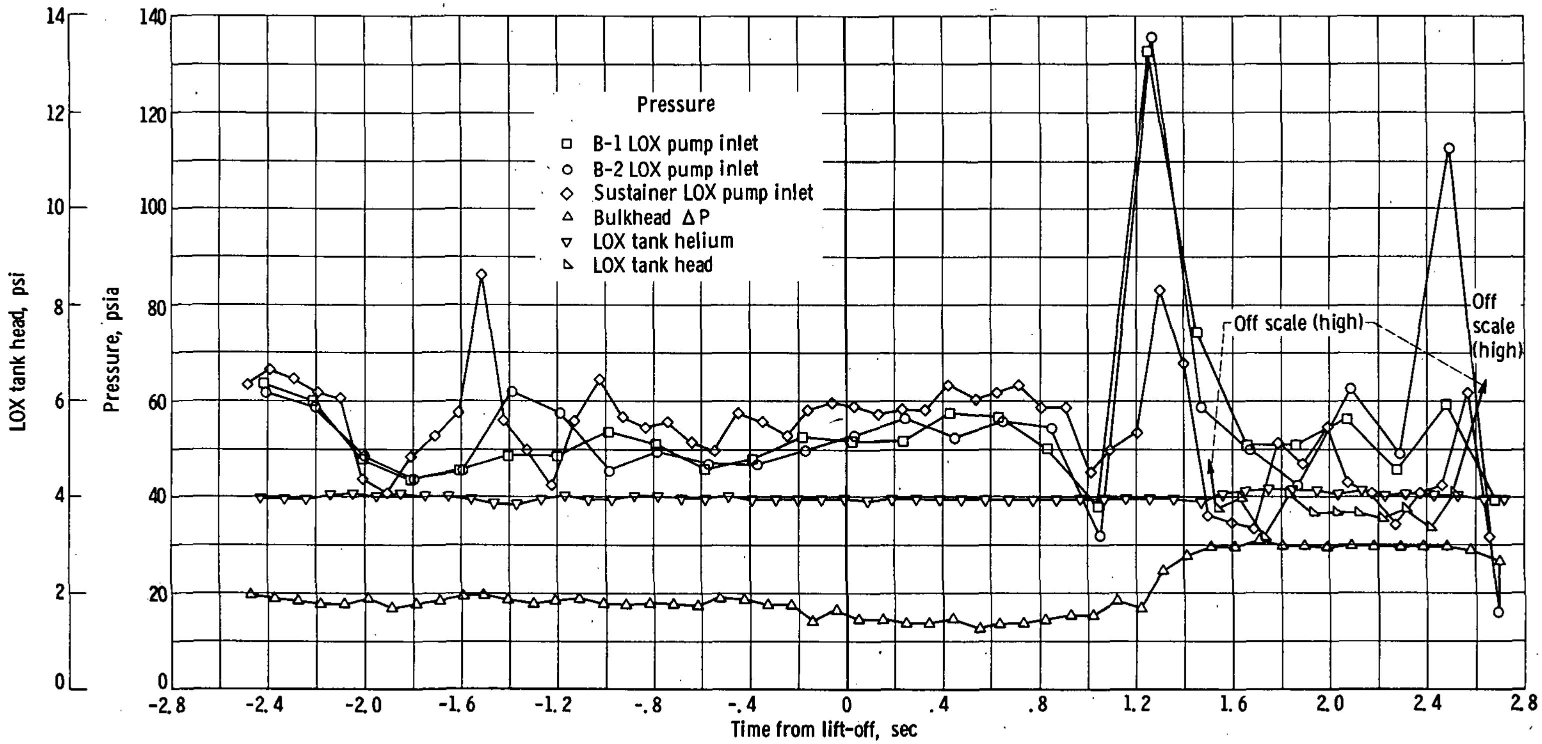

Figure V-6. - AC-5 flight Atlas engine LOX pump inlet pressures bulkhead ΔP.

[redacted]

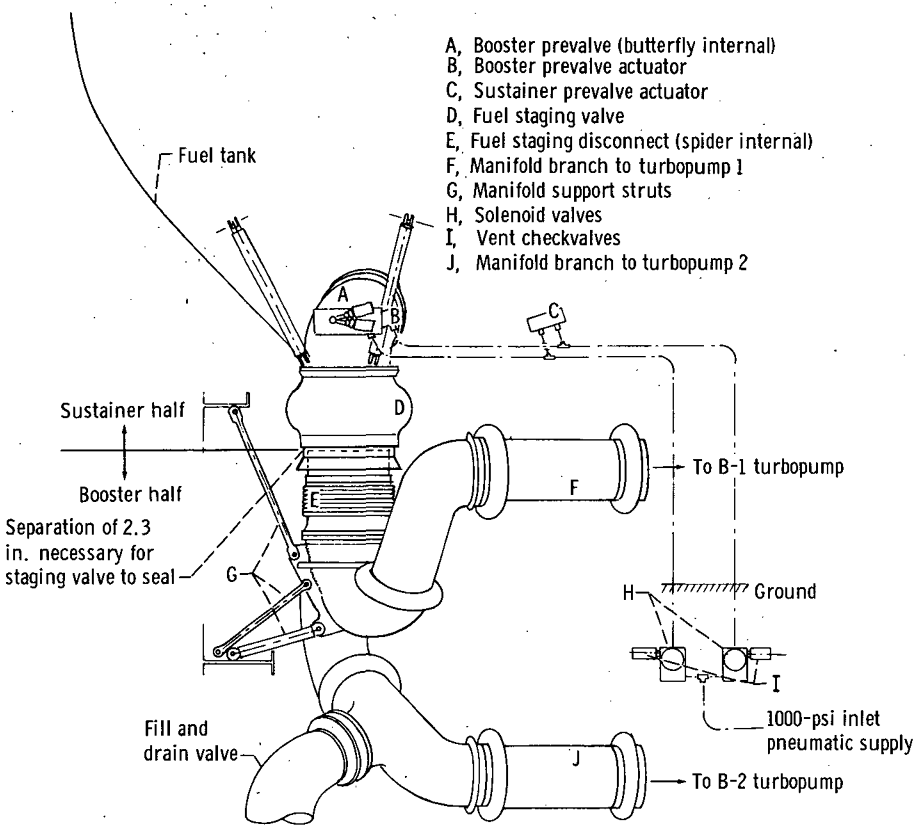

Figure V-7. - Fuel system low pressure ducting configuration between main fuel supply and turbopump inlets.

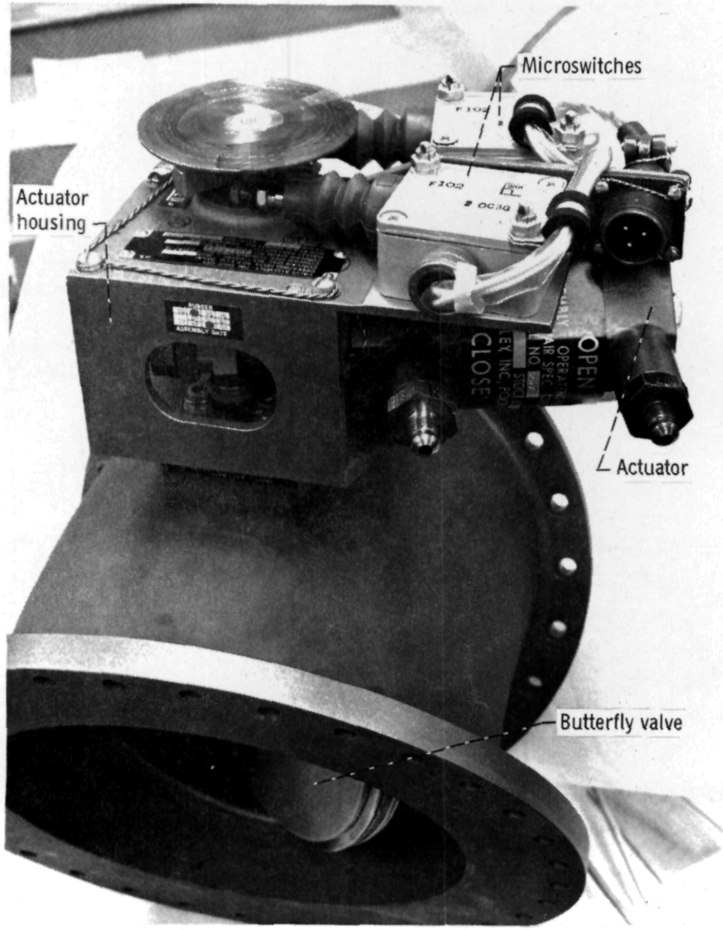

Figure V-8. - Booster fuel prevalve assembly. (Disk in upper left portion of figure installed for testing purposes only).

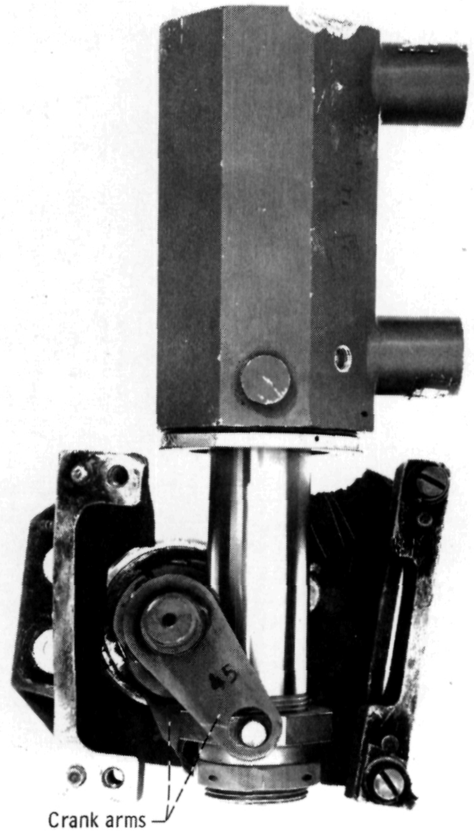

Figure V-9. - Recovered AC-5 actuator and crank arm assembly. (Actuator in the open position).

CONFIDENTIAL

CONFIDENTIAL

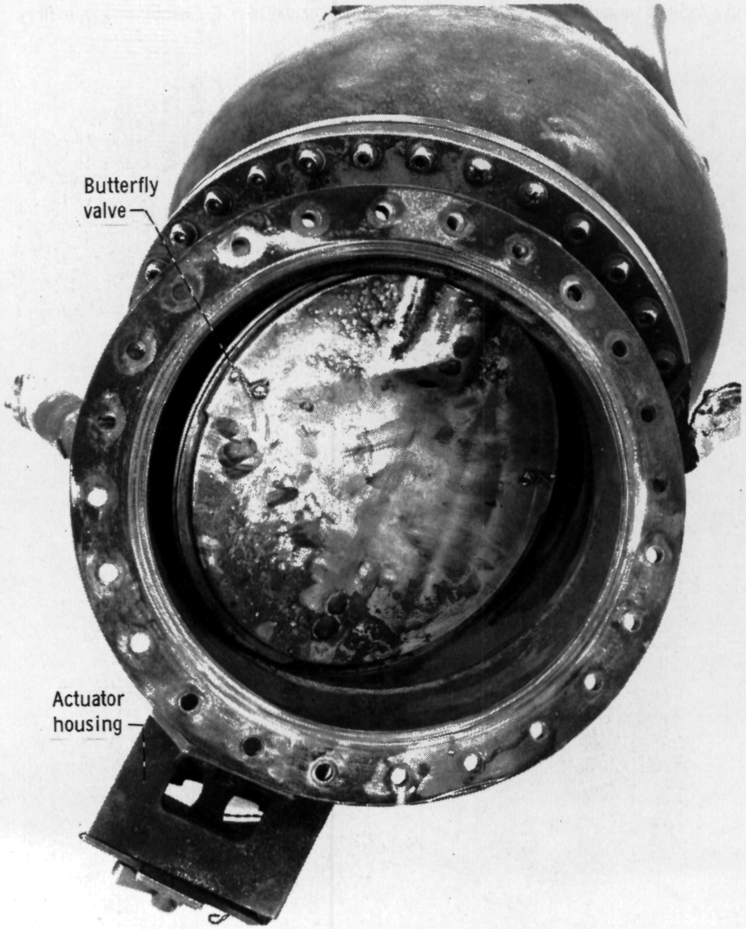

Figure V-10. - Recovered AC-5 booster fuel prevalve. View looking into booster fuel prevalve (still assembled to staging valve) showing butterfly position.

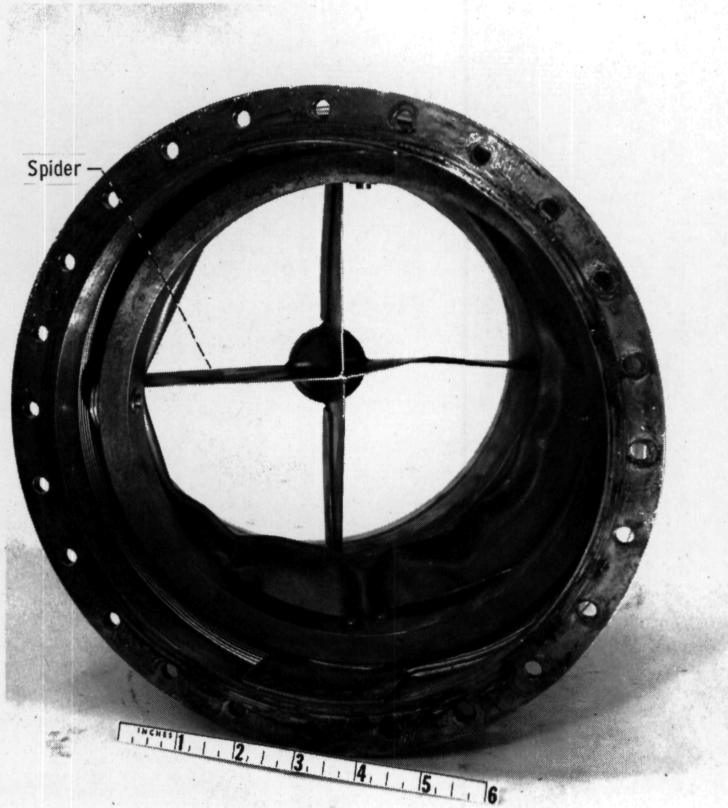

Figure V-II. - Rear view of recovered staging disconnect showing spider still intact.

CONFIDENTIAL

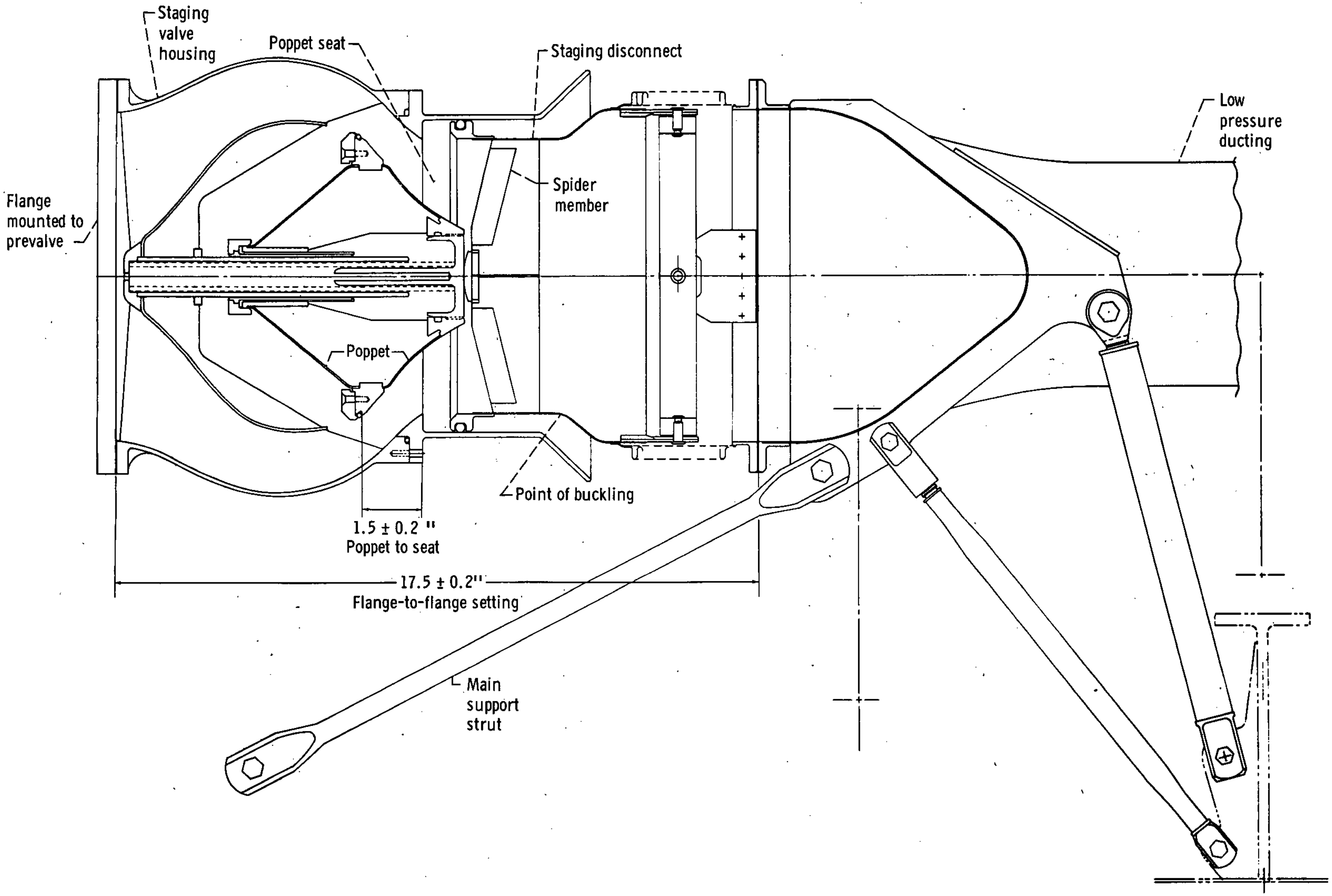

Figure V-12. - Schematic drawing of Atlas Fuel staging valve and staging disconnect.

CONFIDENTIAL

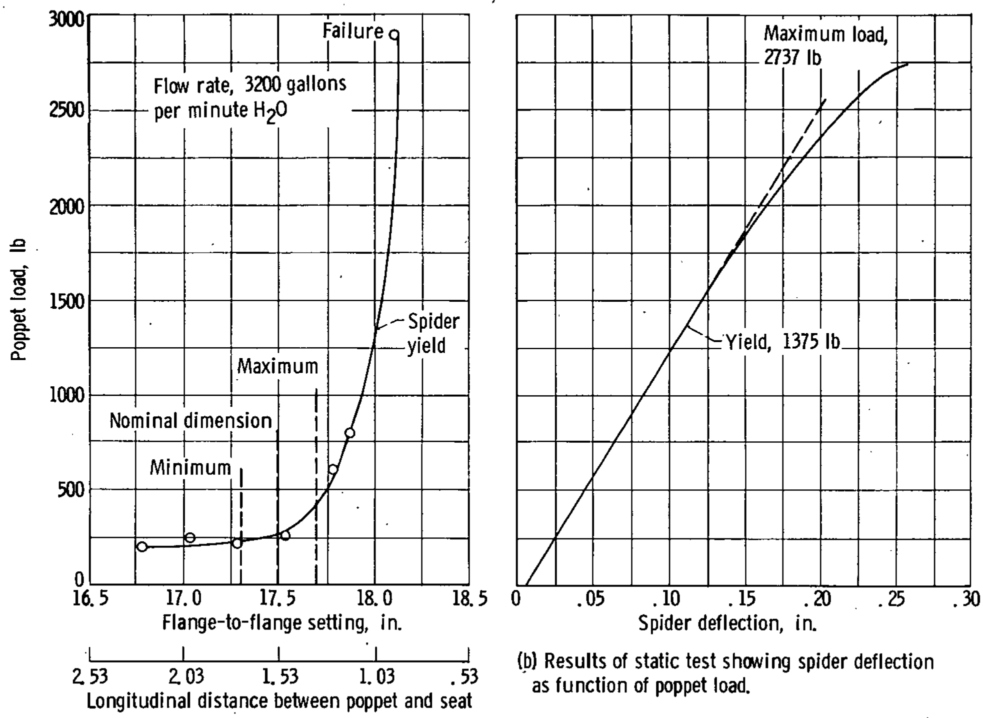

(a) Results of flow tests showing poppet load as function of valve setting.

(b) Results of static test showing spider deflection as function of poppet load.

Figure V-13. - Results of flow and static tests.

[redacted]

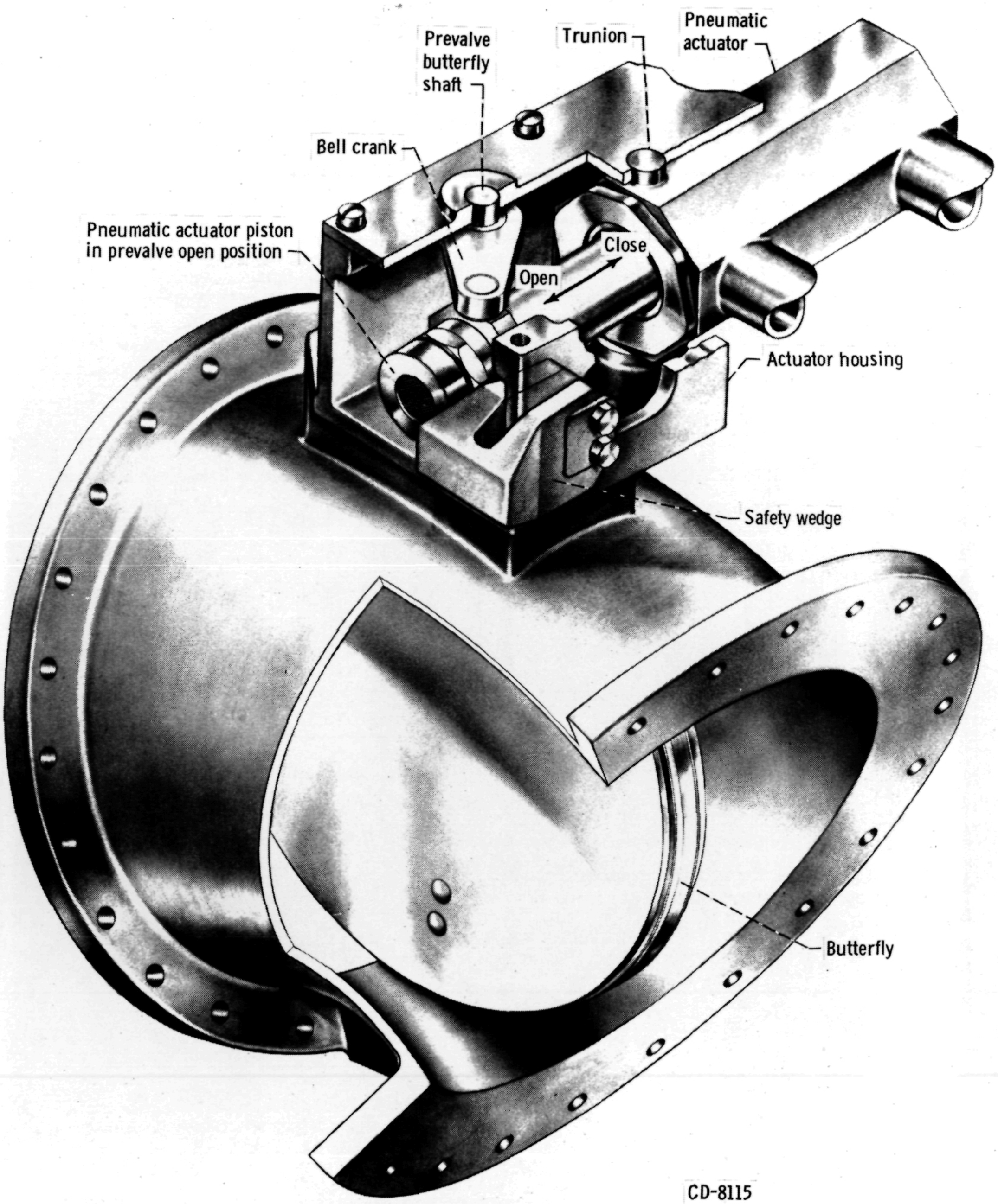

Figure V-14. - Interim fix safety-wedge design to prevent inadvertent closure of fuel prevalve.

[redacted]

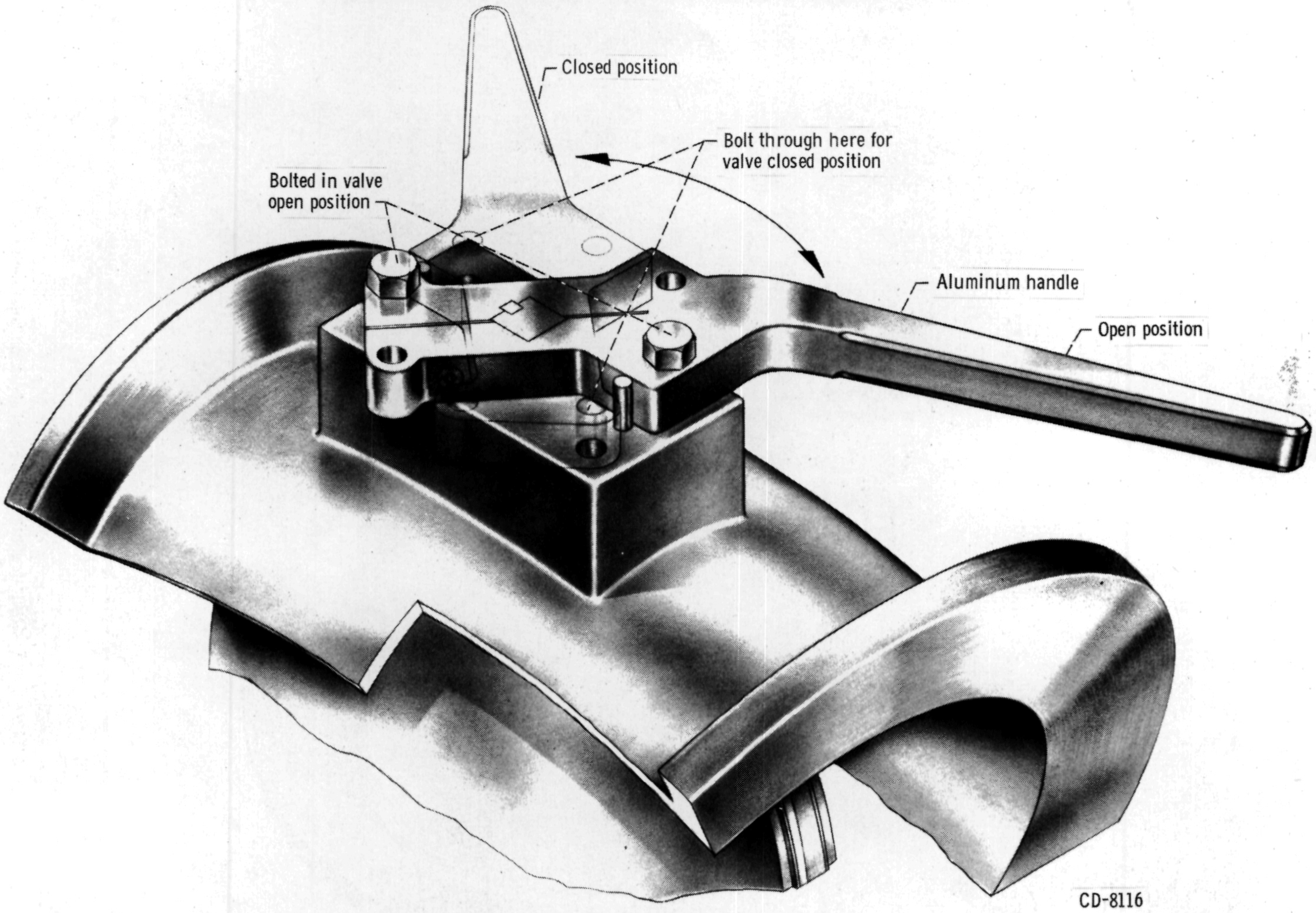

Figure V-15. - Schematic drawing of booster prevalve manual actuator aluminum (6061-T6) handle.

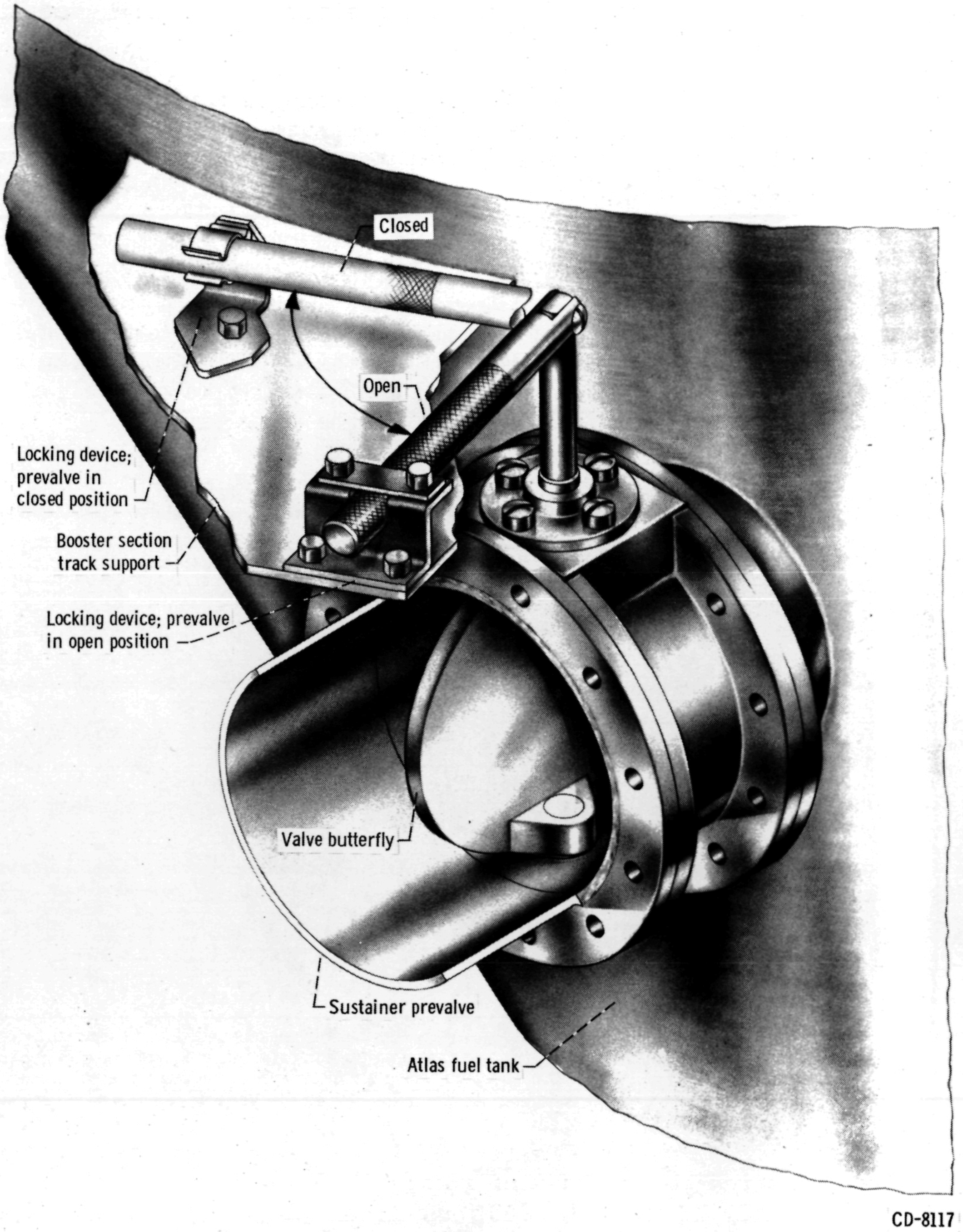

Figure V-16. - Sustainer fuel prevalve manual actuation and locking device.

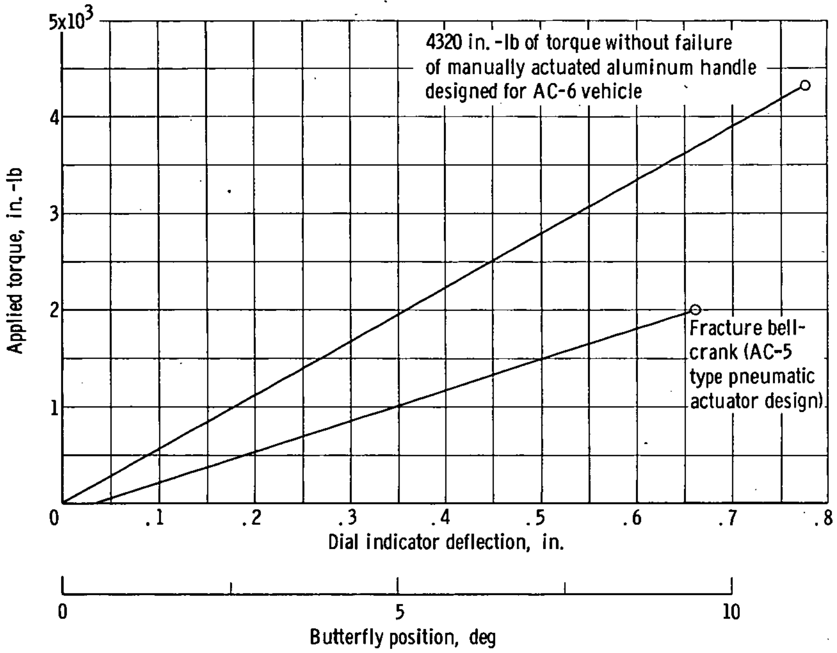

Figure V-17. - Test results of Atlas fuel prevalve and actuator static test.

VI. ATLAS SYSTEMS PERFORMANCE

Summary

Other than the propulsion system, all the Atlas systems functioned normally from their prelaunch condition to vehicle failure. The hydraulic system maintained proper pressure level until T + 2.8 seconds at which time the vehicle was in a general state of disintegration. The electrical and telemetry system operation was satisfactory and within specification. The flight control system maintained vehicle stability throughout. The pitch, yaw, and roll displacements were all less than 0.7° from their lift-off values. The tank pressurization program resulting from introduction of 165k engines was satisfactorily accomplished by the pneumatic system. A return to LOX tank full flight pressures could not be demonstrated because of early loss of the vehicle.

Atlas Hydraulic System

The booster and sustainer hydraulic systems are totally independent and are powered by two variable-displacement pressure-compensated pumps. The two hydraulic pumps are driven by the sustainer and B-2 turbopumps with each system delivering 3000 psi for engine gimbal requirements during flight.

Prior to main engine start and the associated hydraulic power changeover, the two systems are supplied by a ground unit at 2000 psi. The changeover from 2000 to 3000 psi at main engine start is sensed by airborne instrumentation and is a launch release ladder requirement.

Booster and sustainer hydraulic systems reacted normally through the start transient and on to T + 2.8 seconds (see fig. VI-1). Power changeover from ground to airborne pressures started at T - 2 seconds and was complete at T - 1.5 seconds. The ground pressures reflected to the airborne transducers were 1900 psi for the booster and 1950 psi for the sustainer. The pressures after main engine start were 3000 psi on the booster and sustainer systems except for the normal pressure transients expected at start and after vehicle lift-off. Loss of pressure occurred at T + 2.8 seconds, sometime during vehicle disintegration. The system functioned normally throughout, and no anomalies were noted.

Atlas Electrical and Instrumentation System

Atlas electrical power system. - The booster electrical power sources, distribution, and transfer systems operated satisfactorily. All electrical functions and levels were within specifications and adequately supported the flight from countdown to vehicle destruct. The a-c power was supplied by a 400-cycle 3-phase 115-volt rotary inverter. This was the first Atlas launch vehicle to use a manually activated battery, and the first Centaur booster to use a 19-cell battery.

The booster vehicle battery voltage exhibited a voltage transient drop on power changeover. The voltage reached a minimum value of 26.3 volts. The steady-state voltage was 27.9 volts and remained constant. The minimum allowable battery voltage was 26.5 volts.

Figure VI-2 illustrates the inverter frequency and voltage and the missile system d-c input. The inverter frequency after initial dip to 399.5 cps at power changeover remained constant at 402.1 cps. The inverter voltage remained constant at 115.4 volts from power changeover until vehicle destruct.

The booster vehicle electrical system schematic is shown in figure VI-3.

Atlas telemetry and instrumentation system. - One telemetry radiofrequency link was established to telemeter 109 Atlas measurements and three angle-of-attack measurements. The telemetry package provided between 4 and 10 watts to dual antennas. Minimum radiated power requirements from the two antennas are 1 watt from pod 1 antenna and 0.8 watt from pod 2 antenna. Prelaunch measurements indicated 2.5 and 1.9 watts for pod 1 and pod 2 antennas, respectively.

Telemetry and instrumentation system performance was satisfactory. Signal strength was adequate and no transducer failures were reported.

Atlas range safety command system. - Dual receivers were used on the AC-5 boost vehicle. Normal operation of receiver 1 was confirmed by the receiver automatic gain control (AGC) measurement (AD 7V). Figure VI-2(c) shows the receiver AGC level at 457 microvolts prior to lift-off and increasing to 833 microvolts at T + 2 seconds. Minimum required AGC level for command destruct is 5 microvolts. Receiver 2 AGC was not telemetered.

Atlas Pneumatic System

Operation of the airborne pneumatic system was satisfactory. All pressurization and control functions were properly performed during the countdown and powered flight.

Tank pressures. - LOX and fuel tank ullage pressures were satisfactorily maintained by the airborne pneumatic system subsequent to changeover from the ground pressurization unit. The programed pressurization system for the LOX tank demonstrated proper operation through to vehicle destruction; this system was programed to terminate at T + 20 seconds. A transient minimum pressure difference across the intermediate bulkhead of 11.9 psid was recorded 1/2 second after lift-off.

Controls pressurization. - The controls and staging bottles were adequately pressurized to support pneumatic control functions. No further evaluation of this system can be conducted because of vehicle destruction.

Helium storage. - The liquid-nitrogen - helium loading system ground equipment operated satisfactorily by loading helium aboard the vehicle to the prescribed pressure and chilling it to the required temperature.

Atlas Flight Control System

Telemetry indicated no unusual vehicle transients or shocks as observed from rate and displacement gyro data prior to the loss of booster thrust. The operation of the Atlas flight control system was normal.

Flight control system telemetry data received is shown in figures VI-4 to 8. Rate gyro data (fig. VI-4) show normal characteristics during the thrust build-up period. Prior to the loss of booster thrust, vehicle lift-off was typical of previous Atlas-Centaur launches. A lift-off roll transient started at 0.92 second resulting in a maximum roll rate of 2.0 degrees per second (fig. VI-4) at T + 1.1 seconds and a maximum roll displacement of 0.5 degree (fig. VI-5) at T + 1.3 seconds. On the recovery maneuver, the roll rate reached 2.5 degrees per second. A large roll rate overshoot occurred at T + 1.27 seconds and probably was caused by the decaying of booster thrust. At this time booster thrust was less than 10 percent of its nominal value when the peak roll rate was reached.

Autopilot activation occurred at approximately T + 0.9 second (42-in. motion). Engine displacements shown in figures VI-6 to 8 demonstrated proper response to the respective rate and displacement gyro outputs. Figure VI-9 shows the polarity conventions defining positive directions of pitch, yaw, and roll. Booster, sustainer, and vernier engine deflections are shown as negative in figures VI-6 to 8, when correcting for positive pitch, yaw, or roll dispersions.

The loss of booster thrust left the vehicle with no yaw control, but only vernier pitch/roll control. Vehicle attitude errors prior to the time the vehicle returned to its initial lift-off position, as indicated by displacement gyro outputs, were 0.7 degree in pitch, 0.4 degree in yaw, and 0.2 degree in roll at T + 2.77 seconds.

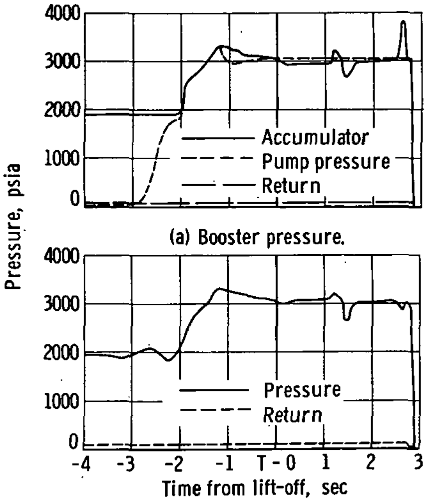

(a) Booster pressure.

(b) Sustainer pressure.

Figure VI-1. - Atlas hydraulic data (AC-5).

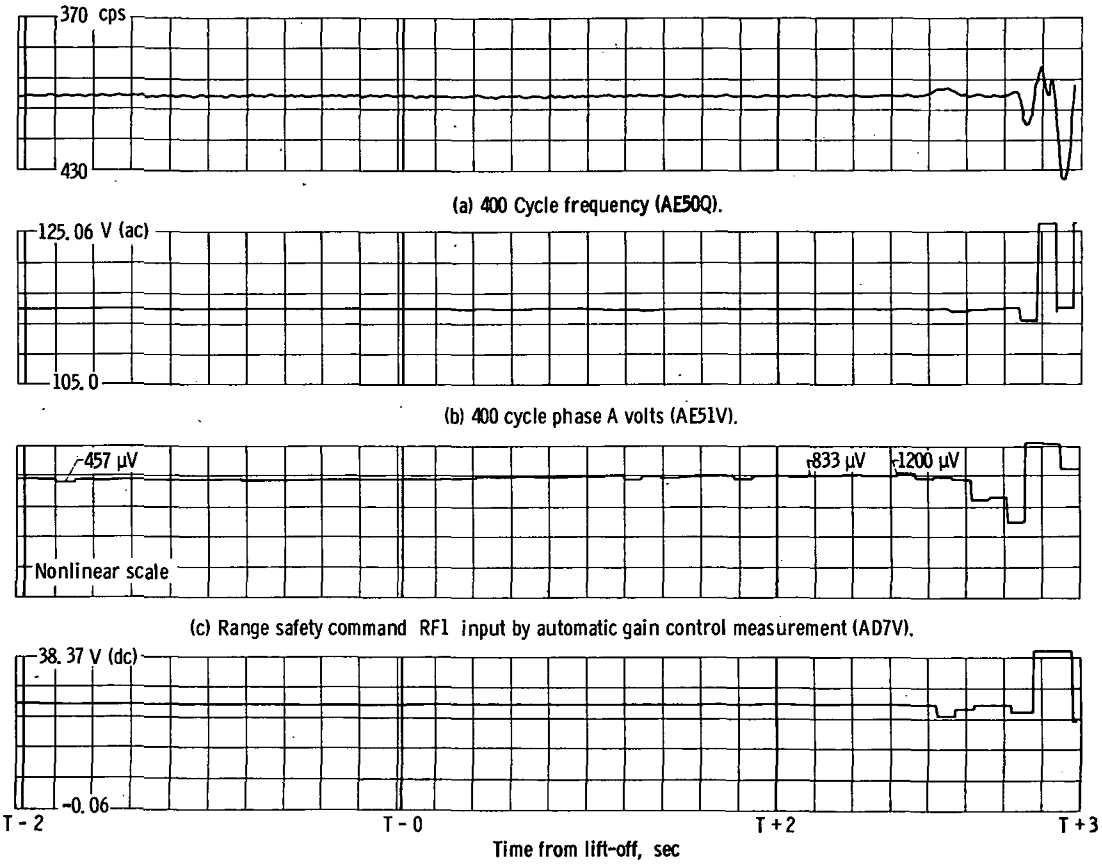

(a) 400 Cycle frequency (AE50Q).

(b) 400 cycle phase A volts (AE51V).

(c) Range safety command RF1 input by automatic gain control measurement (AD7V).

(d) Missile system input (AE28V).

Figure VI-2. - Booster electrical and range safety measurements.

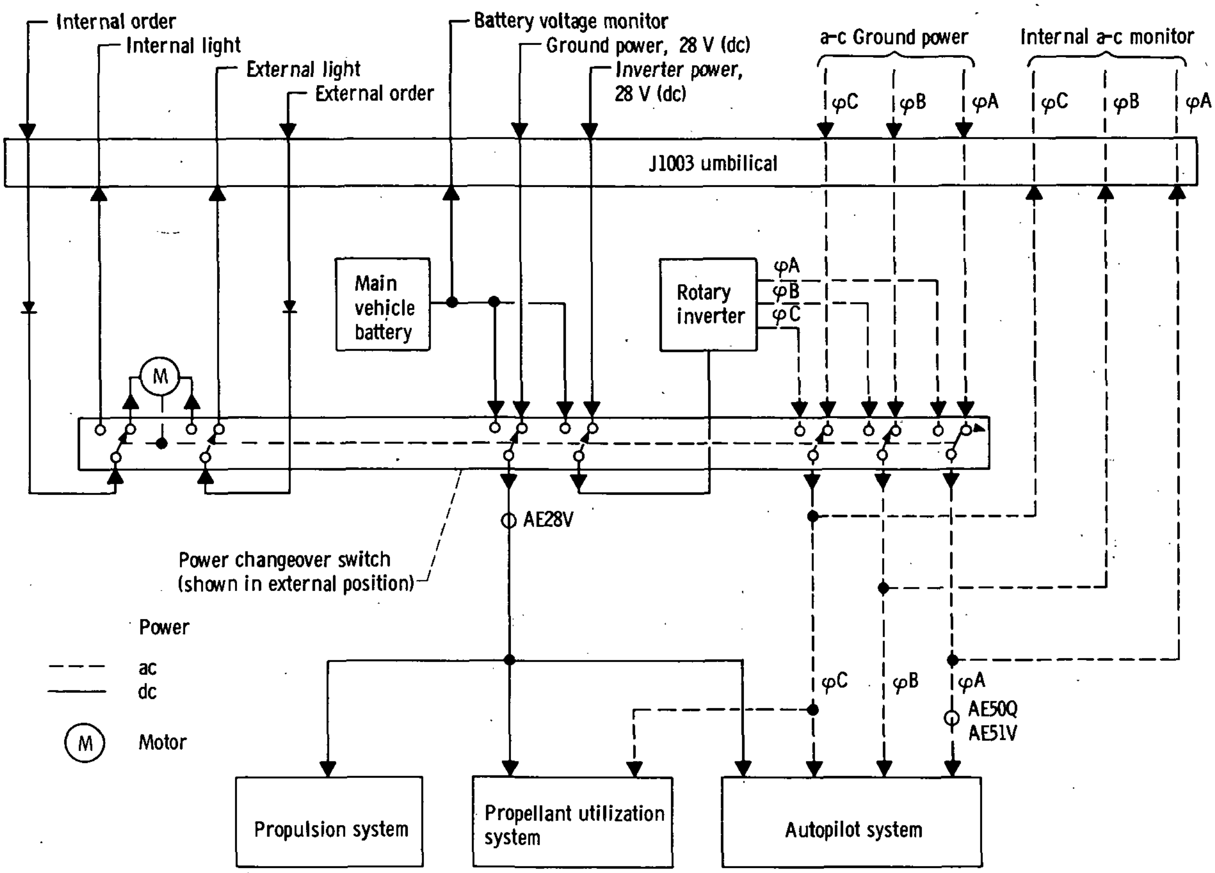

Figure VI-3. - Atlas electrical system.

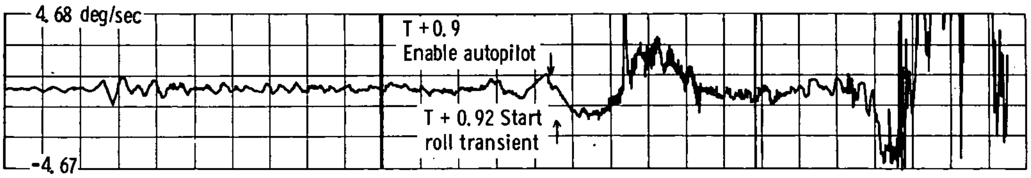

(a) Roll rate gyro signal (AS52R).

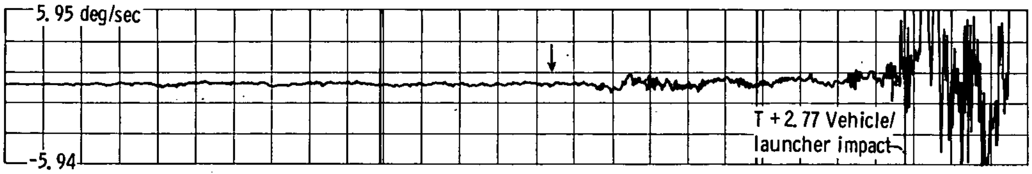

(b) Yaw rate gyro signal (AS54R).

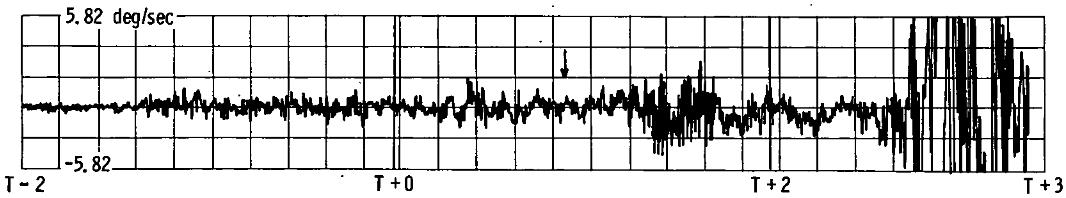

(c) Pitch rate gyro signal (AS53R).

Figure VI-4. - AC-5 Atlas rate gyro telemetry.

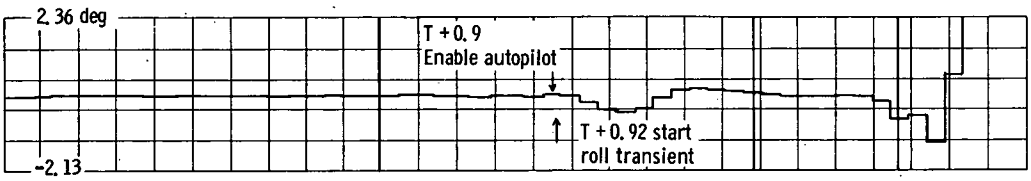

(a) Roll displacement gyro signal (AS61D).

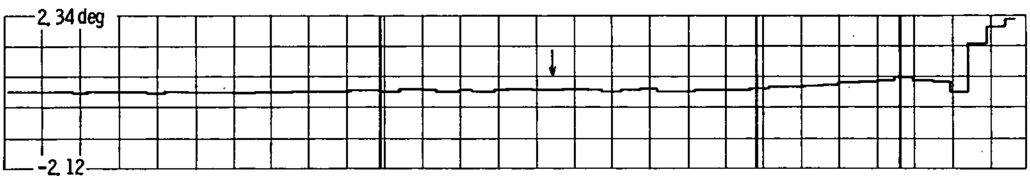

(b) Yaw displacement gyro signal (AS63D).

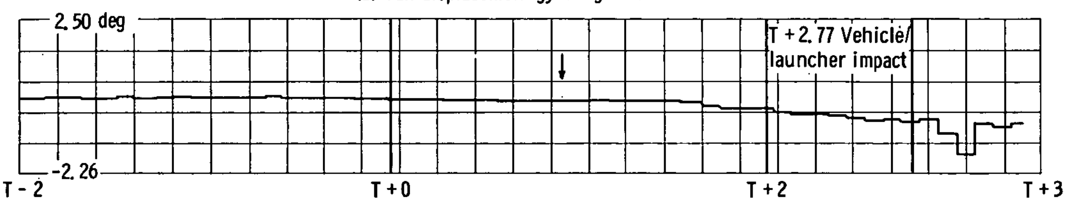

(c) Pitch displacement gyro signal (AS62D).

Figure VI-5. - AC-5 Atlas displacement gyro telemetry.

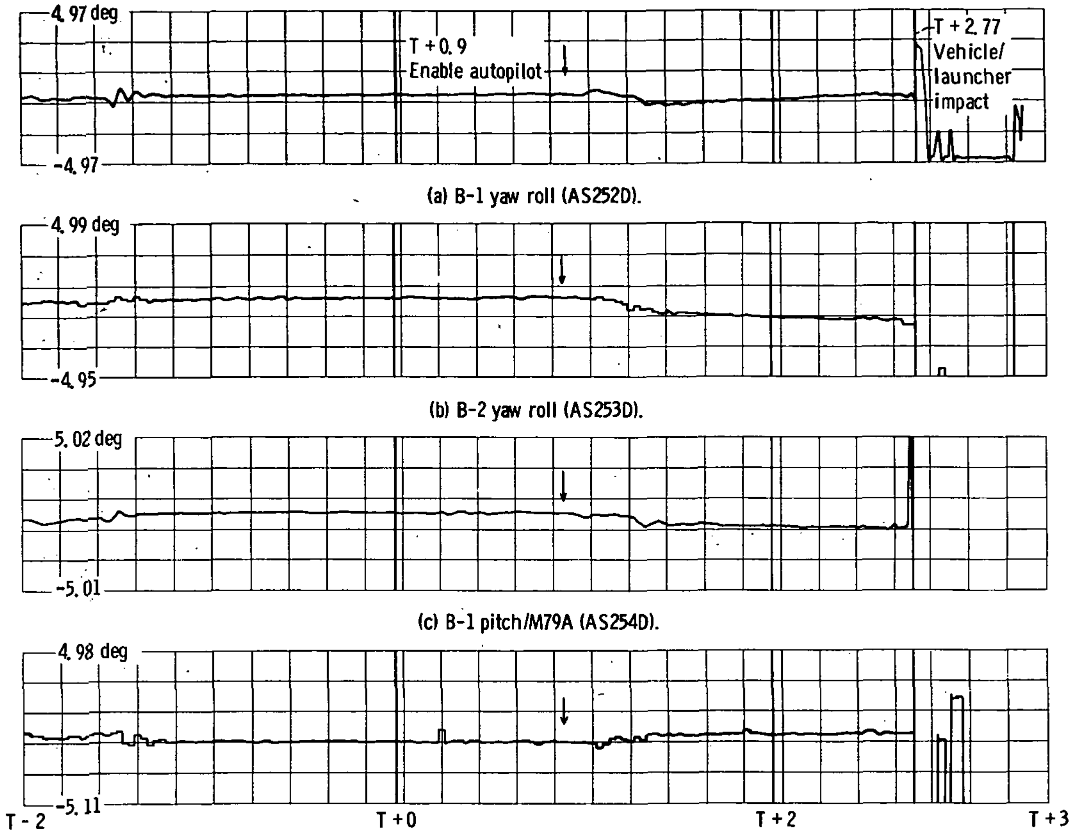

(a) B-1 yaw roll (AS252D).

(b) B-2 yaw roll (AS253D).

(c) B-1 pitch/M79A (AS254D).

(d) B-2 pitch (AS255D).

Figure VI-6. - AC-5 Atlas booster engine displacement.

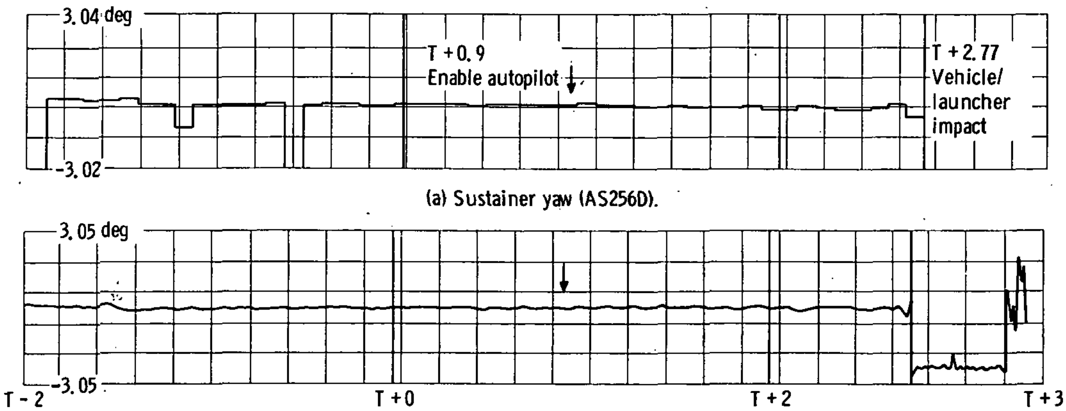

(a) Sustainer yaw (AS256D).

(b) Sustainer pitch (AS257D).

Figure VI-7. - AC-5 Atlas sustainer engine displacement.

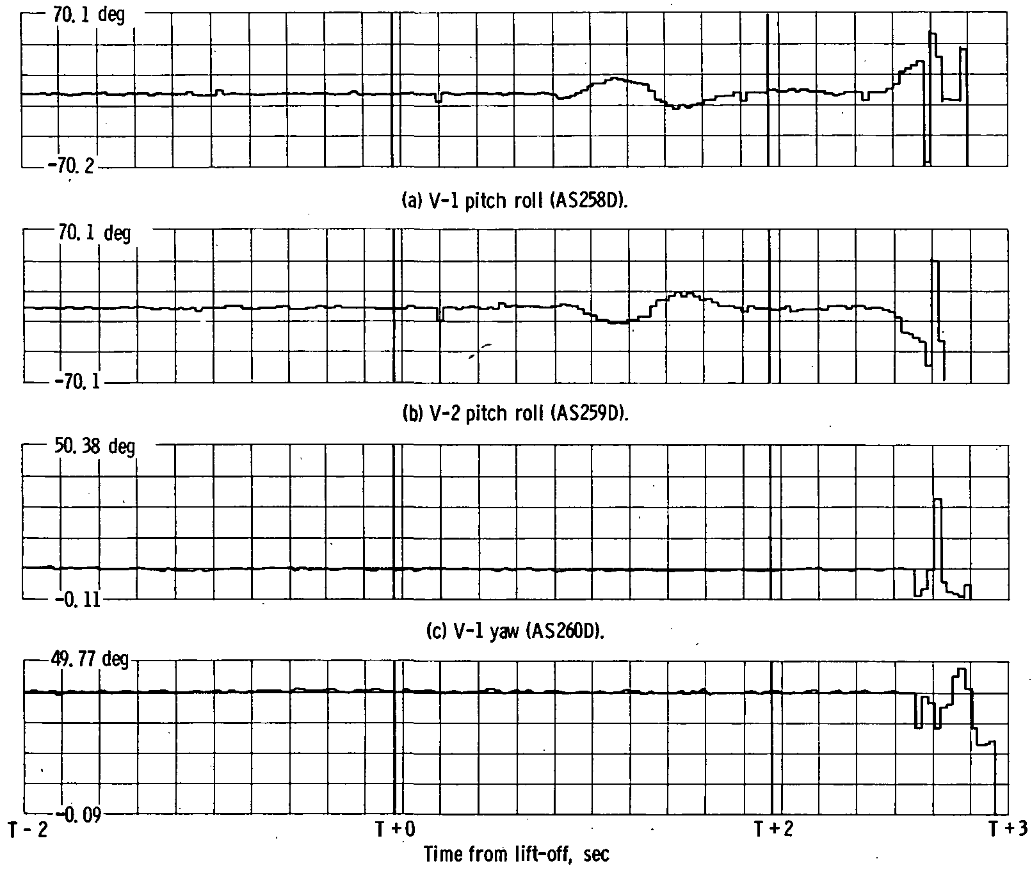

(a) V-1 pitch roll (AS258D).

(b) V-2 pitch roll (AS259D).

(c) V-1 yaw (AS260D).

(d) V-2 yaw (AS261 D).

Figure VI-8. - AC-5 Atlas vernier engine displacement.

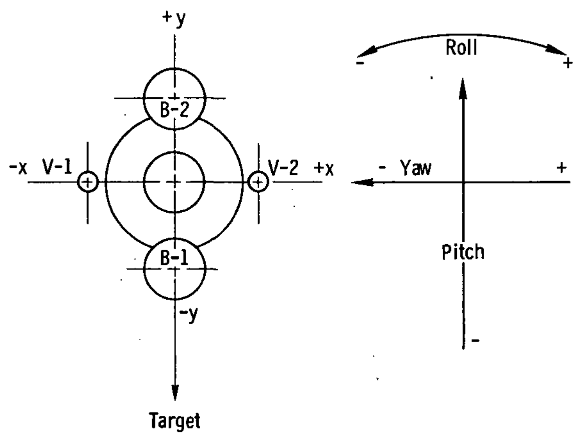

Figure VI-9. - Atlas polarity convention for flight control system.

[redacted]

VII. GUIDANCE

Summary

Investigations after the aborted AC-5 launch have disclosed that, in addition to the Atlas propellant feed system failure, a serious malfunction also occurred in the power control circuitry of the navigation computer unit of the missile guidance set. The failure resulted in the computer going to essentially a nonoperative mode at lift-off. The computer malfunction was in no way related to the Atlas propulsion problem. An interim configuration for the computer has been established for use on AC-6 and AC-7 that eliminates unused parts, thoroughly tests the power control circuitry, and eliminates redundant voltage carrying leads from the computer, through the umbilical connector, to GSE. A final configuration for AC-8 and later flights has been established, which, additionally, simplifies the power control circuitry by reducing the number of relays from ten to three.

AC-5 Guidance Analysis

Malfunction analysis. - Postlaunch analysis of the telemetered digital data word (DDW) showed that the DDW assumed a neutral state (corresponding to a nominal 2.5-V level) and hence was conveying no information. This was the only indication of a possible malfunction within the missile guidance set (MGS). The DDW recording was compared with other recordings to determine if there was a malfunction and to isolate or pin point the probable cause of the malfunction. The DDW is generated in the navigation computer unit (hereinafter called the computer) of the MGS and then modulates a telemetry pack that telemeters the information from the vehicle. The information conveyed by the DDW is a function of the input information to the computer and the computer itself. Prior to umbilical ejection the same DDW is transmitted on a landline to the launch control facility.

Trace (a) of figure VII-1 shows the computer digital data word (DDW) from several seconds before the switch of guidance to inertial mode, at T - 7.868 seconds, until vehicle breakup. The interruption at T - 7.868 seconds normally occurs when the system is switched into the inertial mode; however, at T - 1.292 seconds a complete loss of the telemetered digital data word (DDW) occurred. After loss of the digital data word the telemetry signal voltage level was 2.5 volts, which indicates that the wire to the telemetry transmitter was intact, and the computer was supplying 2.5 volts bias. Later bit-by-bit examination of the DDW showed that, up until the time of data loss, the computer was operating normally.

Trace (b) of figure VII-1 shows the main missile battery current. Two obvious transients are visible. At the time of DDW loss, the current dropped from about 53.8 to 46.3 amperes (7.5-A change). It is shown later in this report that the ejection of the J401, J402, J403, and J404 Centaur umbilical plugs also occurred at approximately this time. The second transient is a drop in current from 46.3 to about 39.5 amperes. It has been determined that this drop occurred at the time of ejection of the J412 umbilical plug, and can be attributed to cutoff of the hydraulic circulating pumps that normally occurs at this time. During FACT plugs out test, the measured current on AC-5 after J412 ejection was measured as 46.5 amperes with telemetry and 46 amperes on the landlines. This value of 46 amperes is also typical of values measured on other vehicles. Therefore, the 39.5 amperes for the AC-5 flight is about 7 amperes below normal, and this corresponds, with expected accuracy, to the current drop that occurred when the J401, J402, J403, and J404 umbilical plugs were pulled.

Traces (c) and (d) of figure VII-1 show that the 35- and 22.2-volt d-c guidance power supplies are normal throughout this entire sequence of events.

In trace (a) of figure VII-2 the DDW is again shown for reference with other guidance signals. Trace (b), the 14.4-kilocycle accelerometer demodulator output, shows effects of vibration at engine ignition and is normal until loss of data. Traces (c) and (d), the W-accelerometer delta "V" and the W-gyro 7.2-kilocycle demodulator outputs, show proper operation of the guidance accelerometer and gimbal control loops until loss of data.

Figure VII-3, traces (b) to (d), the U-, V-, and W-gyro torquing traces, show normal changes at transfer to inertial mode, and little activity from then until loss of meaningful data. To check computer operation further after loss of DDW, the gyro torquing traces were examined in greater detail. If the computer had lost power, no changes in the gyro torquing should occur. Telemetered delta "V's" were used to calculate the W-axis (vertical) acceleration history. The acceleration values were used with gyro "d" values, and known computer cycle lags, to calculate the W-gyro torquing profile for the period after lift-off. The calculated profile is shown, together with the measured torquing, in figure VII-4. Although measured torquing shows some variation, the variations are not time correlated to the calculated profile and are believed to be a result of telemetry noise. The observed and calculated variations are of the same order as the known TLM accuracy; therefore the gyro torquing data is considered inclusive.

The U-, V-, and W-steering traces ((b) to (d) in fig. VII-5) appear nominal and stable throughout this interval, excepting changes that were determined to be decommutator dropout. Examination of the wave train data for this signal revealed that the trace remained constant throughout the "flight".

In summary of the preceding analysis, guidance system performance appeared normal until the vehicle broke up, with the exception that DDW was lost at T - 1.292 seconds. This time corresponded approximately to the time of ejection of the J401, J402, J403, and J404 plugs; an abnormal drop in battery current of about 7.5 amperes occurred at the same time.

Henceforth, in this discussion GMT time shall be used. For reference, loss of DDW at 1325:02.904 GMT corresponds to T - 1.292 seconds.

Figure VII-6 is a high-speed readout showing DDW, and U-, V-, and W-delta V's, and main missile battery current. In addition to the loss of DDW at

1325:02.904 GMT, some distortions of the DDW and delta V waveshapes occurred in the time period of 1325:02.884 GMT (T - 1.312 sec) until 1325:02.887 GMT. Also of interest in figure VII-6 is the transient on the DDW trace that occurred 10 milliseconds after the loss of digital data. These anomalies will be discussed in a later section of this report.

Malfunction isolation. - Examination of computer schematics and computer testing established several possible failure modes that could account for the observed loss in DDW. Among these failure modes are

(1) Grounding of any of the electronics associated with functions K5, $\overline{K5}$, K6, T_0 flip-flops, or the P_0 emitter follower

(2) Failure of the K5 relay, the relay set control, or associated circuitry

(3) Complete loss of 28-volt power to the computer

Of these failure modes, only (2) and (3) would account for the observed drop in d-c current. Equivalent d-c load currents for systems other than guidance are as follows:

System	Equivalent d-c current, A
Autopilot	5.1
Propellant utilization	.8
C-band beacon	.9
Range safety command 1	1.6
Inverter no-load	12.0
H_2O_2 heaters	2.4
Boost pump heaters	2.8

All these systems were verified to be operating normally after lift-off, with the exception that the H_2O_2 and boost pump heaters were difficult to verify in the short time before vehicle breakup. However, these heaters were switched to internal at power changeover and are thereafter isolated from the umbilicals. It is therefore concluded that the observed current drop occurred within the guidance system. Further, since only the computer exhibited any anomalies before vehicle breakup, it is concluded that the observed current drop is related to the loss of computer power.

Previous testing at ETR has shown that when the computer is switched from coast phase to run there is approximately a 7-ampere increase in battery current; when switched from off to run approximately 9 amperes are required. Testing of a computer at Honeywell has shown that switching from coast phase to run requires an additional 14 watts of d-c power (0.5 A at 28 V), and an increase in a-c power of 129 watts (7.1 A dc, assuming 65 percent inverter efficiency). This gives a total equivalent d-c current of 7.6 amperes. Also, the total computer requirement (off to run) was about 10 amperes equivalent d-c current.

Thus the current requirements measured on the computer at Honeywell and those measured in vehicle testing are in fair agreement. Furthermore, it is apparent from the observed current change that the computer went essentially to the coast-phase mode and did not suffer total loss of power (the coast phase power required is essentially all ac).

Figure VII-7 is a schematic drawing of the computer power control circuitry. A simplified schematic drawing showing only pertinent details is presented in figure VII-8. Referring to figure VII-8 in the startup cycle and applying a 28-volt signal to the warmup line from GSE pulls in relays K6 (400 cps power computer) and K9. The K9 contact closure in turn applies power to K8. Airborne 28 volts is routed through umbilical plug J404 to the GSE and back through J404 to a set of contacts on relay K6. When K6 is actuated, this airborne 28 volts electrically latches K6 and K9 and (through K9 contacts) K8. When the computer is commanded to run, K5 (a set-reset relay) is put into the set position. Airborne 28 volts through K5 contacts provides another path to latch K6, K9, and K8 electrically. If K5 is not in the set position when umbilical plug J404 is pulled, the electrical latch on K6, K9; and thus K8 is lost, and most computer power will be cut off. Power will also be cut off if airborne 28 volts is lost with the computer in the run condition (even if plug J404 is engaged). Because the computer output was lost at essentially the time that the J404 plug was ejected, the former failure mode is considered by far the most probable.

Establishment of umbilical eject times. - Because of the apparent relation between the computer failure and the ejection of Centaur umbilical plugs, it was necessary to establish precisely the time of ejection of the J404 umbilical plug. To accomplish this, blockhouse E-A (event recorders) and high-speed recordings of landline data were used. The following table gives the ejection times of various umbilical plugs as read from these recordings.

Umbilical	Event recordings, sec	High-speed landline recordings	Difference
J401	1325:02.92	02.885	0.035
J402	02.92	------	-----
J403	02.915	02.865	.050
J404	02.925	------	-----

Since the resolution and response times of the high-speed recordings are much better than those for the E-A recordings, the high-speed values must be considered the most precise. Unfortunately there were no continuous high-speed recordings of data through the J404 plug. However, the E-A data do indicate that the J404 plug was the last one ejected and that it was ejected approximately 5 milliseconds after the J401 plug. Thus the best estimated time for the J404 plug is 02.885+0.005 seconds, or 02.890 seconds. This value is considered accurate to a few milliseconds. Photographs of the umbilical ejection indicated that the order of mechanical ejection was the same as that indicated by the landline recordings. However, in spite of the high photograph frame rate (400 fps), resolution was not sufficient to verify the landline values of ejection time.

Referring to figure VII-6 shows that the estimated J404 plug ejection time of 02.890 seconds is about 3 milliseconds after the last waveform distortion occurred in the DDW and delta "V" traces. Examination of data from the AC-4 flight and the AC-5 FACT (plugs out) revealed that similar waveform distortion occurred during umbilical ejections. Later testing showed that the distortions were particularly related to the ejection of the J402 and the J404 plugs. It is therefore concluded that the J404 umbilical plug was ejected within ±3 milliseconds of 1325:02.887 GMT. This is 17 milliseconds before loss of the telemetered digital data word at 1325:02.904. The delay before loss of the DDW may be accounted for by relay dropout times in the computer power control circuitry.

Special postflight test results. - During the week following the aborted launch of AC-5, extensive system and computer testing was conducted at Kearfott, Honeywell, AFETR, LeRC, and GD/C. The following paragraphs summarize the various test procedures and results.

(1) AFTER testing.

(a) L-30 computer (S/N 3).

K5 disabled to simulate reset condition. Removal of 28 volts power to simulate umbilical J404 ejection gave the following delay times:

5 milliseconds until K9 open
8 milliseconds until K8 open
9 milliseconds until loss of DDW

Complete removal of 28 volts gave essentially the same results.

(b) L-31 computer (S/N 017).

K5 not disabled (in set condition). Complete removal of 28 volts power:

9 milliseconds until K9 open
10.5 milliseconds until K8 open
13.5 milliseconds until loss of DDW

In these tests, DDW sometimes went to the 2.5-volt state.

(2) Honeywell testing.

MGS 10 tests, L-31 computer (S/N 001).

With and without K5 disabled, all tests showed a loss of 400 cps power (K6 and K9 open) in 8 to 9 milliseconds and loss of DDW in 11 milliseconds or less. Telemetry outputs went to 0 and 2.5 volts randomly.

(3) Kearfott testing.

L-31 computers, K5 disabled.

DDW loss in all cases occurred in 10 to 14 milliseconds after interruption of 28 volts power. However, in about 100 tests, the TLM output never went to 2.5 volts, and only once to 5 volts.

(4) GD/C testing.

AC-6 vehicle, MGS 21, L-31 computer (S/N 021).

(a) Simulated umbilical ejection with K5 disabled:

The DDW went to the 2.5-volt level 14 milliseconds after J404 plug ejection. After another 10 milliseconds, the DDW went to the 0-volt level. The vehicle battery current dropped 6 amperes. The profile of the current drop was very similar to that observed on AC-5. These results are presented in figure VII-9.

(b) Complete removal of 28 volts dc from the computer:

The profile of the vehicle battery current drop was somewhat steeper than that obtained with K5 disabled. In figure VII-10 the current profiles from the GD/C tests are compared with the profile from AC-5.

(5) LeRC testing.

L-30 computer (S/N 5).

Relay K5 disabled, simulated umbilical ejection:

11 milliseconds until K9 open
11 to 13 milliseconds until loss of DDW
20 milliseconds until K8 open
20 to 21 milliseconds - transient occurs or DDW trace, which sometimes changed the voltage level of the DDW trace. Typical oscilloscope traces from these tests are shown in figure VII-11.

These special postflight tests have shown

(1) Loss of DDW in from 10 to 14 milliseconds after simulated umbilical ejection (K5 disabled), or after complete removal of 28 volts from the computer. The time delay varies from computer to computer and reflects the difference in relay dropout times. Loss of DDW occurs just after relay K9 opens. At loss, the DDW may go to the 5-, 2.5-, or 0-volt state.

(2) When 28 volts are completely removed, relays K8 and K9 open at about the same time.

(3) When K5 is disabled and umbilical ejection is simulated, K8 opens on the order of 10 milliseconds after K9. Opening of K8 results in a transient on the DDW channel which may or may not change the state of the DDW flip-flops (output voltage). A similar transient was observed in the AC-5 flight data 10 milliseconds after loss of DDW (see fig. VII-5).

(4) The AC-6 vehicle tests, with K5 disabled, showed a missile battery current profile closely duplicating that observed on AC-5. When 28 volts were completely removed from the computer, the current drop was somewhat steeper.

In view of the aforementioned results it is concluded that a failure most likely occurred in the K5 relay, or its associated circuitry, so that it was effectively in the "reset" condition. When the J404 umbilical plug was ejected, GSE 28 volts were removed from relays K6 and K9. Opening of these relays, and subsequently of the K8 relay, removed power from the arithmetic section of the computer (essentially the coast-phase mode). Another, but less likely failure, could have been the loss of 28 volts of power to the computer.

Preflight testing. - Investigation has disclosed that approximately 1 year ago, when the computer coast-phase circuitry was disabled, all tests that would check the operation of K5 set control at the unit level were eliminated. The only known test that checks the operation of this relay is the vehicle system plugs out test. The computer installed in AC-5 was replaced after FACT plugs out test, and insofar as can be determined, operation of K5 was never tested.

Since one possible failure mode is the loss of 28 volts of power to the computer, the wiring harness history was investigated. On F - 1 day, an open connection was discovered in the harnessing to the platform electronics unit. Two additional wires in this harness failed during subsequent pull testing. The PE harness connectors were "Poke-Home" type, and the same type connectors are used in the computer harnessing. Visual tests were performed on computer connectors; however, pull tests were not run. Microscopic inspection of the failed pins indicated that faulty crimping tools were probably used.

Concluding Remarks

(1) The computer went into a state similar to "coast phase" (power removed from the arithmetic section of the computer) resulting in loss of the digital data at 1325:02.904 GMT (T - 1.290 sec).

(2) Most likely the cause was failure of the K5 relay, or its associated circuitry. This resulted in the loss of 28 volts of power to hold in relays K6, K9, and subsequently K8 when the J404 umbilical plug was ejected. Opening of these relays removed power from the arithmetic section of the computer. Evidence substantiating this failure mode includes

(a) Time of loss of the DDW after ejection of the J404 plug agrees with test results to within the knowledge of J404 ejection time

(b) Magnitude of the main missile battery current drop

(c) Shape of the current drop profile

(d) Occurrence of a transient on the DDW channel about 8 milliseconds after loss of digital information; this transient indicates sequential opening of relays K9 and K8

(e) Computer and guidance system test procedures, did not adequately test the operation of relay K5

Corrective action. -

(1) The following action is underway for AC-6 and AC-7 effectivity:

(a) Remove from the computer or completely isolate electrically all circuitry which is no longer required.

(b) Modify computer power control GSE so that proper operation of all airborne computer power control relays and wiring can be verified before lift-off. This modification will remove power lines that went directly from the computer to GSE through the umbilical connector which paralleled power lines to the computer from the MGS.

(c) Test operation of K5 on the unit level.

(d) Change P_0 emitter follower circuit to relieve wattage overstress on a resistor.

(e) Review all other guidance and autopilot Atlas-Centaur GSE interfaces, to check for "sneak paths" and other potential failure modes.

(f) Review computer test procedures for adequacy.

(2) Additional action, effectivity AC-8: Redesign computer airborne and GSE power control circuitry. This redesign will simplify power control relays and circuitry not absolutely required by using three relays in place of ten. This is possible because of elimination of the coast-phase requirement. Power control relays will be used in a failsafe mode (not energized during flight).

(3) Airborne harnessing fabrication techniques have been reviewed. Use of approved wire stripping tools and properly calibrated crimping tools will be ensured.

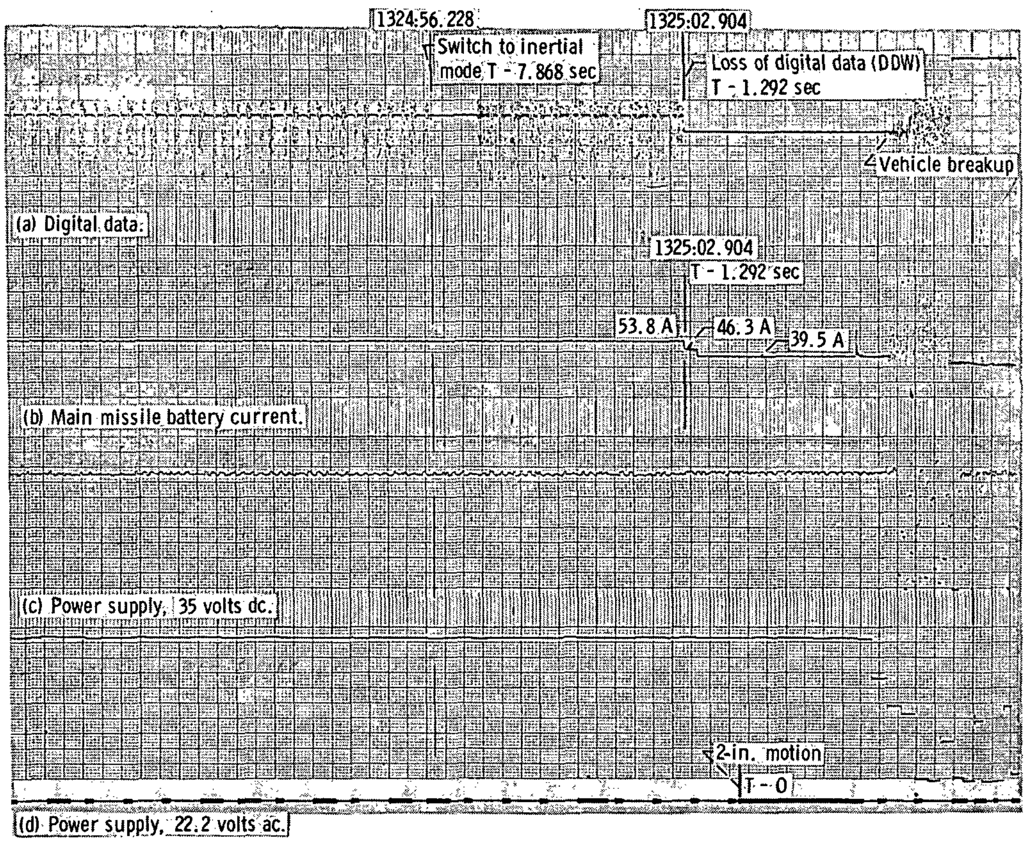

Figure VII-1. - Telemetered guidance signals.

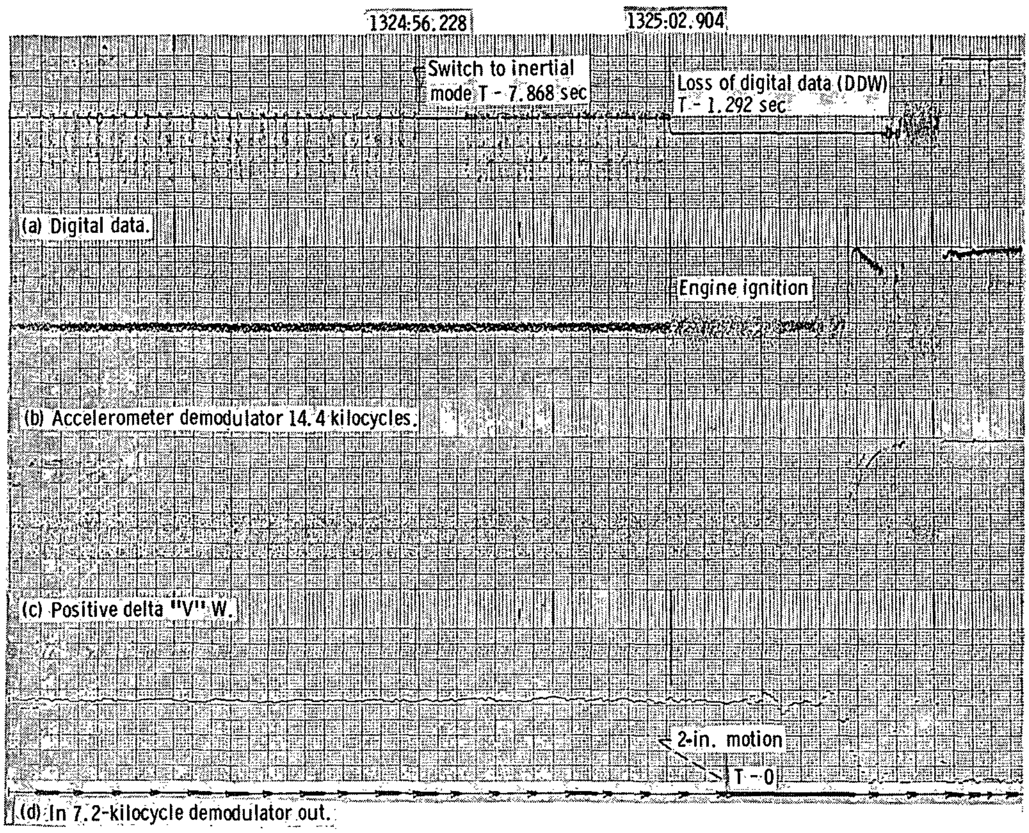

Figure VII-2. - Telemetered guidance signals.

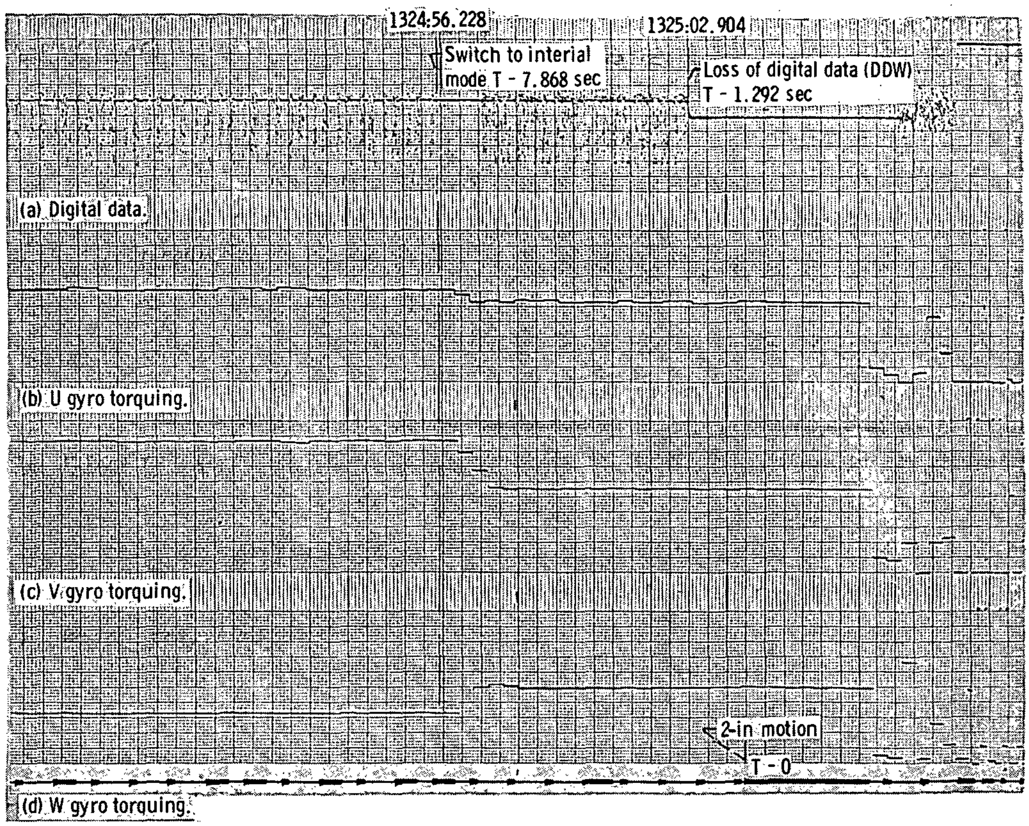

Figure VII-3. - Telemetered guidance signal.

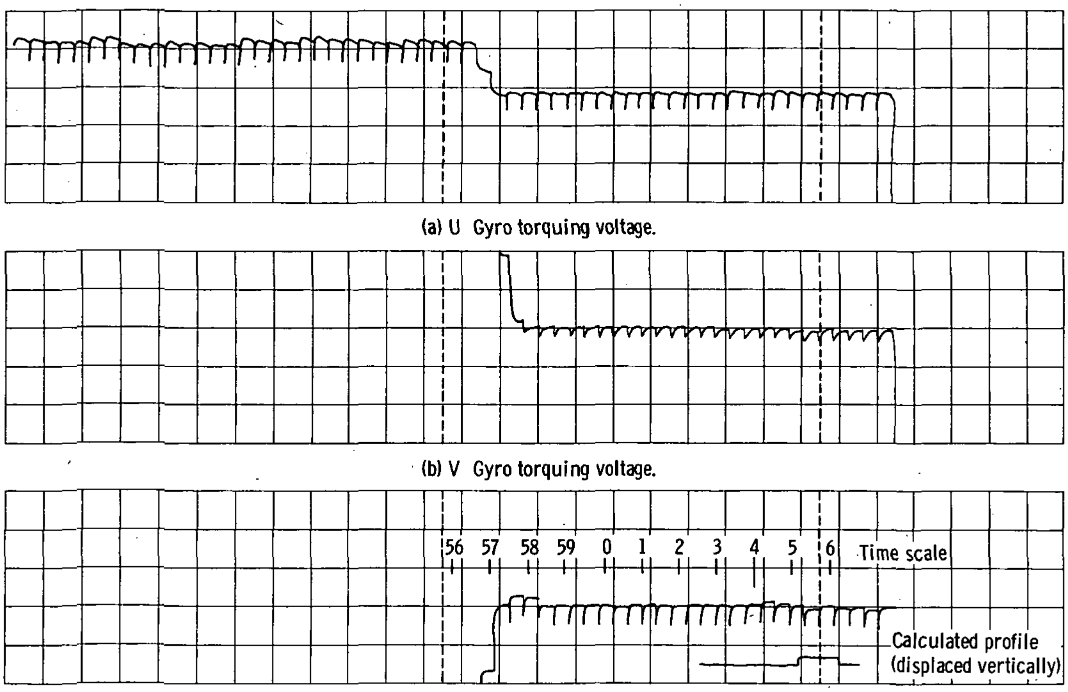

(a) U Gyro torquing voltage.

(b) V Gyro torquing voltage.

(c) W Gyro torquing voltage.

Figure VII-4. - Gyro torquing traces.

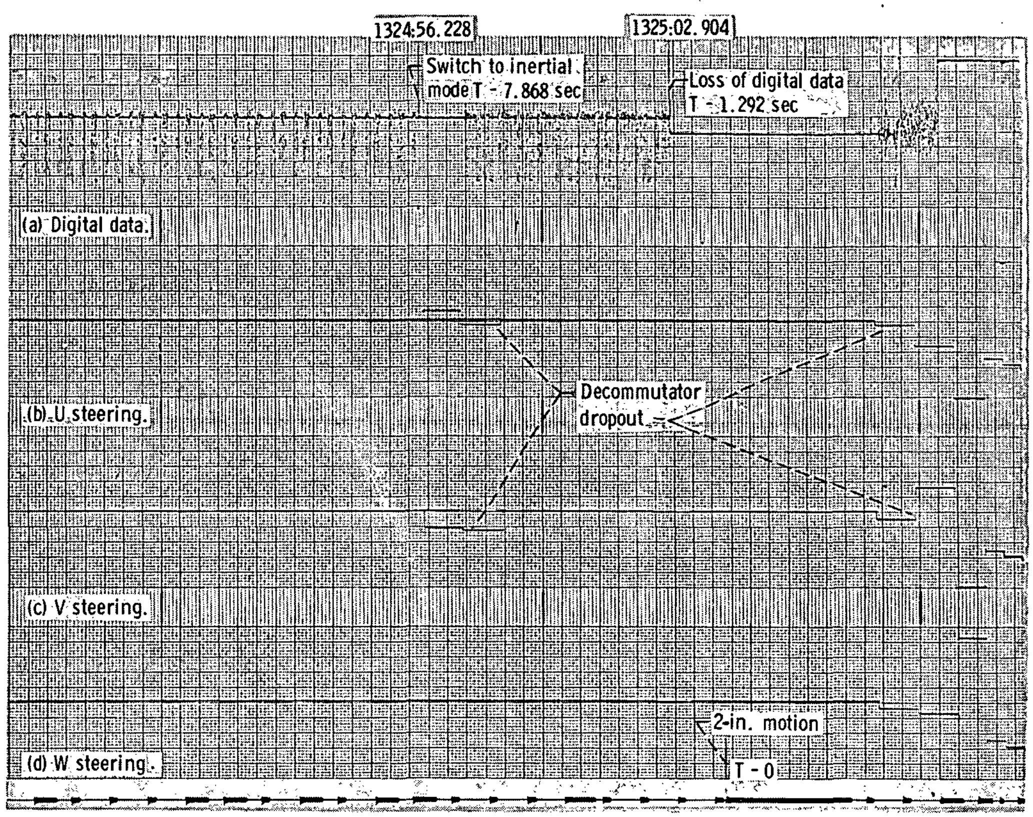

Figure VII-5. - Telemetered guidance signals.

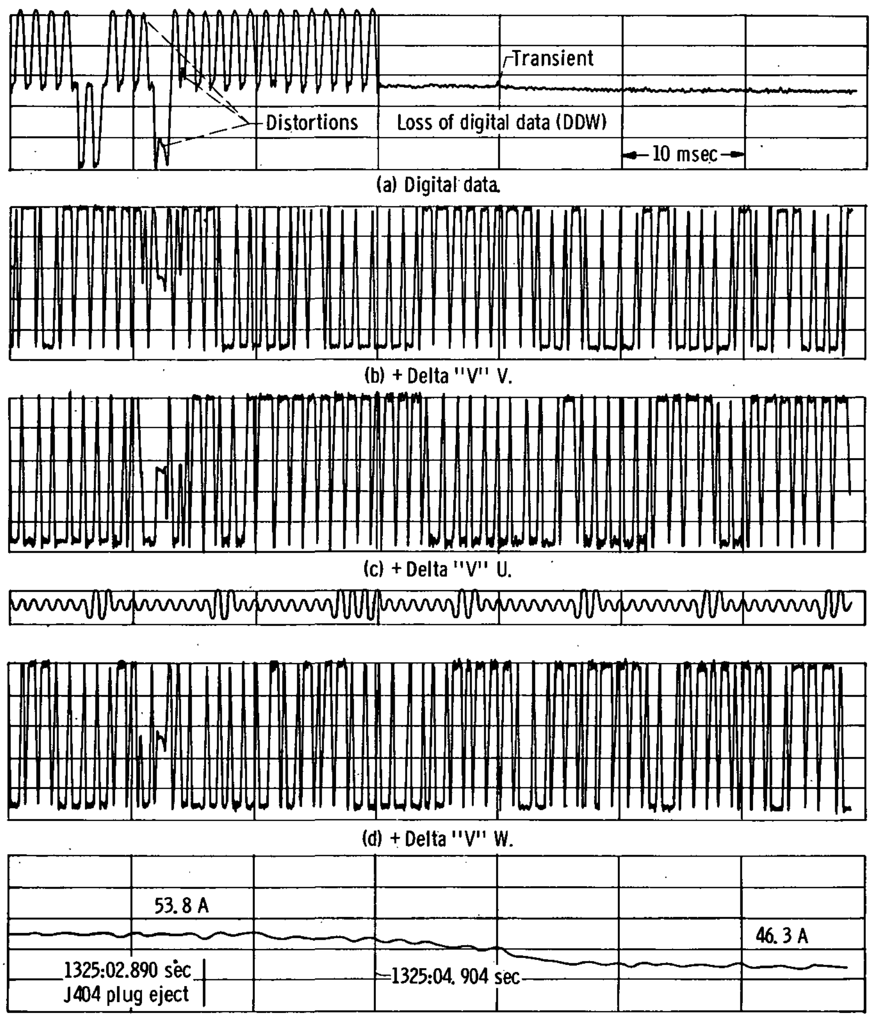

(e) Main missile battery current.

Figure VII-6. - High-speed recordings of guidance signals.

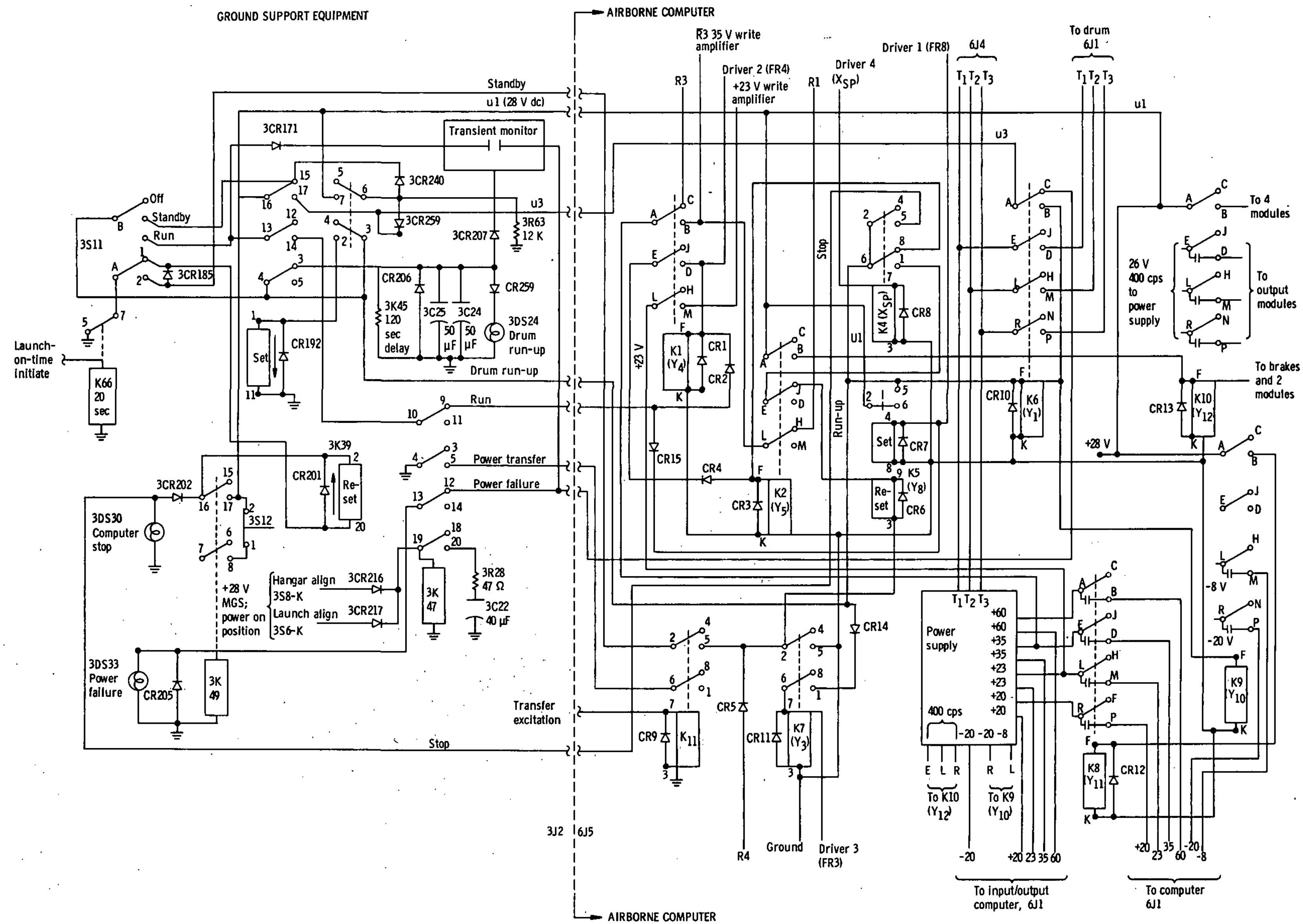

Figure VII-7. - Computer control circuitry.

[redacted]

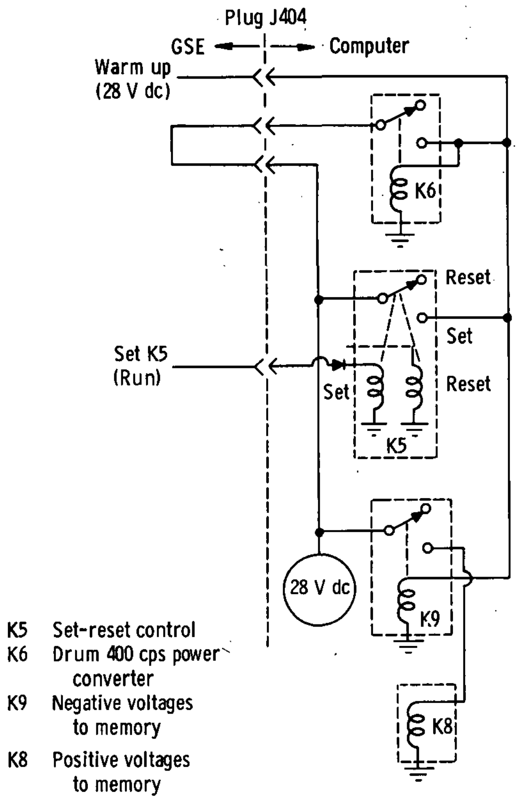

Figure VII-8. - Simplified schematic of computer power control circuitry.

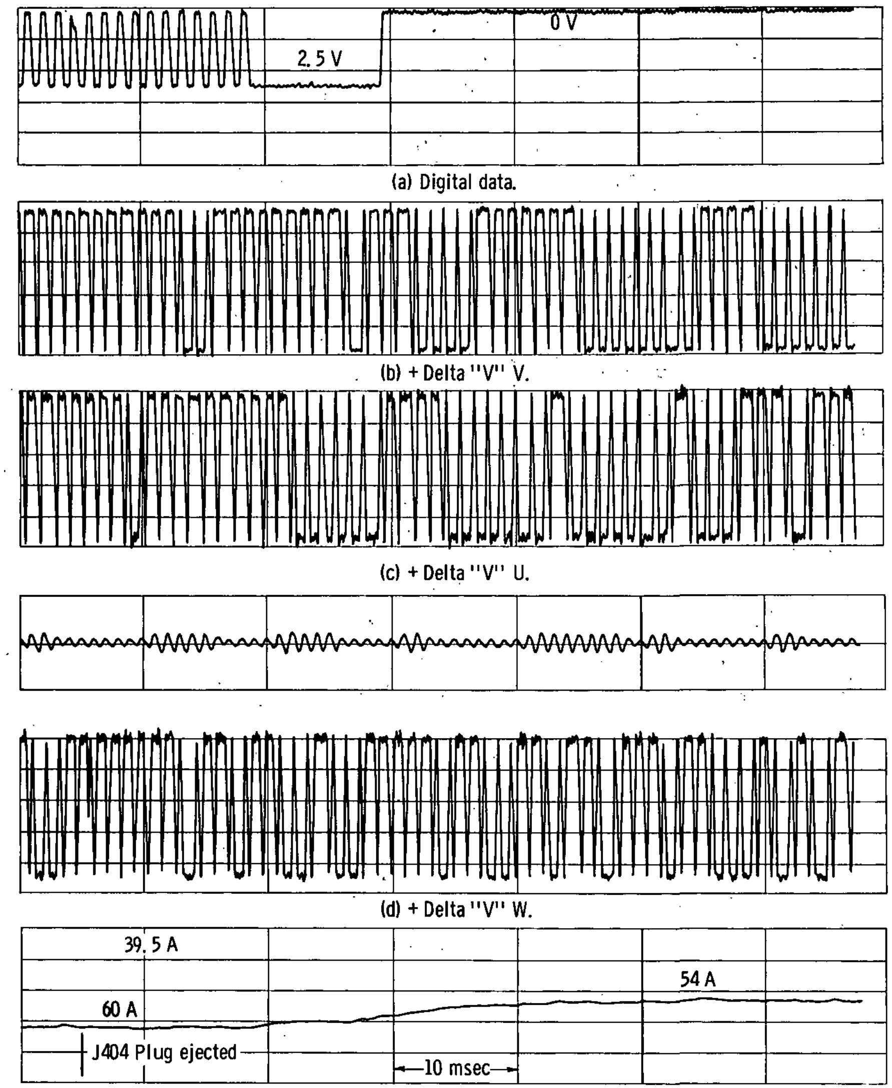

(e) Main missile battery current.

Figure VII-9. - AC-6 vehicle tests. Relay K5 disabled.

CONFIDENTIAL

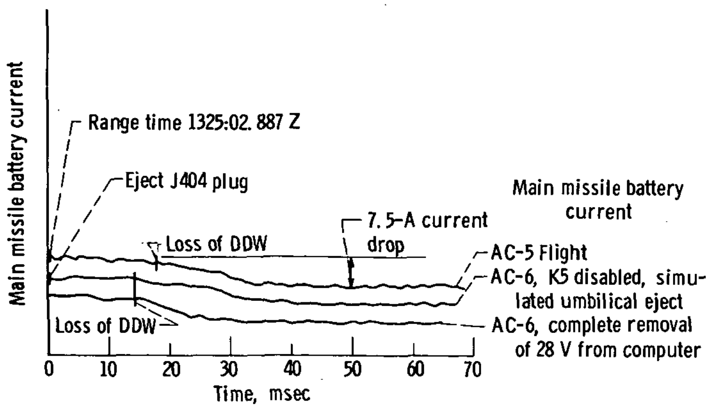

Figure VII-10. - Comparison of main missile battery current profiles from AC-5 flight and AC-6 vehicle tests (profiles displaced vertically for clarity).

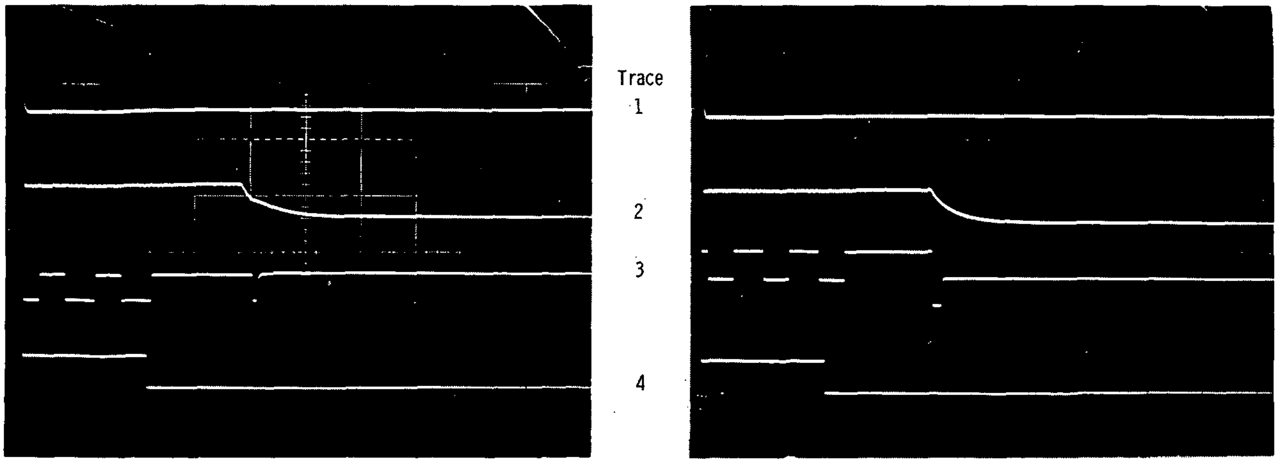

Trace 1 - U-3 voltage, 50V/cm
2 - Relay K8 monitor, 50V/cm
3 - TLM digital data word, 5V/cm
4 - Relay K9 monitor, 50V/cm

Figure VII-11. - Typical oscilloscope traces from LeRC computer tests. Computer S/N 5(-1 model); oscilloscope triggered by removal of 28 volts from U-3 line to computer; sweep set 5 milliseconds per centimeter.

VIII. CENTAUR ELECTRICAL SYSTEM

Summary

The airborne electrical system provides on-board electrical power storage, conversion, distribution, and protection as well as fulfilling the requirements of instrumentation, telemetry, tracking, and range safety command systems.

All electrical power systems adequately supported the flight, from countdown operations to vehicle destruct. The only significant anomaly occurred in the main missile battery current. A two-step dropin system load was noted that resulted from dropouts of user systems.

System power was supplied by a 100-ampere-hour main missile battery, a 100-ampere-hour telemetry battery, and a 650-volt-ampere static inverter. The pyrotechnic power for the thrustor bottles, nose-fairing explosive bolts, vent door, and insulation-panel latches was supplied by two redundant 1/2-ampere-hour batteries. The range safety command system power was supplied by two batteries identical to the pyrotechnic batteries.

Performance of the Centaur telemetry and instrumentation system was satisfactory on AC-5. There were 275 measurements of Centaur and the dynamic model parameters made. The LH_2 vent pressure measurement was the only one failing to produce data.

The range safety and tracking systems experienced no anomalies.

Centaur Electrical Power System

Performance of the Centaur electrical power system was satisfactory during prelaunch operations and until the vehicle was destroyed. A schematic diagram of the Centaur electrical system is shown in figure VIII-1.

The only significant anomalies in system performance were two step decreases in battery current prior to T - 0 accompanied by a corresponding rise in main missile battery voltage (fig. VIII-2). The first drop in current occurred at T - 1.3 seconds and coincided with the loss of the digital data link. Current decreased from 54 amperes to approximately 47 amperes. Details of this malfunction are given in the section <u>CENTAUR GUIDANCE</u>. The second drop in main missile battery current occurred at approximately T - 0.9 second when the aft prelaunch umbilical was ejected. At this time, power to the hydraulic recirculation pump motors was cut off resulting in a 7.5-ampere drop in current. Investigation revealed that recirculation motors were not turned off manually at T - 2 minutes as planned. Main missile battery voltage increased from 27.9 to 28.25 volts as a result of the decreased load (fig. VIII-2). Voltage increases appear in steps, since the measurement is commutated at a rate of one sample per second. Neither current step decrease had any adverse effect on the electrical system.

The staging disconnect actuator temperature reached a minimum of 61° F at lift-off. The red-line temperature was 50° F minimum.

The inverter performance was satisfactory. The inverter skin temperature, as indicated by landline measurement, was 61.8° F at lift-off. The inverter phase voltages varied a maximum of 0.4 volt throughout launch countdown and up to vehicle destruct. The voltages for phases A, B, and C were 115.4, 115.8, and 114.5, respectively, during countdown and until flight termination.

Centaur Range Safety Command System

Operation of the Centaur range safety command system was satisfactory throughout launch operations. Dual receivers were used on the Centaur vehicle. The automatic gain control (AGC) level of both receivers was approximately 1200 microvolts at lift-off. Receiver 1 AGC increased to approximately 1830 microvolts at T + 3 seconds, while receiver 2 AGC level remained at 1200 microvolts.

Centaur Tracking

Azusa, C-band, and S-band transponders functioned satisfactorily. The S-band transponder was located on the SD-1 dynamic model, and the Azusa and C-band beacons were located on the Centaur. Azusa AGC level was -52 decibels, or 560 microvolts. The Azusa was the only instrumented tracking system.

Telemetry and Instrumentation

Four pulse amplitude modulations (PAM) FM/FM links were carried on AC-5 for Centaur and the dynamic model airborne measurements. Telemetry systems 1 and 2 monitored Centaur vehicle parameters. Telemetry subsystems 2 and 3 monitored the payload environment. Subsystems 1 and 2 were located on the Centaur vehicle in the forward equipment area. Subsystems 3 and 4 were located in the retromotor simulator portion of the Surveyor dynamic model. Telemetry system power output was 3 to 5 watts. Frequencies were as follows:

RF 1 225.7 Mc

RF 2 235 Mc

RF 3 243.8 Mc

RF 4 251.5 Mc

Six telemetry system parameters were telemetered including telemetry battery current, thermocouple reference junction temperature, and four telemetry package skin temperatures. All parameters were as expected, well within acceptable limits. Telemetry battery load current for subsystems 1 and 2 was

11 amperes. Subsystems 3 and 4 were powered by a separate battery on the dynamic model. The reference junction temperature was constant, and the telemetry package skin temperatures remained at acceptable limits. Subsystems 1 and 2 had stabilized at approximately 75° F, and the subsystems on the dynamic model stabilized at approximately 45° F.

Signal strength from the Centaur telemetry packages and from Atlas RF 1 was adequate as shown in figure VIII-3 (ref. 7). Receiver threshold was approximately 0.75 microvolt. Some flame attenuation is evident at booster engine ignition but signal strength remained well above receiver threshold level.

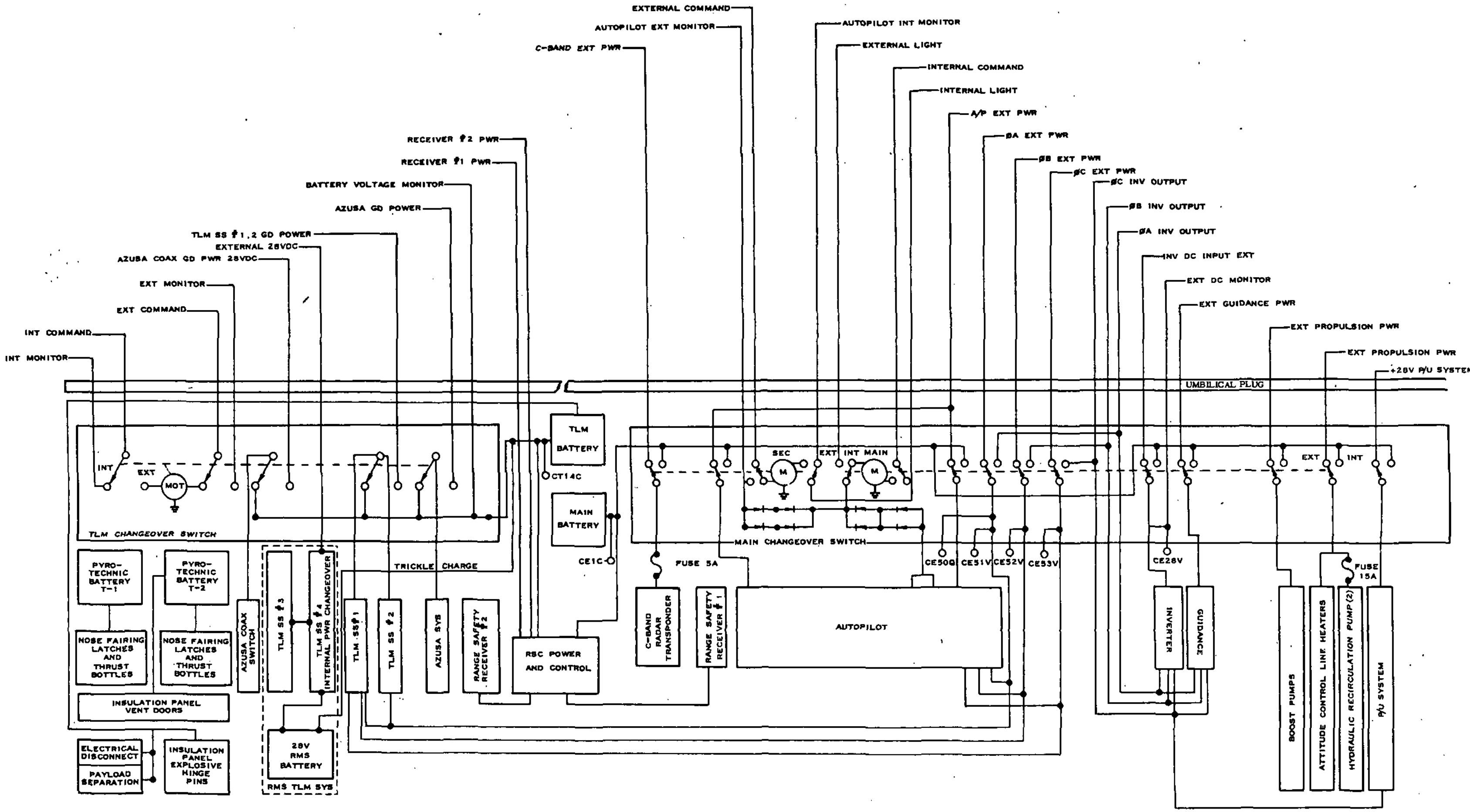

Figure VIII-1. - Centaur electrical system.

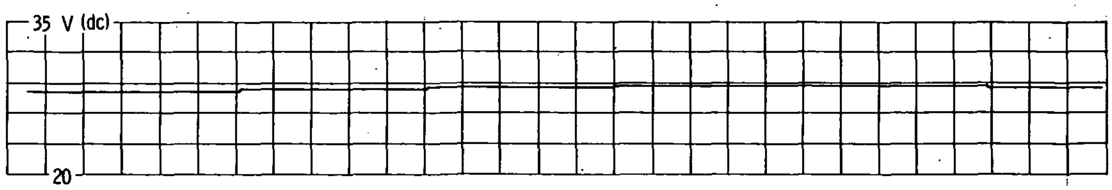

(a) Power supply, 28 volts dc (CE28V).

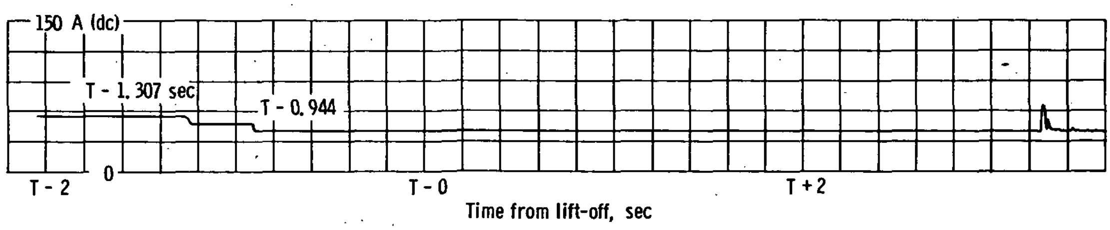

(b) Main missile battery current (CE1C).

Figure VIII-2. - Centaur direct-current power measurements.

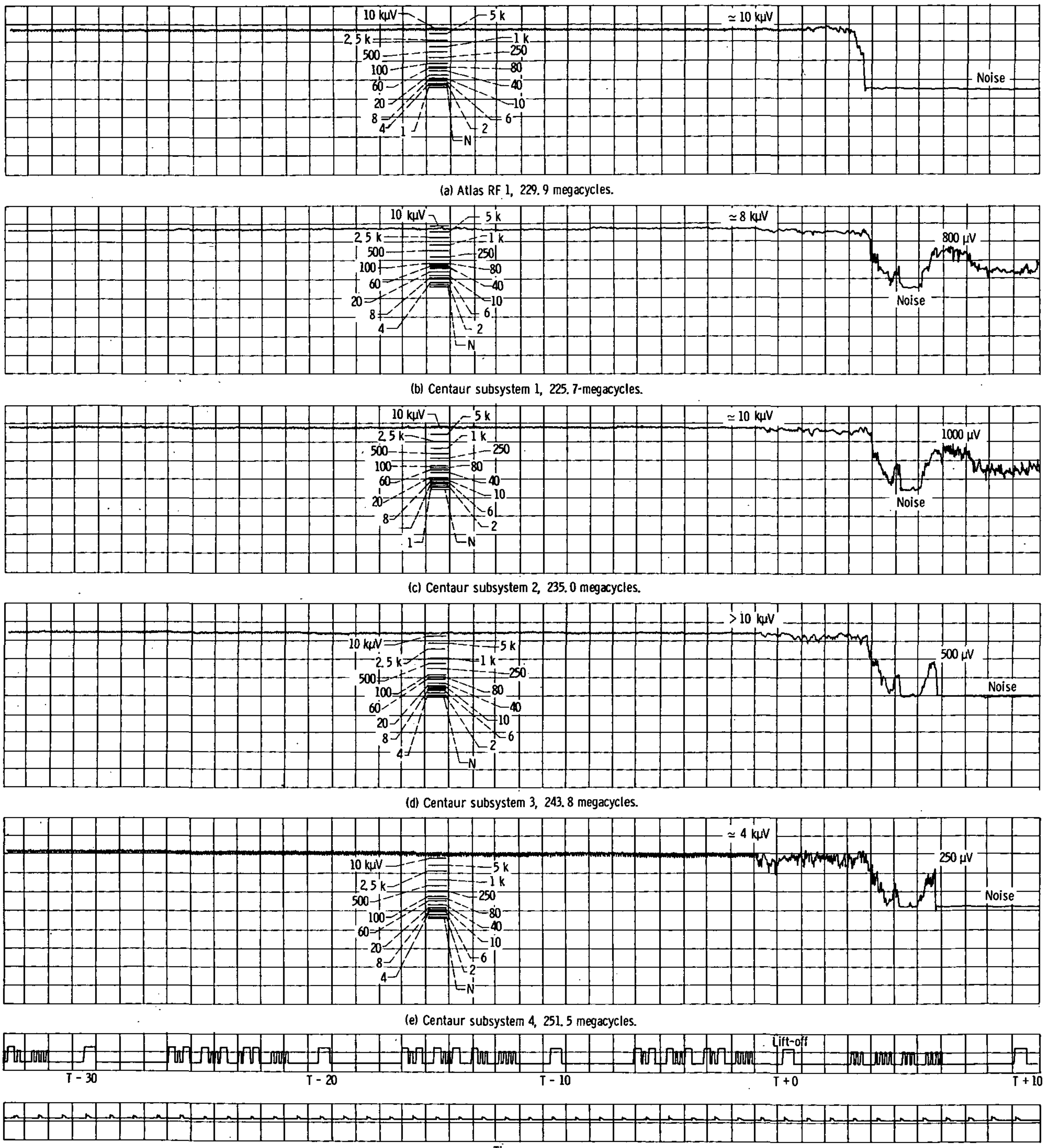

(a) Atlas RF 1, 229.9 megacycles.

(b) Centaur subsystem 1, 225.7-megacycles.

(c) Centaur subsystem 2, 235.0 megacycles.

(d) Centaur subsystem 3, 243.8 megacycles.

(e) Centaur subsystem 4, 251.5 megacycles.

Figure VIII-3. - Atlas-Centaur telemetry signal strengths (ref. 7).

IX. CENTAUR PROPELLANT UTILIZATION SYSTEM

AC-5 was the first Centaur vehicle to utilize the newly developed capacitance probe propellant utilization (PU) system (ref. 8). All system checks were satisfactory during the countdown, and the system showed normal operation up to the time of vehicle destruct.

The PU System is shown schematically in figure IX-1. The basic operation of the system is one of sensing and comparing the mass of propellants and correcting engine flow rates to maintain a desired ratio of oxidizer to fuel in the tanks. In Centaur, the capacitance probes sense the mass of each propellant and compare them in the electronics package. If the ratio varies from a predetermined value, LOX flow to the engines is varied to return the ratio to the proper value.

The launch countdown system checks started at T - 105 seconds. All parameters, as shown in table IX-I, were within tolerance. LOX and LH_2 quantities during tanking are shown as a function of time in figure IX-2.

The electronics package skin temperature is shown in figure IX-3. The temperature remained within the 25° to 129° F limit throughout the countdown.

Centaur Propellant Loading - AC-5

LH_2 and LOX were satisfactorily tanked to planned flight levels by the propellant level indicating system (PLIS). The PLIS also utilized two 100-percent dual element level sensors, one in each tank to ensure loading to the proper level. The propellant levels and weights at lift-off are presented in the following table (ref. 9).

Propellant	PLIS, percent	Ullage pressure, psia	Density, lb/cu ft	Station, in.	Volume, cu ft	Weight, lb
LOX	98.7	31.2	68.72	382.3	354.0	24 330
LH_2	99.7	21.6	4.32	190.32	1191.44	5 147

TABLE IX-I. - COUNTDOWN SYSTEM CHECKS

Time, min	Checkout function
T - 105	The engine LOX flow control valves were exercised; valve rotation rates were 8.7 and 8.0 degrees per second (allowable is 6 to 12 deg/sec)
T - 62	The valves crossed over from LOX-rich stops to LH_2-rich stops; the crossover points must satisfy the following equation: $5LH_2 - LOX = 160 \pm 500$ pounds $LOX = 13.087$ $LH_2 = 2668 \times 5 = 13\ 340$ $\therefore 5LH_2 - LOX = 253$ pounds
T - 54	Same as T - 62 min: $LOX = 19\ 330$ $LH_2 = 3848 \times 5 - 19\ 240$ $\therefore 5LH_2 - LOX = -90$ pounds
T - 53	The full quantity checks must satisfy the following: $LOX = 19\ 870 \pm 1000$ pounds $LH_2 = 3880 \pm 200$ pounds Measured LOX = 20 030 pounds M = 160 pounds Measured LH_2 = 3848 pounds M = -32 pounds
T - 52	Valve rotation rates: 9.6 and 9.2 degrees per second
T - 5	Valve rotation rates: 9.26 and 9.15 degrees per second

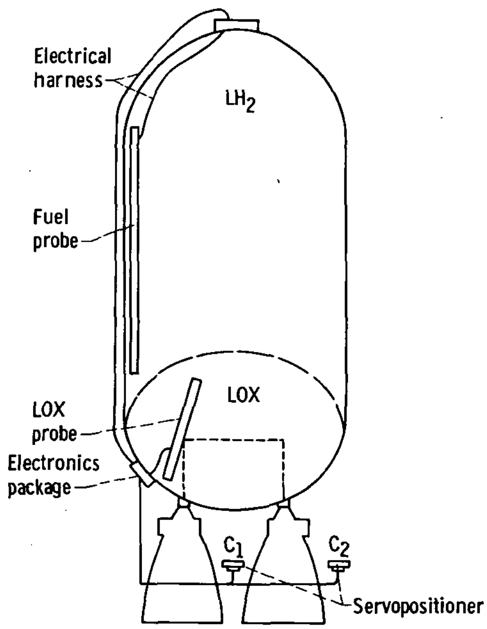

Figure IX-1. - Propellant utilization system.

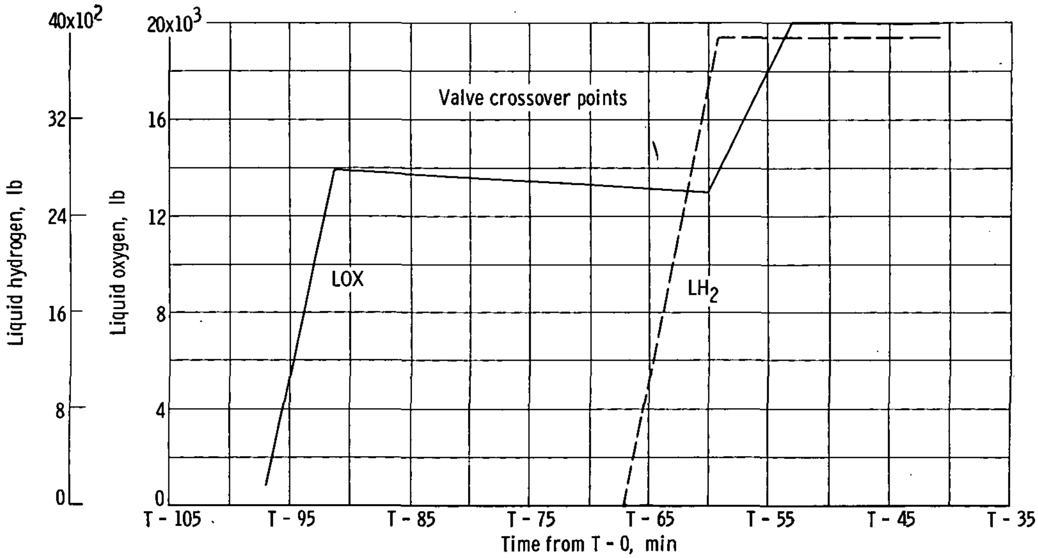

Figure IX-2. - Liquid oxygen and liquid hydrogen quantities.

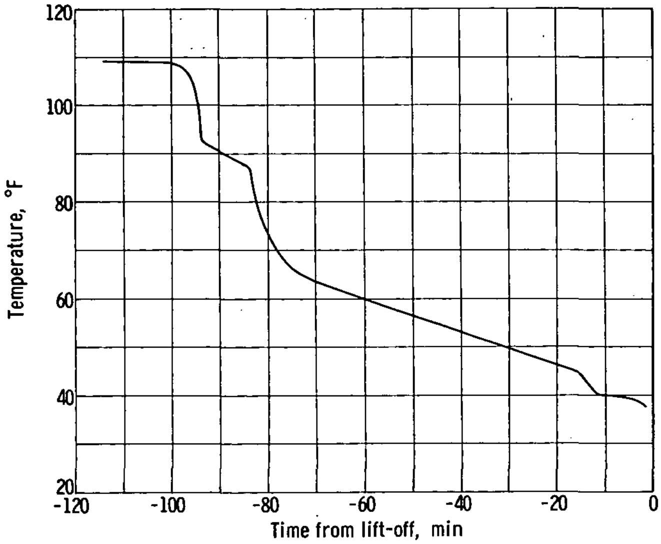

Figure IX-3. - Electronics package skin temperature.

X. STRUCTURES

Loss of the AC-5 vehicle after approximately 3 seconds precludes any extensive structural performance evaluation. Pressure and temperature environments were essentially at their prelaunch values and presented no surprises. These environments have been adequately substantiated on the previous three successful flights. Flight loads, both lateral and longitudinal, during the few seconds immediately following launch are at their minimum values and present no critical problems. Structural performance was satisfactory prior to loss of the vehicle.

In spite of general mission failure, it was possible to evaluate Atlas intermediate bulkhead differential pressure history. Because the uprated booster engines were used for the first time on the AC-5 vehicle, it was feared that the differential pressure might attain negative values and result in bulkhead reversal. In order to obviate this possibility, a programed pressure system was used for the LOX tank ullage. The system was programed to maintain a pressure of 5 psi less than the 28.5 psig minimum normal flight pressure for the first 20 seconds after launch. Because of the vehicle failure so soon after lift-off, the return of the LOX tank to the nominal flight pressure range (28.5 to 30.0 psig) could not be substantiated. However, the bulkhead differential pressure history showed a value of 16.8 psi at T - 10 seconds and 11.9 psi at T + 0. This indicates that the programed pressure system is adequate to maintain intermediate bulkhead structural integrity.

XI. VEHICLE DYNAMICS

Atlas roll-rate gyro measurement (AS52R, fig. XI-1) indicated a short duration oscillation at T - 1.5 seconds with a maximum peak to peak (P-P) amplitude of 1.7 degrees per second at a frequency of 10 cps. In the payload area at this flight time, a combined lateral and torsional oscillation of 1 g P-P at a frequency of 11 cps occurred (fig. XI-2). The excitation source was thought to be engine position oscillations during starting transient indicated by B-1 engine yaw-roll measurement (AS252D, fig. XI-3) as 1.2 degrees maximum P-P gimbaling.

Correlation of AC-5 (165k engines) main stage with other D series Atlas starts was made by comparing B-1 engine yaw feedback voltages (feedback voltage is proportional to gimbaling angle) with 32 vehicles having 150k engines and two having 165k engines. As seen in table XI-I, the feedback voltages of the two 165k engine vehicles were comparable with the feedback voltages of the 150k engine vehicles. Booster 156D (AC-5) experienced higher than average feedback voltages and, therefore, gimbaling angles, but eight vehicles have seen amplitudes as high or higher. This correlation indicated that, during starting transient, the gimbaling amplitudes were higher than average, but within the normal deviations seen on other Atlas starts.

A longitudinal oscillation of 0.8 g P-P amplitude at a frequency of 8 cps occurred at T + 0.3 second of flight (fig. XI-4). It was believed that this perturbation was caused by Atlas LOX pressurization instability at lift-off. However, it did not compare well with Atlas LOX pressurization instability oscillations at lift-off of 0.35 g P-P and 6 cps, which have been evident on other Atlas-Centaur flights. More analysis must be performed to ascertain the cause and possible effect from this oscillation.

TABLE XI-I. - COMPARISON OF B-1 ENGINE YAW FEEDBACK VOLTAGES DURING STARTING TRANSIENT OF ATLAS D SERIES VEHICLES

[Vehicles 7101, 7102, and 156 had 165k engines.]

B-1 yaw feedback voltage (rms)										
0.2	0.3	0.4	0.5	0.6	0.7	0.8	0.9	1.1	1.3	1.6
Atlas D vehicle identification number										
29	14	3	10	11	26	45	17	15	195	5
49	20	7	28	289	199		44		288	
	22	27	50	7102	7101		156			
	48	43	83				216			
	51	56					250			
		67								
		90								
		91								

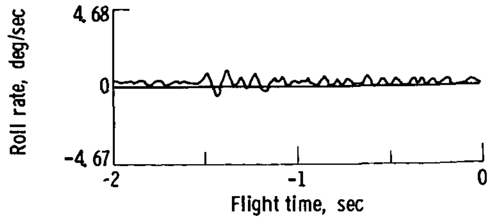

Figure XI-1. - Roll rate gyro signal (AS52R).

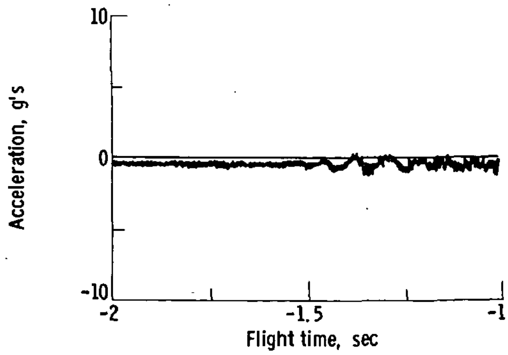

Figure XI-2. Spacecraft mounting leg accelerometer at position 0° and station 125 with x-x axis sensitivity.

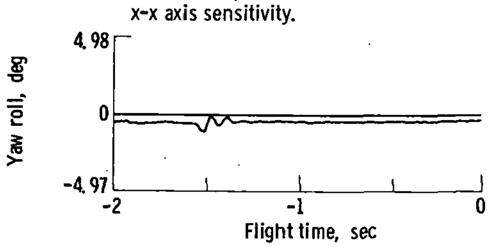

Figure XI-3. - B-1 yaw roll (AS252D).

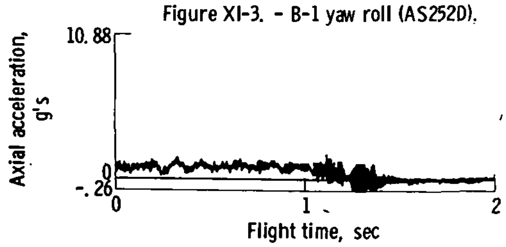

Figure XI-4. - Axial acceleration (CM101A).

XII. GROUND-SUPPORT AND LAUNCH-AREA DAMAGE

Summary

Performance of the mechanical ground-support equipment was satisfactory during the countdown. Temperatures, pressures, and time-sequenced functions were maintained within prescribed limits.

Complex damage due to blast forces was not severe and was limited to the immediate launcher area and secondary structures. Heat damage was extensive on the launch deck, in the mezzanine of the Launch and Service Building, and on the umbilical tower.

Ground-Support Equipment

The mechanical ground-support equipment (GSE) operated satisfactorily during final preparations and countdown. Although there were no countdown holds due to GSE operations, a power outage was experienced at T - 140 minutes (0501 EST) as a result of a fuse link failure in the industrial power supply that caused a 15-minute delay. Power was switched to "critical power," repairs were made, and transfer made back to industrial power during the scheduled T - 90 minute hold.

Prelaunch temperatures and pressures were satisfactorily maintained within limits for propellants and environmental control.

A total of 28 fixed cameras at nine camera pads were used to give optical data coverage. Film coverage was good and provided significant detailed sequential timing of events.

Propellants supplied for the launch were:

Liquid hydrogen	21 000 gal	
Liquid oxygen	38 000 gal	
Liquid helium	2 929 gal	
Gaseous nitrogen	28 trailers	First- and second-stage air conditioning
	6 trailers	Payload air conditioning
	1 trailer	Atlas thrust section heater
Gaseous helium	12 trailers	Insulation panel purge
	3 trailers	LOX storage tank pressurization

Shortly after the AC-5 launch failure, all tanks and bottles were blown down to avoid any possible dangers with the propellants. No gas quantity measurements were taken.

Complex Damage

Explosion data were obtained by blast gages and thermal sensors in the launch abort monitoring system and by photography. These data indicated three separate explosions and a possible fourth explosion. Temperatures in excess of 6000° F were measured at the top of the umbilical tower and on the launch deck. The data indicated that more of the energy yield was released in thermal form than in pressure form. This was generally confirmed by actual complex damage. Except in the immediate vicinity of the launcher, blast damage was limited to doors, windows, louvres and similar secondary structures; the basic frameworks of the service tower, umbilical tower, ramp, and other primary structures were unaffected. Heat damage was extensive, resulting in complete destruction of much electrical equipment, pipe insulation, and aluminum handrails. Some of the damage is shown in the photographs included in this section (figs. XII-1 to 10). In addition to equipment that must be replaced, there is a general need to clean, paint, inspect, test, and revalidate most of the equipment in the pad area. Damage to specific items of facility and ground-support equipment was as follows:

Service Tower

The primary tower structure was not damaged. Secondary damage was as follows:

(1) Some aluminum siding was blown loose.

(2) Windows were shattered.

(3) Fiberglass panels on sliding doors were blown off.

(4) Electrical wiring at the southeast corner was destroyed.

(5) About 35 percent of the painted surface suffered heat damage.

Umbilical Tower

The primary tower structure was not damaged. Secondary damage was as follows:

(1) Approximately 90 percent of the paint on the tower structure was burned.

(2) All wiring and associated equipment, with the possible exception of explosion-proof equipment, was damaged beyond repair.

(3) All pipe insulation was burned.

(4) The majority of piping on the tower suffered heat damage and will require removal, cleaning, and testing to determine reusability.

Launch and Service Building

(1) Two concrete block walls were blast damaged and require partial replacement.

(2) One structural steel beam was bent.

(3) Miscellaneous handrails, ladders, and doors were damaged beyond repair.

Ramp

The damage was minor and was limited to handrails, stair grating, and vent louvres.

Water Pump Building

(1) A door and an air louvre were blown out.

(2) Masonry block walls were cracked.

Propulsion System

(1) Two liquid-helium Dewars, located on the ramp near the umbilical tower, suffered minor damage.

(2) About 50 percent of the liquid-helium transfer lines on the umbilical tower were damaged beyond repair.

Propellant Systems

(1) The LOX and RP-1 propellant lines in the launcher area were destroyed.

(2) The LH_2 vent burner stack was bent, and the electrical conduit was destroyed.

(3) The LH_2 flex assemblies from the top level of the umbilical tower to the Centaur fill and drain valve were destroyed.

(4) Two GH_2 flex lines from the vent fin were damaged.

(5) The LOX dump valve was destroyed.

(6) Centaur LOX flow control and boom vent valves were burned.

Air Conditioning System

(1) All duct insulation from the bottom of the umbilical tower to the end of both booms was damaged.

(2) The Centaur thrust section heating duct was damaged from the second to the fifth level of the umbilical tower.

Hydraulic System

(1) All hydraulic lines on the launcher and ramp were destroyed.

(2) The nitrogen charge panel on the ramp and all lines above the ramp to this panel were destroyed.

(3) The hydraulic pumping unit suffered smoke damage.

Umbilical Booms

The booms suffered heat and blast damage but no major structural damage. The booms are to be removed from the tower, disassembled, and refurbished.

Launcher

The launcher was completely destroyed except for a few small components that may be salvageable.

Pressurization System

(1) The Atlas and Centaur pressurization control units, and the pressure reducing panel located on the mezzanine of the transfer room, suffered smoke and corrosion damage. Much of the corrosion resulted from the use of foam-type fire extinguishers.

(2) All pressure tubing on the launcher was destroyed.

Electrical Systems

(1) Approximately 30 major items of equipment were destroyed. Most of this equipment was in the transfer room; some was on the ramp and at the base of the umbilical tower. This equipment consists of racks, junction boxes, relay boxes, power supplies, and terminal cabinets.

(2) Long-run cables entering the transfer room from the cable tunnel were damaged, and require cutoff, splicing, and retermination.

(3) All cabling in the pad area and up the umbilical tower was damaged beyond repair.

RF and TV Systems

(1) The RF transmission lines on the umbilical tower and the termination box at the end of the cable tunnel require replacement.

(2) The C-band and Azusa test sets require replacement.

(3) Five TV cameras require overhaul due to heat and blast damage. All cabling to these cameras must be replaced.

Landline Instrumentation

All distribution boxes, cabling, and transducers located on and around the launcher, umbilical tower, and transfer room were damaged beyond repair.

Figure XII-1. - Aerial view showing general damage to pad area.

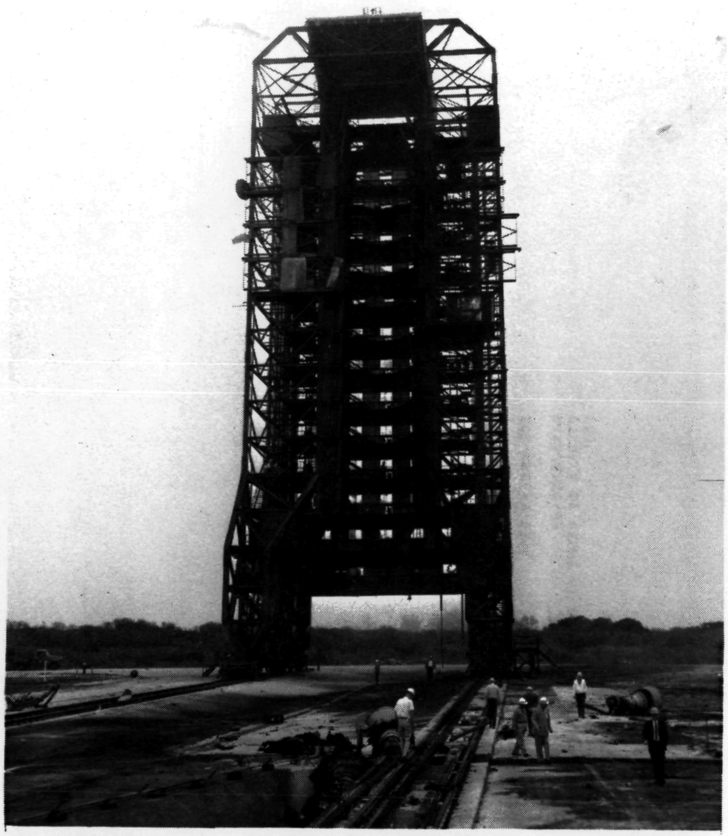

Figure XII-2. - View of service tower showing damage to Fiberglas panels.

Figure XII-3. - View of southeast corner of service tower showing heat damage to electrical wiring.

Figure XII-4. - View from ramp showing general damage to umbilical tower.

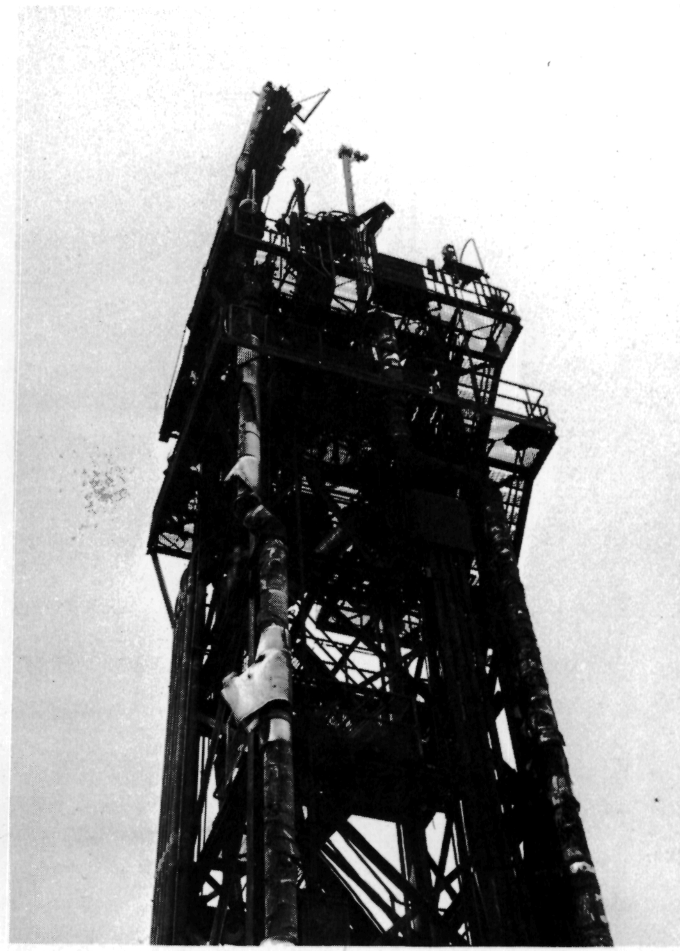

Figure XII-5. - Closeup view of umbilical tower showing damage to air-conditioning ducts.

CONFIDENTIAL

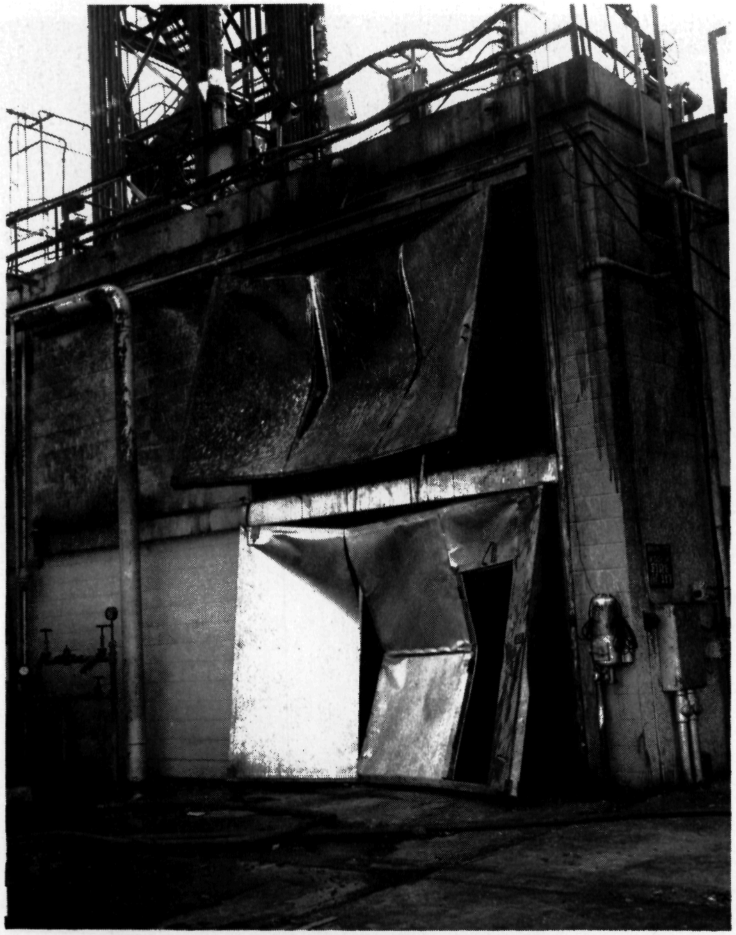

Figure XII-6. - View of launch and service building showing damaged doors.

Figure XII-7. - View at top of ramp showing melted aluminum handrails and damage to grating.

CONFIDENTIAL

Figure XII-8. - Closeup view of damaged Atlas-Centaur launcher.

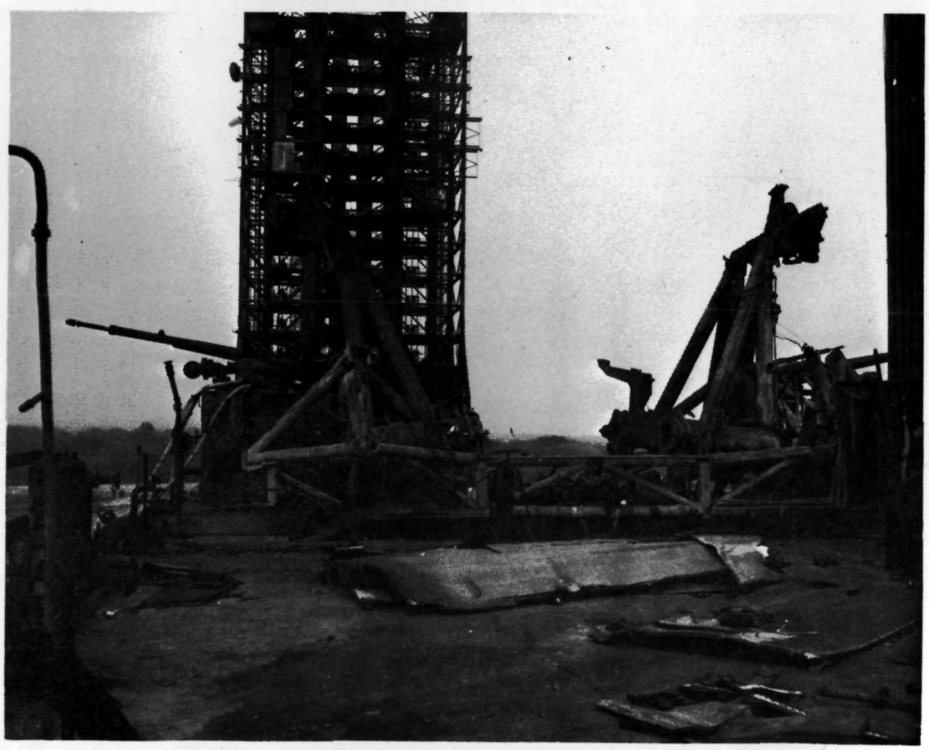

Figure XII-9. - Damaged launcher with vehicle debris in foreground.

Figure XII-10. - View at top of ramp showing typical destruction of electrical equipment and cameras.

APPENDIX

ABBREVIATIONS

A-C	Atlas-Centaur
AFCRL	Air Force Cambridge Research Laboratories
AFETR	Air Force Eastern Test Range
AGC	automatic gain control
ac	alternating current
BECO	booster engine cutoff
cps	cycles per second
CRT	composite readiness test
DDW	digital data word
DSIF	deep space instrumentation facility
dc	direct current
EST	Eastern Standard Time
ETR	Eastern Test Range
F -	-days prior to launch day
FACT	flight acceptance composite test
FPIP	fuel pump inlet pressure
GD/C	General Dynamics/Convair
GH_2	gaseous hydrogen
GMT	Greenwich Mean Time
GSE	ground-support equipment
H_2O_2	hydrogen peroxide
I/A	interstage adapter
IGS	inertial guidance system
k	thousands of pounds of thrust

LeRC	Lewis Research Center
LH_2	liquid hydrogen
LOX	liquid oxygen
LV-3	launch vehicle 3 Centaur
MECO	main engine cutoff
MES	main engine start
MGS	missile guidance set
PE	platform electronics
PLIS	propellant level indicating system
P-P	peak to peak
PU	propellant utilization
psi	pounds per square inch
psia	pounds per square inch absolute
psid	pounds per square inch differential
psig	pounds per square inch gage
Q	quadrant
QUAD	quadrant
Q_1, Q_2, Q_3, Q_4	quadrants I, II, III, and IV, respectively
RF	radiofrequency
rms	root mean square
RP-1	rocket propulsion fuel
rpm	revolutions per minute
RSC	range safety command
SD-1	Surveyor dynamic model
SECO	sustainer engine cutoff

REFERENCES

1. Anon.: Trajectory and Performance Data, Appendix B. Rept. No. 63-0495-22, General Dynamics/Convair, Mar. 21, 1965.

2. Gossett, John D.: Centaur Test Report (AC-5). Tanking (CTP-INT-0006H), Conducted Feb. 11, 1965. Field Projects Branch, Atlantic Missile Range, NASA Goddard Space Flight Center, Feb. 18, 1965.

3. Gossett, John B.: Centaur Test Report (AC-5). Flight Acceptance Composite Test CTP-INT-0001H, Conducted Feb. 18, 1965. Field Projects Branch, Atlantic Missile Range, NASA Goddard Space Flight Center, Feb. 19, 1965.

4. Gossett, John B.: Centaur Test Report (AC-5). Composite Readiness Test CTP-INT-0005C, Conducted Feb. 25, 1965. Field Project Branch, Atlantic Missile Range, NASA Goddard Space Flight Center, Feb. 27, 1965.

5. Rocketdyne Engineering Staff: Design Information Report for the Atlas MA-5 Propulsion System. Rept. No. R-3026-5, Rocketdyne, North Am. Aviation, Dec. 30, 1964.

6. Anon.: Failure Analysis Report. Rept. No. CT-9B-06-131, General Dynamics/Convair, Mar. 11, 1965.

7. Anon.: AC-5 Postflight Analysis. Rept. No. BTD-65-064, General Dynamics/Convair, Apr. 19, 1965.

8. Hansen, G. L.: Model Specification for Centaur 6C Second Stage Vehicle. Rept. No. 55-01506, General Dynamics/Astronautics, Nov. 1, 1963.

9. Test Evaluation Group: Atlas/Centaur Flight Evaluation Report Vehicle AC-5. Rept. No. GD/C-BNZ65-019, General Dynamics/Convair, Apr. 1, 1965.